GEORGIA INSTITUTE OF TECHNOLOGY
OFFICE OF CONTRACT ADMINISTRATION
SPONSORED PROJECT INITIATION

Date: February 29, 1980

Project Title: Precision Tracking Radar Antenna Measurements

Project No: A-2585

S

Project Director: Dr. Robert W. McMillan

Sponsor: Battelle Columbus Laboratories

Agreement Period: From February 8, 1980 Until ~~June~~ July 30, 1980 (Delivery Order Period)

Type Agreement: Delivery Order No. 1462 (Time and Materials Subcontract under Prime DAAG29-76-D-0100)

Amount: $19,965 Ceiling Price

Reports Required: Summary of Results; Oral Reports; Final Report

Sponsor Contact Person (s):

Technical Matters

Contracting Officer's Technical Representative (COTR)

Mr. Henry M. Grass
ATTN: DRSMI-REL
USA MICOM
Redstone Arsenal, AL 35809

(205) 876-1831

Contractual Matters
(thru OCA)

Mr. L. G. (Jack) Franklin
Contracting Officer
Battelle Columbus Laboratories
Durham Operations
3333 Chapel Hill Boulevard
P. O. Box 8796
Durham, NC 27707

(919) 489-2366

Defense Priority Rating: None

Assigned to: EML/EOD (School/Laboratory)

COPIES TO:

- Project Director
- Division Chief (EES)
- School/Laboratory Director
- Dean/Director—EES
- Accounting Office
- Procurement Office
- Security Coordinator (OCA)
- Reports Coordinator (OCA)
- Library, Technical Reports Section
- EES Information Office
- EES Reports & Procedures
- Project File (OCA)
- Project Code (GTRI)
- Other

GEORGIA INSTITUTE OF TECHNOLOGY
OFFICE OF CONTRACT ADMINISTRATION

SPONSORED PROJECT TERMINATION

Date: 10/17/80

Project Title: Precision Tracking Radar Antenna Measurements

Project No: A-2585

Project Director: Dr. Robert W. McMillan

Sponsor: Battelle Columbus Laboratories

Effective Termination Date: 7/30/80

Clearance of Accounting Charges: 7/30/80

Grant/Contract Closeout Actions Remaining:

_X_ Final Invoice and Closing Documents (STAS Claims Voucher/Final)
_ Final Fiscal Report
_ Final Report of Inventions
_ Govt. Property Inventory & Related Certificate
_ Classified Material Certificate
_ Other _____

Assigned to: EML/EOD (School/Laboratory)

COPIES TO:

Project Director
Division Chief (EES)
School/Laboratory Director
Dean/Director–EES
Accounting Office
Procurement Office
Security Coordinator (OCA)
Reports Coordinator (OCA)
Library, Technical Reports Section
EES Information Office
Project File (OCA)
Project Code (GTRI)
Other Project Code (OCA)

CA–4 (1/79)

PRECISION TRACKING RADAR ANTENNA MEASUREMENTS

(A-2585)

by

R. C. Rogers III, R. W. McMillan,
G. F. Smith III, and J. J. Gallagher
Georgia Institute of Technology
Engineering Experiment Station
Atlanta, Georgia 30332

A STUDY PERFORMED FOR

U.S. Army Missile Command
Advanced Sensors Directorate
Redstone Arsenal, Alabama 35809

through

Battelle Columbus Laboratories
Durham Operations
Durham, North Carolina 27707

Under Scientific Services Agreement Contract DAAG29-76-D-0100
Delivery Order Number 1462

July 18, 1980

FOREWORD

This final report describes work done for the U. S. Army Missile Command through Battelle Columbus Laboratories. The technical monitor for MICOM was Mr. Henry Grass of the Advanced Sensors Directorate, and the period of performance was 11 February to 18 July 1980. Those participating in the Study for Georgia Tech included R. C. Rogers III, R. W. McMillan, G. F. Smith III, and J. J. Gallagher. The authors gratefully acknowledge the contributions of D. O. Gallentine and his mechanical design personnel as well as those of personnel in the Georgia Tech Engineering Experiment Station Machine Shop. Helpful discussions were held with Messers. Henry Grass, Tom Barley, Gus Rast, and Dr. George Emmons of MICOM.

TABLE OF CONTENTS

TABLE OF CONTENTS (CONT.)

SUMMARY

This report represents a continuation of a study done by McMillan and Riley [1] on the possibility of designing an antenna which is siumltaneously pointed by a large, relatively crude gimbal which would support an entire system and a smaller highly accurate gimbal which is used for fine steering of an antenna beam. As originally envisioned, the antenna would be used in a millimeter wave system and should be cheaper than a conventional antenna steered by a simple gimbal because the larger load-bearing pointing mechanism could be relatively crude, while the smaller, precision pointing gimbal would not have to support the entire antenna weight.

The original report [1] examined the possibility of steering a Cassegrain antenna beam by moving either subreflector or feed, in addition to a large number of additional feed approaches including phased arrays, a Luneberg lens, and various electro-optic effects. In that study, it was concluded that, based on present technology, precision steering of a Cassegrain antenna beam can best be accomplished by moving either subreflector or feed. The experimental and theoretical work described in this report therefore had as an objective the determination of the best method for steering the antenna beam in this way.

Determination of the best beam pointing method was accomplished by making measurements of actual steered antenna patterns on the Georgia Tech antenna range. A parallel theoretical effort supported these measurements and confirmed the results obtained. It is concluded that rotation of the Cassegrain antenna subreflector is the best method of beam pointing from the points of view of both steering efficiency and minimum beam distortion.

Since the theoretical results on beam pointing closely agreed with the measurements, the theory was used to design an antenna more amenable to beam pointing than those commercially available. This design is discussed in this report, and it is recommended that this antenna be built and tested.

LIST OF FIGURES

LIST OF FIGURES (CONT.)

LIST OF FIGURES (CONT.)

LIST OF FIGURES (CONT.)

1.0 INTRODUCTION

1.1 Background

The ability of systems employing frequencies in the millimeter wave (MMW) portion of the electromagnetic spectrum to penetrate adverse weather, and the improved resolution with smaller antennas attainable in this frequency band, have led to increased systems development activity in this spectral region. Examples of this activity in Army systems are the millimeter beamrider, differential guidance, and various radar programs.

Although MMW antennas are generally much smaller than conventional radar antennas, they may still be large from the standpoint of achieving rapid scanning and accurate pointing, with diameters of 50-60 cm being fairly common for high resolution applications. These antennas may weigh 10-15 kg, and since no rotary joints are available for use in most of this spectrum, it is generally necessary to mount all transmitter and receiver waveguide components directly on the antenna. If it is necessary to mount this device on a gimbal, it is obvious that a very rigid, sturdy structure is required. If it is further desired to achieve tracking accuracies on the order a few tenths of milliradians, the servo system components become expensive because high accuracy and large load bearing capability are required simultaneously. The use of a gimbal-mounted splash plate for steering alleviates this problem to some degree, but the stiffness and flatness requirements for this reflector still make it very heavy for mounting on a precision gimbal. In addition, a splash plate system is significantly larger in terms of space required for mounting and achieving a clear field-of-view. This study addresses the problems involved in building an antenna which can be used for accurate tracking without the requirement for precision gimbaling of the antenna or its main reflector.

It is recognized that very large and heavy gimbal mounting structures are available at moderate prices as long as the accuracy

requirements are not too severe. When a gimbal system has simultaneous high accuracy, heavy load, and fast scan requirements, however, its price rapidly increases. In order to avoid such escalation the approach taken in this report to obtain accurate tracking without mounting the antenna or splash plate on a precision gimbal involves the use of a crudely steered primary antenna which is fed by a precisely steered feed system. In this way, while the large relatively crude gimbal moves the heavy antenna, its inaccuracies are compensated by the precision feed. Since the large gimbal has a heavy load-bearing but minimal accuracy capability, and the precise feed can achieve high accuracy with light load, the result should be an accurate tracking antenna which is also moderate in cost. Figure 1-1 is a schematic diagram of this approach, shown implemented with a parabolic reflector antenna. Note that it is possible to fine steer the antenna beam by moving either the feed horn or the subreflector. Furthermore, the beam may be steered by either translating or rotating the horn or subreflector, although it will be seen that movement of the subreflector is more effective because of the magnification of this element.

It will be shown that the antenna beam can be effectively steered by moving either of the elements mentioned above, but this report does not address some of the control system difficulties inherent in this approach. For example, fine steering to 0.1 milliradian accuracy will require position encoders with resolution of 16 bits on each of the gimbal axes. Such encoders tend to be large and will therefore distort the antenna beam because of increased central oscuration in the case of subreflector steering. Crossover between the coarse and fine gimbals may also be difficult to implement.

This report describes the results of measurements made at Georgia Tech on antenna beam steering by rotation and translation of both subreflector and feed of a Cassegrain antenna. These measurements are compared to a simple geometrical theory to determine the degree of steering and are compared to optical diffraction theory to determine sidelobe levels and other beam distortions. Good agreement is obtained in both cases.

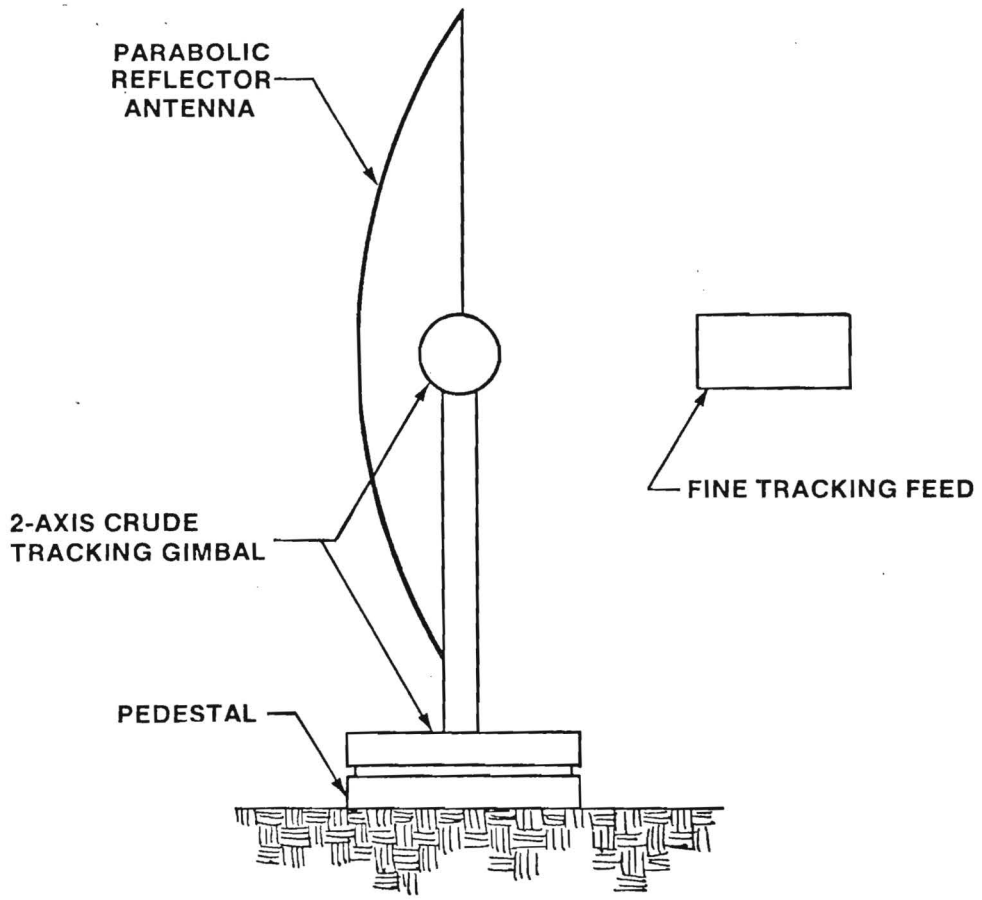

Figure 1-1. Schematic of crude tracking antenna with fine tracking feed.

A preliminary analytical study [1] on the same subject as this report covers has been done by McMillan and Riley. This earlier work will be referred to extensively in this report and parameter choices will be made consistent with its calculations.

1.2 Summary of Measurements

A modified TRG Model W822-24 61 cm (24 inch) Cassegrain antenna was used for the measurements discussed in this report. A rotation-translation system was used to vary both feed and subreflector position and angle.

1.2.1 Subreflector Translation and Rotation

For subreflector measurements, the subreflector support struts were removed and the subreflector was supported on a brass rod which was mounted to the rotation/translation stage. The center of rotation passed through the focus of the hyperbolic reflector for most measurements, but a series of experiments was also conducted in which the rotation center passed through the hyperbola vertex. Both pure translational measurements, and measurements in which the subreflector was first translated and then rotated to point toward the feed, were made.

1.2.2 Feed Translation and Rotation

In performing feed steering experiments, the subreflector mounting struts were replaced and a fixture similar to that used for subreflector measurements was used for feed translation and rotation. Rotations were carried out about the phase center of the feed horn, which is assumed to be located at the horn output. Horn translation measurements were also made. It will be shown that feed horn motion is less effective in antenna beam steering than subreflector motion because of the magnification of this latter element, which is 5.67 for the antenna used for the measurements described herein.

1.3 Pointing and Tracking Requirements

Although accuracy requirements vary greatly from one MMW system to another, it is possible to formulate some general guidelines based on a hypothetical battlefield scenario. The maximum range of interest for most MMW systems is a few kilometers and a reasonable estimate for aimpoint accuracy at this range is on the order of one meter, giving an overall system accuracy of a few tenths of a milliradian. Because of large contributions of other subsystems to this error budget, the ideal case would be for the contribution of the antenna subsystem to be negligible, which implies that its accuracy should be 0.05 mrad. It is emphasized that this error is the contribution of the gimbal subsystem and its associated electronics only. This level is chosen so that other tracker system errors will dominate the error budget. Although stringent, this accuracy is within the state-of-the-art of tracker systems.

A reasonable tracking rate requirement may be derived by considering a target moving transversely to the line-of-sight at a rate of 50 km/hr at a range of 100 m, a minimum range that is considered consistent give a tracking rate of only about 8 degrees per second, which should not be difficult to attain.

Jitter and boresight requirements are more difficult to evaluate. It would be desirable for the combination of these errors with tracking errors not to exceed the 0.05 mrad mentioned earlier, but this degree of accuracy is not realistic. It is probably reasonable to require the combined tracking, jitter, and boresight errors not to exceed twice this amount, or 0.1 mrad.

A MMW antenna system will probably also be required to operate in some type of search mode over a limited sector. In this case, the fine steering feed would be disabled, and the feed boresighted with the

primary antenna. To maximize search mode coverage, it is desirable to have the primary antenna scan as rapidly as possible. For a raster scanning format, the most rapid scan velocity occurs in azimuth, and a reasonable angular velocity of scan for a MMW antenna of 60 cm aperture is considered to be about 100 deg/sec.

In summary, the nominal system requirements for a MMW scanning and tracking antenna system are as follows: (1) tracking, jitter and boresight errors 0.1 mrad, (2) tracking rate $\sim$ 8 deg/sec, and (3) scan rate $\sim$ 100 deg/sec. Although error analyses for the steering methods treated in this report have not been performed, it is expected that typical MMW system accuracies will not be compromised by any of these approaches.

1.4 Summary of Conclusions

The conclusions reached in this report may be summarized by stating that beam steering of a Cassegrain antenna is possible by moving either the feed horn or the hyperbolic subreflector. Of these two methods, the latter is most effective because of the magnification of this subreflector. Rotation and translation of the hyperbola are essentially equally effective as regards beam steering but translation gives higher sidelobe levels. It is recognized that translational motion of a subreflector would be hard to attain because precise linear motion is generally more difficult to implement and control than rotary motion. It will be concluded, therefore, that rotary motion of the hyperbola is the most effective way to implement beam steering with a Cassegrain antenna.

The TRG antenna used for the experiments described in this report is not very suitable for beam steering. It will be shown that long focal length antennas generally give better beam steering and less distortion than those with short focal lengths. The TRG antenna has a 203 mm (8 inch) focal length and a 61 cm (24 inch) diameter, which gives an f-number of 1/3. In Section 5 of this report, an antenna design suitable for beam steering is discussed.

2.0 Beam Deviation Theory

The theory of antenna beam deviation is presented essentially in two parts: (1) a simple geometric theory based on rotation and translation of subreflector and feed separately [2,3], and (2) a diffraction theory approach using the results obtained by Ruze [4] and Lo [5]. The geometric theory accurately predicts beam steering, but does not give any indication of beam distortion, while the diffraction theory gives beam broadening, degradation of sidelobe levels, and gain loss. It may be possible to linearly and accurately deflect an antenna beam by a given method, but this deflection is of limited effectiveness unless the beam distortion is within tolerable limits.

A Cassegrain antenna configuration as shown in Figure 2-1 was chosen as a realistic framework for analysis of the effects of beam steering on tracking mm wave systems. As conceived in this study, the feed is located at the real focus and illuminates a hyperbolic secondary reflector ahead of the dish. The secondary reflector in turn illuminates the paraboloid.

Geometric optical techniques are generally based on paraxial treatment alone, i.e., the system is restricted to operating in an extremely narrow region about the optical axis. Obviously, if rays from the periphery of a parabolic reflector in a low F# (F# = f/D) antenna system are to be evaluated, the paraxial condition $\sin\phi = \phi$ is not satisfactory (ϕ = angle between the optical axis and a converging ray from the aperture at any point off the optical axis). In optical systems where the F# is greater than three the paraxial treatment is sufficient, since $\sin\phi = \phi$ to within 3 percent (i.e., $\phi < 10$ degrees). However, in antenna systems where lower F#'s are used this approximation is no longer valid and higher order terms must be considered. These may be discussed by expanding the sine function which yields:

$$\sin\phi = \phi - \frac{\phi^3}{3} + \frac{\phi^5}{5} - \cdots \qquad (2\text{-}1)$$

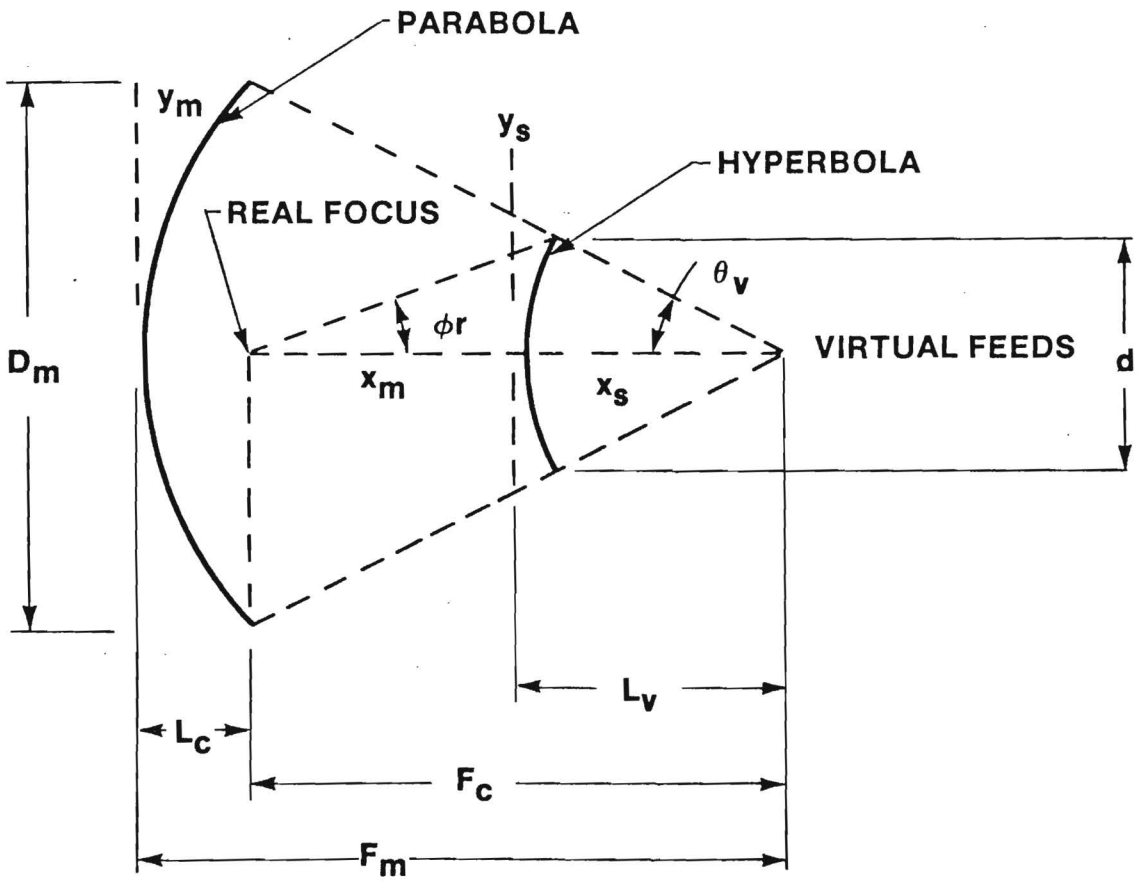

Figure 2-1. Cassegrain antenna system.

If the first two terms of this expression are retained as an improved approximation, the well-known third order theory is obtained. Departures from the paraxial treatment (or first order theory) which then result, are contained in the five primary aberrations (spherical, coma, astigmatism, field curvature, and distortions). In an optical system, the primary interest in these aberrations is the spatial distortion of the image plane from its desired focus. However, in antenna systems these aberrations manifest themselves as phase distortion which have a significant effect on gain, beamwidth, and side lobe levels.

The effects of coma and astigmatism have been evaluated, in this report, assuming the effects of spherical aberrations, field curvature, and distortion are nonexistent. Coma is an aberration associated with the image point lying off-axis. Astigmatism results in light rays passing through the optical system in a vertical plane focussing at a different distance from rays passing through in a horizontal plane.

These results indicate that scanning over a few beamwidths will require an F on the order of one. Scanning techniques such as rotating wedges or flat scan mirrors at or near the image plane only serve to increase spherical aberrations and distortion due to field curvature. The net result of this effect would be to increase the F for a given maximum scan angle and require a feed re-focus as a function of scan angle. Neither situation is desirable; therefore, the standard Cassegrain antenna configuration will be used. In this configuration, spherical aberrations, field curvature, and distortion can be compensated and the effects of coma and astigmatism will dominate.

2.1 Determination of Antenna Parameters [6,7]

Most of the antenna parameters required for calculations of steering performance were provided by TRG, and the remaining parameters were either calculated from these or measured. The parameters are listed in Table 2-1 and a mechanical drawing of the antenna is in Section 3.

Table 2-1

TRG Model W822-24 Antenna Parameters

Type	Cassegrain
Material	Machined Aluminum Casting
Diameter D	610 mm (24")
Focal length f	203.2 mm (8")
Eccentricity of Subreflector ϵ	1.4282
Magnification of Subreflector M	$\frac{\epsilon+1}{\epsilon-1} = 5.67$
Diameter of Subreflector	61 mm (2.4")
Distance from Feed Phase Center to Subreflector Vertex b	104.3 mm (4.106")

The only antenna parameter needed for calculations of beam steering in addition to those given above is the distance c of the hyperbola focus from the hyperbola vertex. This quantity may be calculated from the following set of equations valid for hyperbolas:

$$a(\epsilon - 1) = 2c \qquad (2\text{-}2a)$$

$$a + c = b \qquad (2\text{-}2b)$$

where a is the length of the hyperbola transverse axis (distance between vertices of the conjugate hyperbolas).

Using values from Table 2-1 and solving these equations for c gives c = 18.39 mm (0.724"). These parameters will be used in subsequent calculations of Cassegrain antenna beam steering.

2.2 Determination of the Beam Deviation Factor

The beam deviation factor (BDF) of an antenna is defined [7] as the ratio of beam deflection angle θ_b to the angular displacement of the feed θ_f, both measured from the axis of the reflector with the vertex as origin. The BDF is used in all of the geometrical equations for beam steering by both feed and subreflector motion and must therefore be determined before these calculations can be made. The BDF of a parabolic reflector has been calculated by Lo [5], who shows that this parameter is given by good approximation by

$$BDF = \frac{1 + h(D/4f)^2}{1 + (D/4F)^2} , \qquad (2\text{-}3)$$

where the factor h is a function of f, D, and the illumination function $f(\theta, \phi)$. Lo notes that the value of h is not critical and that it may vary from 0.3 to 0.7, depending mostly on the illumination function. In the earlier report [1], h was chosen to be 0.5, and this value will be used for calculations in this report for consistency. Substituting values of D and f from Table 2-1, together with h = 0.5 into the above equations gives BDF = 0.82. The noncriticality of the choice of h is emphasized by the fact that a choice of h = 0.7 would give BDF = 0.892, which is a change of less that 10%. The value BDF = 0.82 will therefore be used in the geometrical calculations of beam divergence. This factor does not appear in the physical optics calculations; it is inherent in the equations of formulation.

2.3 Subreflector Translation

Two types of hyperbola translation were considered in the work discussed in this report. The first is a pure translation and is easily treated by the simple geometrical theory. The second is a translation followed by a rotation such that the subreflector looks back at the feed. This latter type is more complicated and is treated by the diffraction theory calculations of Ruze [4], to be discussed later.

Translation of the hyperbola vertex normal to the focal axis is reflected as a translation of the source image from the parabola design focus. The beam deviation is determined again by computing the location of the virtual focal point. Referring to Figure 2-2, it is easily seen that $Y = (\delta / M)$ and that the beam deviation is identical to that of a feed displacement of:

$$\theta_{B1} = \frac{\delta(BDF)}{Mf} . \tag{2-4}$$

A second term exists in this translation, but serves only as a beam distortion and an angular deviation of the exit beam defined simply as

$$\theta_{B2} = \frac{\delta(BDF)}{f} . \tag{2-5}$$

The total beam deviation then becomes:

$$\theta_B = \theta_{B1} + \theta_{B2} = - \frac{\delta(BDF)}{Mf} (M-1).$$

It will be seen that beam deviation due to hyperbola translation is identical to feed translation modified by the quantity (M-1). For this reason, hyperbola translation is considered a more effective way of beam steering than feed translation. These calculations will be compared to experiment in Section 4.

2.4 Subreflector Rotation

Subreflector rotations about both the hyperbola focus and the hyperbola vertex were measured, but the results of Section 3 show that there is little difference between these two rotations. The geometry

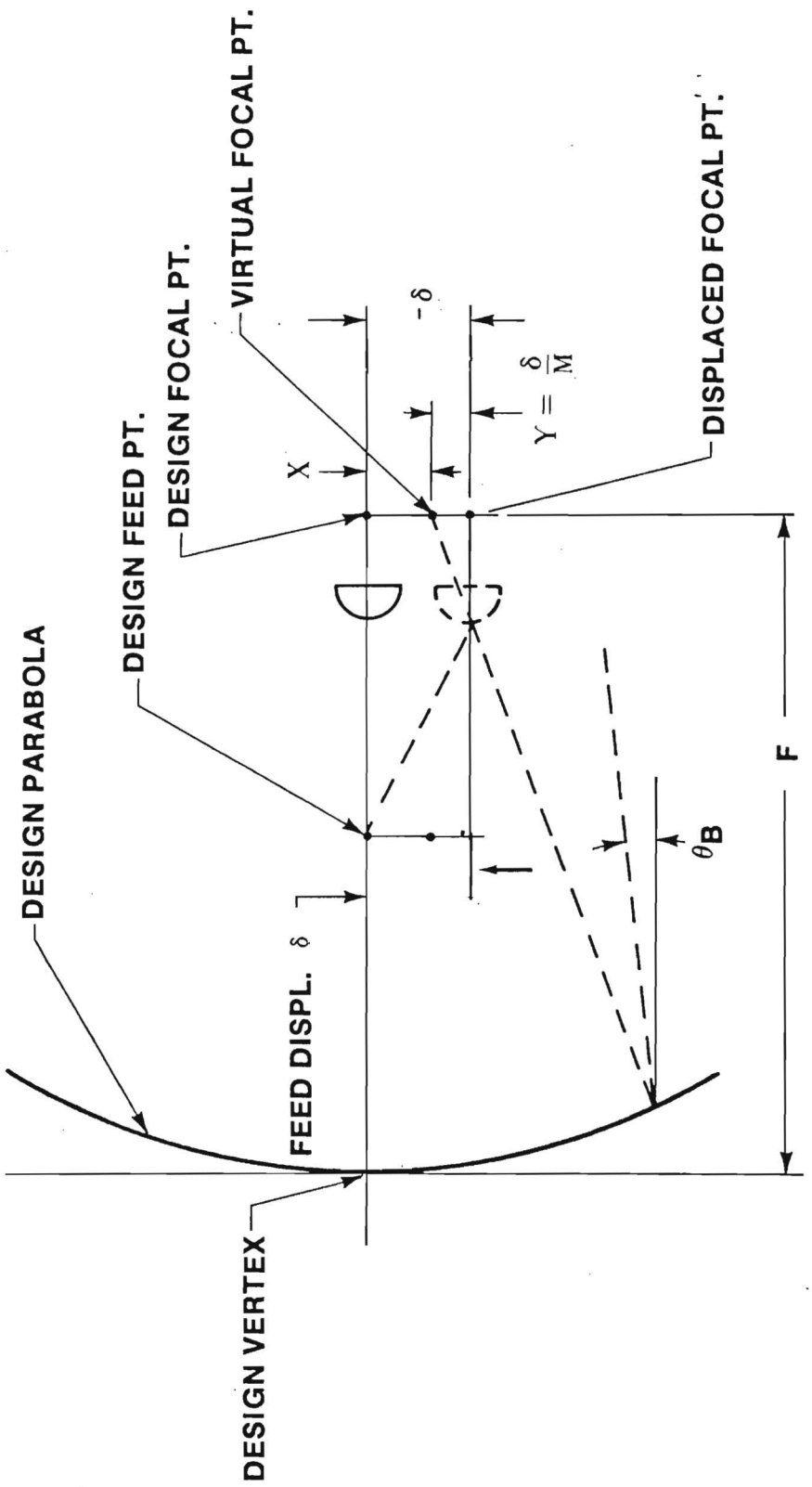

Figure 2-2. Hyperbola and feed translation geometry.

appropriate for subreflector rotation about the vertex is shown in Figure 2-3. In rotating the subreflector, the focus is displaced approximately by an amount [2]

$$C = F \tan \alpha \tag{2-6}$$

where α is the rotation angle. This equation is accurate if α is small, which will be the case for all practical rotation angles. In calculating the beam deflection angle, a correction must be applied to relate the displaced feed point to the design focal axis. This is accomplished by translating the displaced focal point back to the design focal axis by an amount equal to C. This effect is identical to beam deviation due to feed translation and causes a beam deviation angle of

$$\theta_2 = \frac{C(BDF)}{Mf} , \tag{2-7}$$

while displacement of the focus causes a deflection of

$$\theta_1 = \frac{C(BDF)}{f} , \tag{2-8}$$

The total deflection is then

$$\theta_{SR} = F \tan \alpha \frac{(BDF)}{f} \frac{(M + 1)}{M} . \tag{2-9}$$

Beam deflection computed with this equation will be compared to theory in Section 4.

2.5 Feed Translation

The geometry for feed translation is shown in Figure 2-2. The displaced or virtual focal point caused by a feed translation of δ_F is $-\delta_F/M$ and the corresponding beam deviation is therefore

$$\theta_f = - \frac{\delta_F (BDF)}{Mf} , \tag{2-10}$$

where the minus sign indicates that a downward feed deflection gives an upward beam deflection. Note that beam steering by feed deflection will

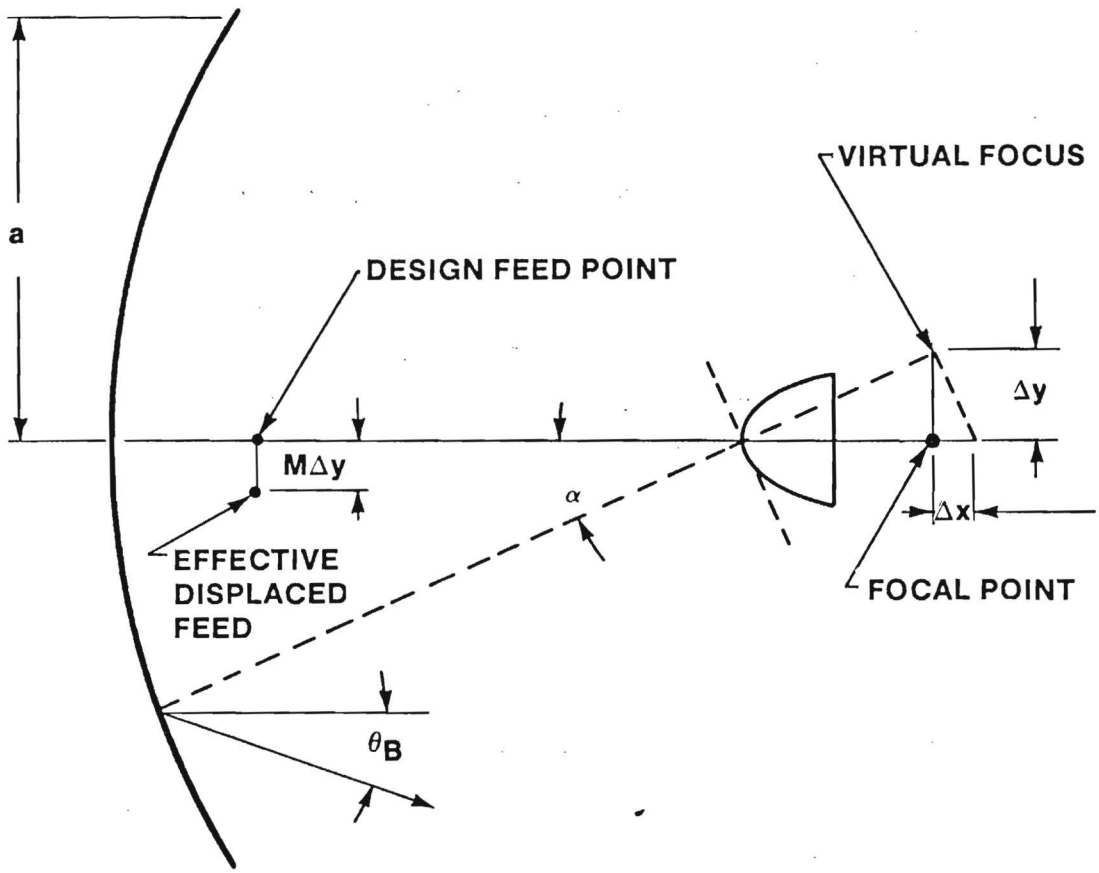

Figure 2-3. Geometry for rotation of subreflector about its vertex. Focus rotation geometry is similar.

not be very effective due to the presence of the factor M in the denominator. Measurements of antenna beam deflection angle as a function of this parameter were also made, and are compared to theory in Section 4.

2.6 Feed Rotation

Rotation of the Cassegrain antenna feed is not explicitly treated in any of the references cited in this report, but may be determined by considering that the BDF calculation of Lo treated the case in which the feed is located at the focus of the parabola. For the case in which the feed is at the focus of the conjugate hyperbola feeding the real hyperbola (Cassegrain antenna case), the beam deflection is reduced by the magnification of the subreflector and the ratio of the focal lengths.

As with feed translation, this method of beam steering is seen to be not very effective because of the magnification of the hyperbola, but this case was also measured and will be compared to theory in Section 4.

2.7 Calculation of Beam Distortions Using Diffraction Theory

The problem of parabolic dish antenna beam deflection by translation of the feed located at the focus of the parabola has been treated by Ruze [4]. Examination of Figure 2-1 will show that translation or rotation of the parabola feed is equivalent to the same motion of the hyperbola in a Cassegrain antenna. The case treated by Ruze is that of translation of the parabola feed followed by a slight rotation such that the axis of the feed points at the vertex. To be consistent with this treatment, one of the series of measurements made during this effort involved translation of the subreflector followed by a rotation to point the hyperbola axis at the parabola vertex.

Ruze shows that the electric field in the far field of the antenna is given by

$$E(\theta) = 2\pi Eo \int_o^a f(r) Jo(krA) r dr, \qquad (2\text{-}11)$$

where $E(\theta)$ is the electric field at angle θ, E_o is the axial value of the field and also serves as a normalization constant, $f(r)$ is the parabola illumination function, k is wave number, r is radial distance measured from the focus of the parabola, and a is the parabola radius. The parameter A is given by

$$A = \sin\theta - \frac{\varepsilon_x}{fM(r)} \tag{2-12}$$

where ε_x is the feed (or hyperbola) displacement and $M(r)$ is given by

$$M(r) = 1 + \left(\frac{r}{2F}\right)^2. \tag{2-13}$$

A useful representation for the illumination function is given by

$$f(r) = 0.33 + 0.67[1-(r/a)^2]. \tag{2-14}$$

which is seen to have a 10 dB taper when squared. This expression for $f(r)$ was used for all calculations of antenna patterns.

Upon making these substitutions into Equation (2-11), there results an integral that cannot be evaluated in closed form, but is not difficult to evaluate by computer. The Georgia Tech CDC 6400 computer was programmed to evaluate this integral which was calculated for several different values of hyperbola translation. These computed antenna patterns are compared to measured patterns in Section 4.

The theory of subreflector rotation has been treated by Lo [4] who used the diffraction integral to determine the beam deviation factor of a parabolic reflector. In an appproach similar to that of Ruze, he treated a paraboloid fed by a horn at its focus, so that his results must be slightly modified for a Cassegrain antenna. This modification factor is the ratio of the focal length of the hyperbola F to that of the parabola f, which multiplies the angle through which the subreflector is displaced.

The diffraction integral in the form

$$E(\theta) = K\iint \frac{f(r)}{\rho} \cos\left[kr(\sin\theta - (F\beta/f)\cos\phi\right]rd\phi dr \qquad (2\text{-}15)$$

was used by Lo. In this equation, K is a constant, f(r) is the aperture distribution and β is the subreflector angular displacement. The parameter ρ is given by

$$\rho = f \sec^2 \theta/2. \qquad (2\text{-}16)$$

which is the equation of the parabola in polar coordinates. The variable θ is the angle measured between a line directed from the antenna axis to the point of measurement and the axis itself. In this integral, the integration over θ is one of several which may be expressed as a Bessel function [8]. As a result, the integration over θ may be performed to give

$$E(\theta) = 2k\int_0^a Jo(z)\frac{f(r)}{\rho} rdr, \qquad (2\text{-}17)$$

where $z = kr(\sin\theta - F\beta/f)$, and a is the parabola radius. As was done earlier for the case of subreflector translation, this integration can be performed numerically to give far-field antenna patterns which shift in angle as a function of the hyperbola rotation angle β.

The results of solving this equation will be given in Section 4 which may be compared to the measurements in Section 3. It will be seen that hyperbola rotation gives much less beam distortion than hyperbola translation, and is therefore the method of choice for fine steering an antenna beam.

It should be noted here that the calculations of this section assume rotation about the hyperbola focus. Although measurements of beam steering by rotation about the vertex were made, this case was not treated theoretically, and the results of Section 3 will show that this method is inferior to that of rotation about the focus, because of increased beam distortion.

3.0 ANTENNA EXPERIMENTS

3.1 Introduction

The antenna experiments were divided into two parts. The first part involved beam steering and antenna pattern degradation effects resulting from subreflector reorientation, i.e. rotation and translation perpendicular to the antenna axis of the subreflector from its optimum position, while the second part was concerned with similar effects associated with feed reorientation.

In each case a TRG 24 inch diameter Cassegrain antenna (Figure 3-1) was modified to meet experimental requirements. Design parameters for this antenna, such as focal length, paraboloid eccentricity, etc., and a description of the antenna are included in Section 2. A discussion of the experimental setup and antenna range is included later in this section.

3.1.1 Subreflection Reorientation Experiment

Reorientation of the subreflector from its optimum on-axis position (i.e. that position which gives a focussed and symmetrical antenna pattern) was achieved using the modified form of the afore-mentioned TRG antenna shown in Figure 3-2 and 3-3. Note that the spider-like subreflector support has been replaced by a cube-cylindrical rod support mechanism, which is in turn attached to the surface of an x-y translation and rotation table assembly. This assembly was fabricated by mounting a rotary table with angular read-out, to an optical quality x-y translation stage, with x and y micrometer read-outs. The subreflector shaft was mounted in a cylindrical hole of the cube such that the convex subreflector surface faced the antenna feed. On-axis mechanical alignment of the subreflector holder was accomplished by inserting an alignment rod into the antenna feed mounting hole which engaged the subreflector mounting hole at the proper subreflector position. Antenna patterns were recorded for various subreflector

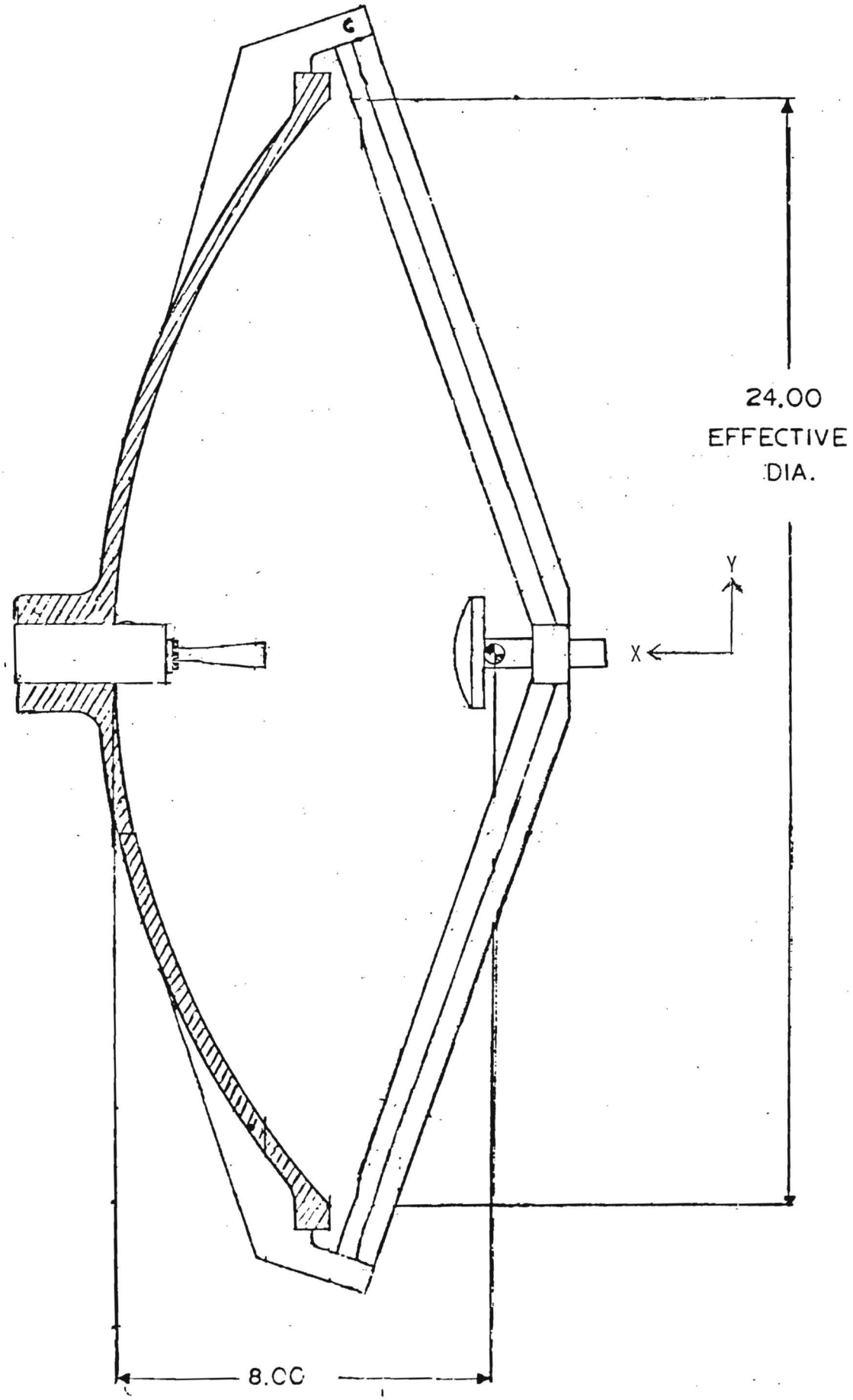

Figure 3-1. TRG (24" Dia.) Cassegrain reflector antenna. (Top View)

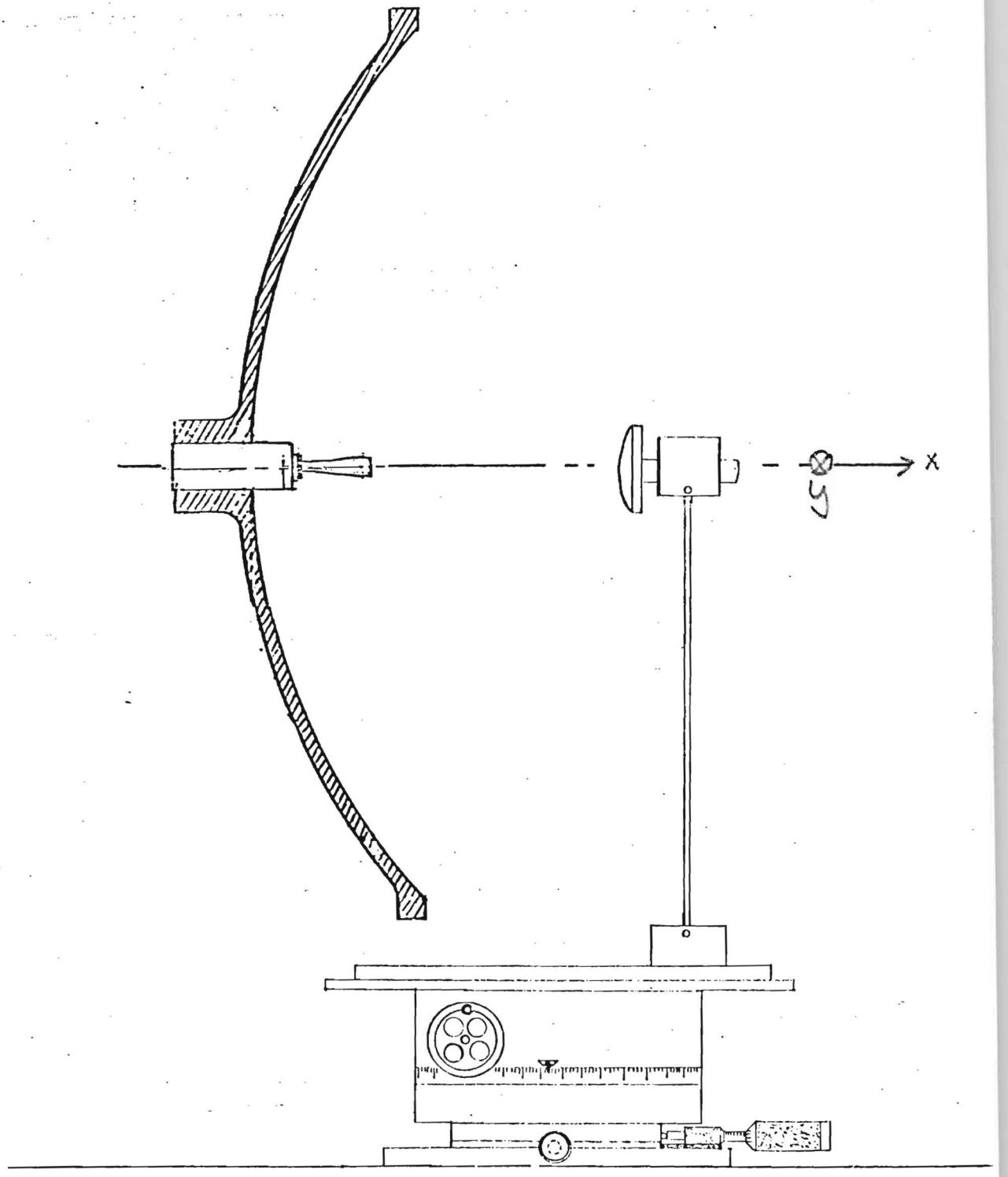

Figure 3-2. Modified Antenna (TRG) system for subreflector translation and rotation.

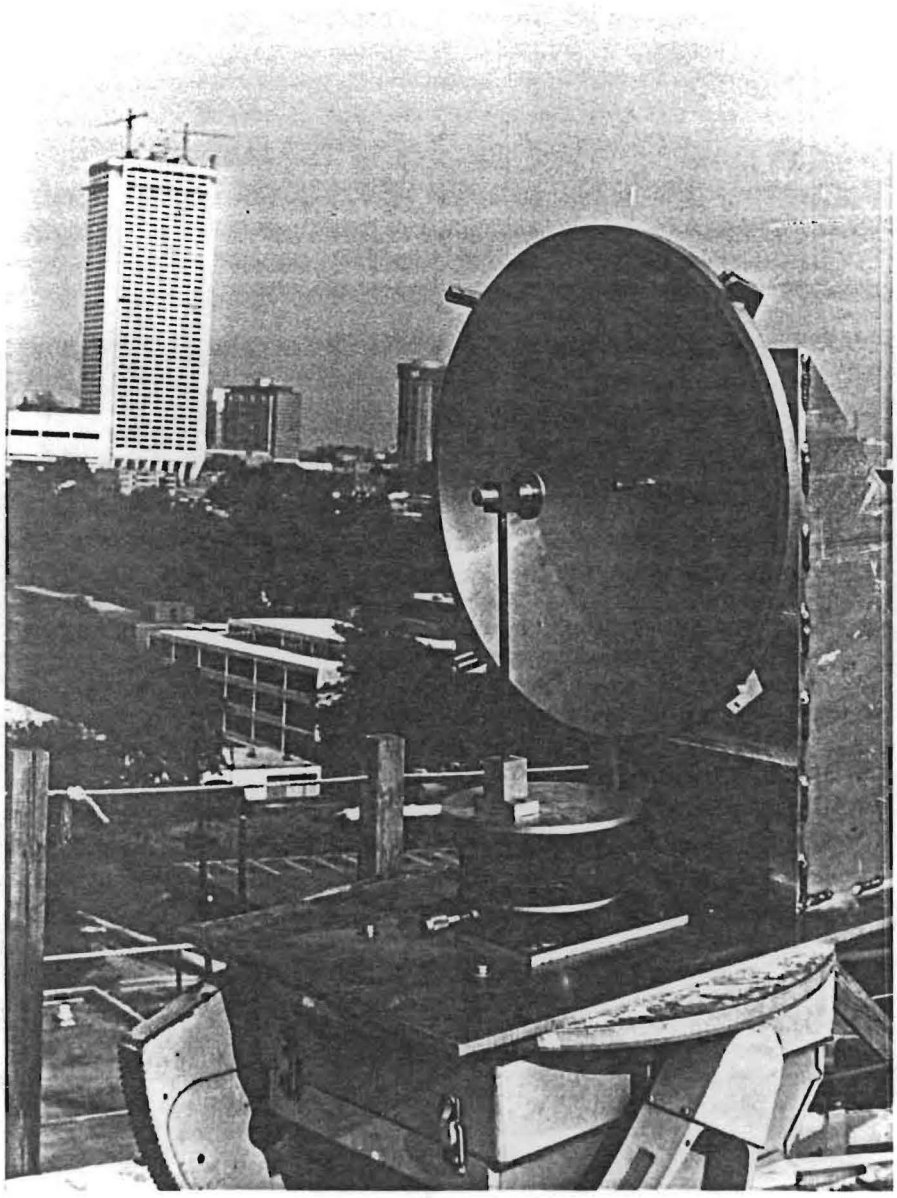

Figure 3-3. Photograph of antenna steering mechanism used for subreflector rotation and translation.

translations, rotations and translation-rotation combinations. Note that for both sets of experiments the antenna under test was horizontally polarized (E field parallel to the horizon) and the antenna focus was optimized with respect to the antenna symmetry axis (x axis of Figure 3-1). All subreflector and feed translations and rotations are with respect to the E-plane.

Figures 3-4 and 3-5 show E- and H-plane antenna patterns respectively for a non-translated, non-rotated subreflector (i.e. no beam steering). Note the deep nulls between the main lobe and sidelobes indicating good antenna focus. The second set of patterns are E-plane patterns (Figures 3-7, 3-8, 3-9, and 3-10) corresponding to feed translation in the E-plane (y axis translation) as illustrated by Figure 3-6. An H-plane pattern (Figure 3-11) corresponding to an E-plane feed translation of 5.08 mm did not differ significantly from that of the optimum H-plane pattern of Figure 3-5.

E-plane patterns resulting from subreflector E-plane rotation about the antenna focus (as illustrated in Figure 3-12) are shown in Figures 3-13, 3-14, 3-15 and 3-16. The H-plane pattern (Figure 3-17) corresponding to a four degree E-plane rotation was essentially the same as that of Figure 3-5.

Figures 3-19, 3-20, 3-21 and 3-22 show E-plane patterns corresponding to rotation of the reflector about its vertex (Figure 3-19). The H-plane pattern of Figure 3-23 for an E-plane subreflector rotation of 3 degrees does not differ significantly from Figure 3-5.

The last pattern set (Figures 3-25 and 3-26) is due to translation and rotation toward the feed of the subreflector as illustrated in Figure 3-24. A sidelobe level increase of 3 dB over that of Figure 3-5 was observed (Figure 3-27) for the H-plane pattern corresponding to an E-plane translation of 7.67 mm and rotation of 3.93 degrees toward the feed. Table 3-1 contains significant antenna pattern degradation data for the subreflector translation part of this experiment.

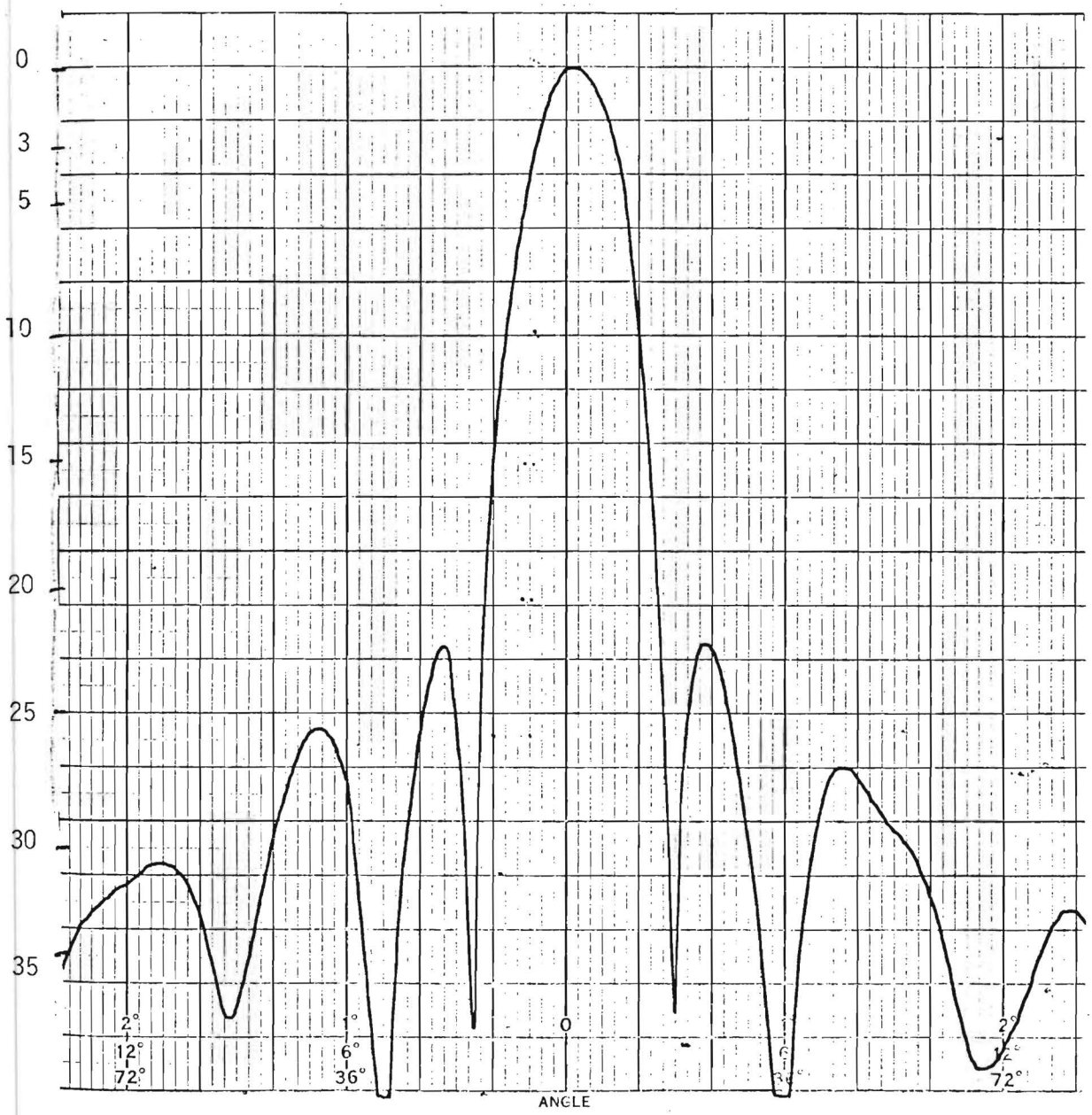

Figure 3-4. Measured E-plane pattern for subreflector in normal position, Frequency 94.58 GHz. Three large divisions $\geq$ 1 degree for all patterns in this report.

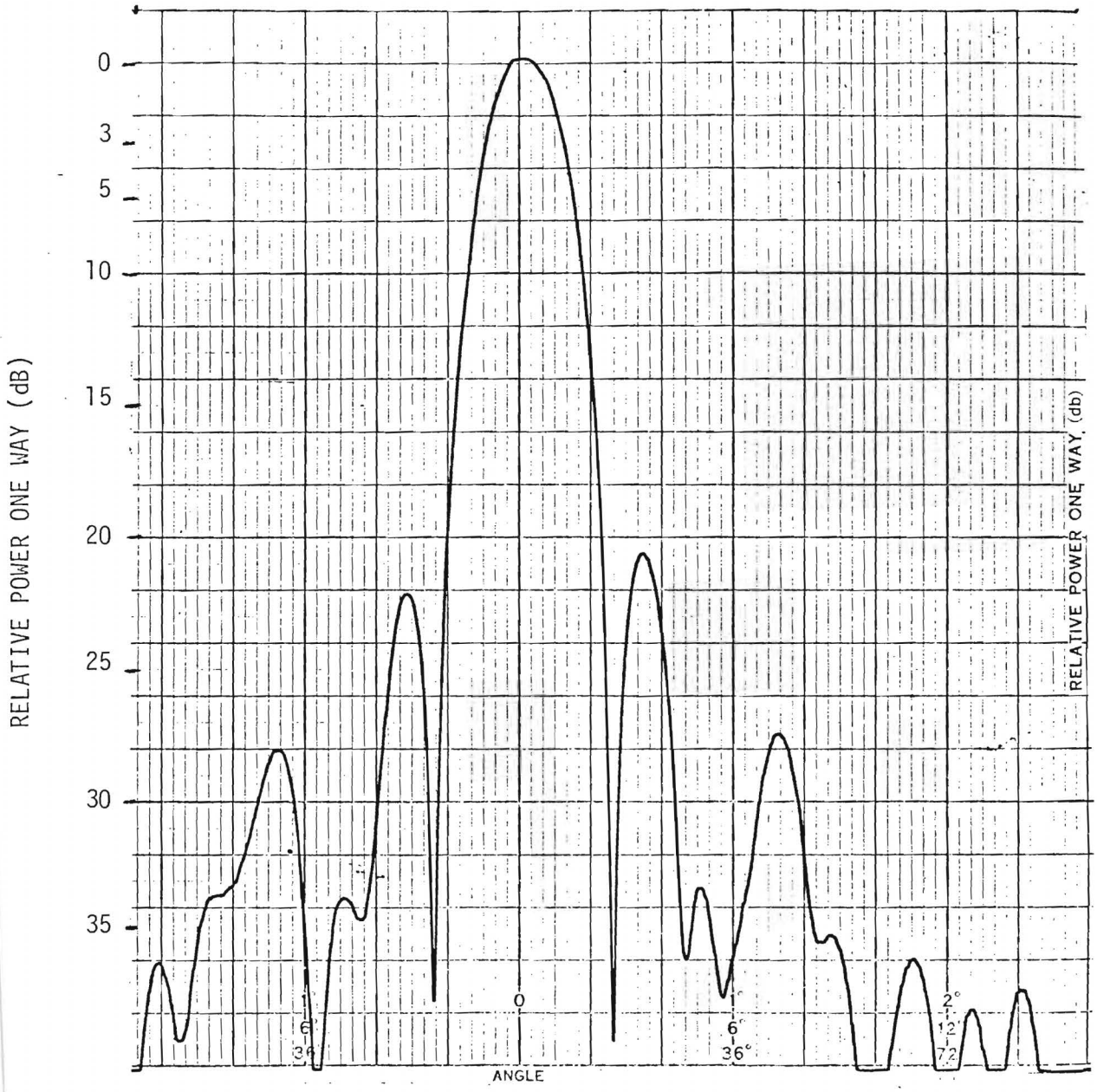

Figure 3-5. Measured H-plane pattern for subreflector in normal position. Frequency 94.58 GHz.

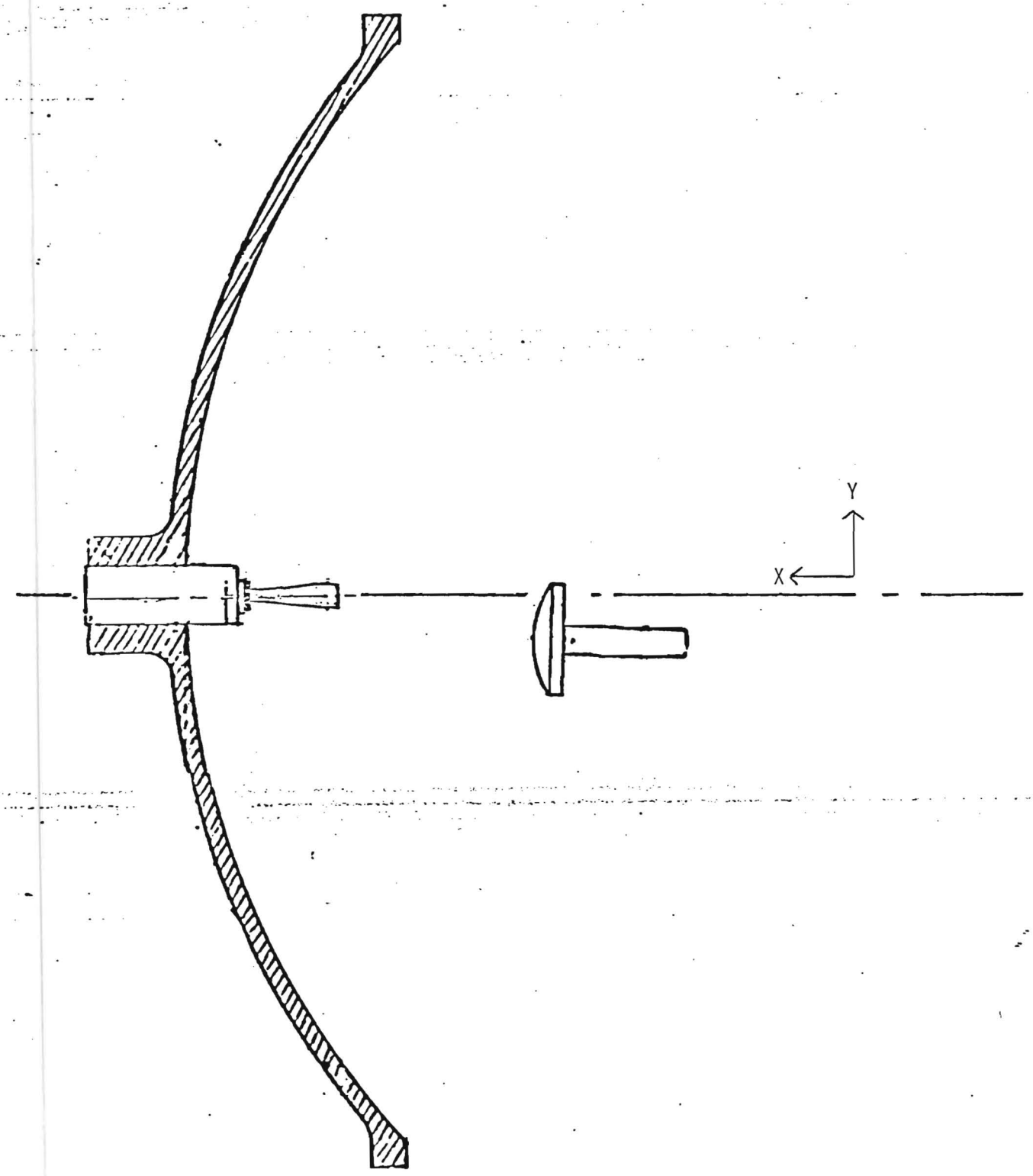

Figure 3-6. Translation of subreflector. (Top View)

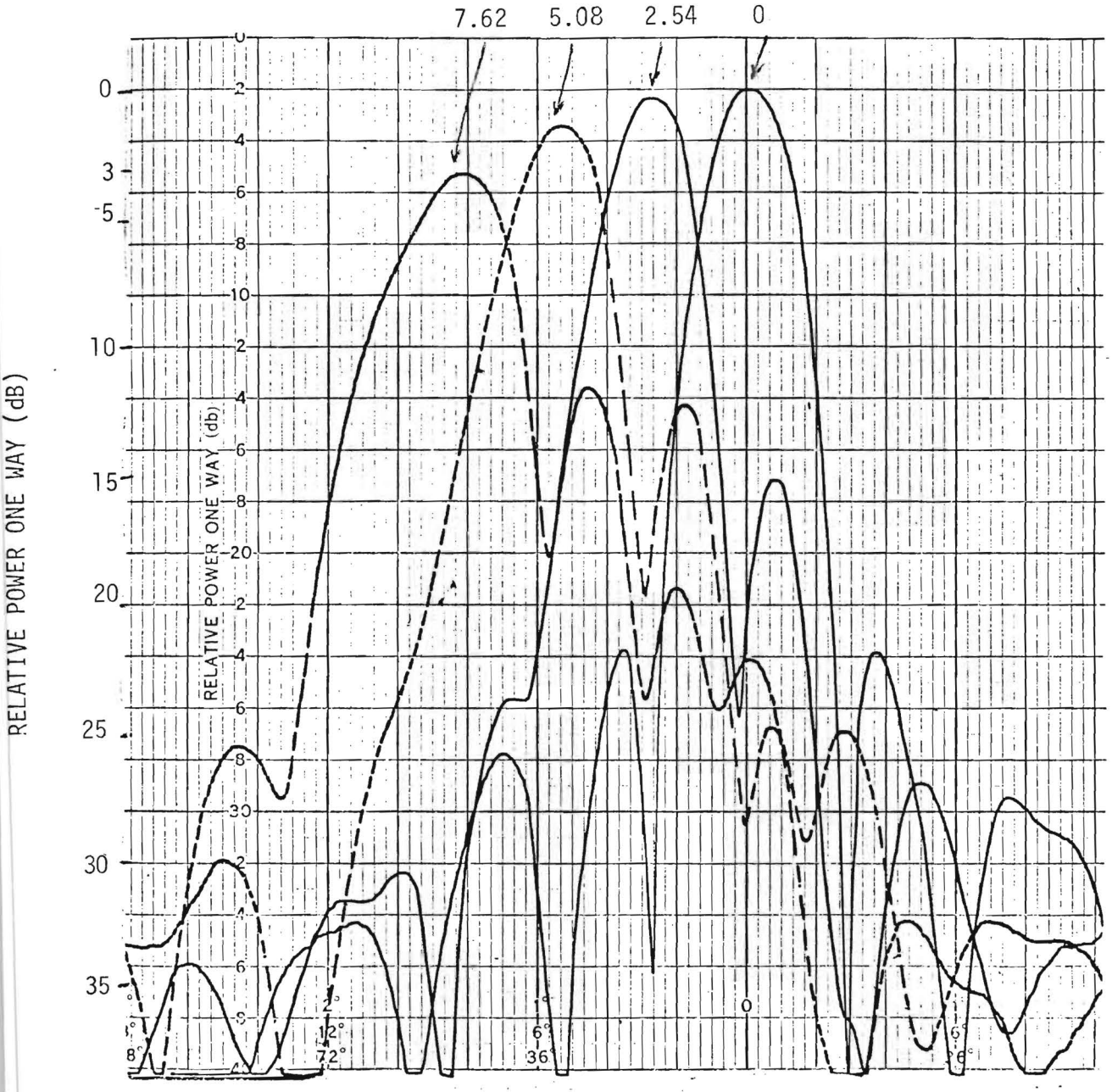

Figure 3-7. Measured E-plane pattern for subreflector translated 0.0, 2.54, 5.08, 7.62 mm. Frequency 94.58 GHz.

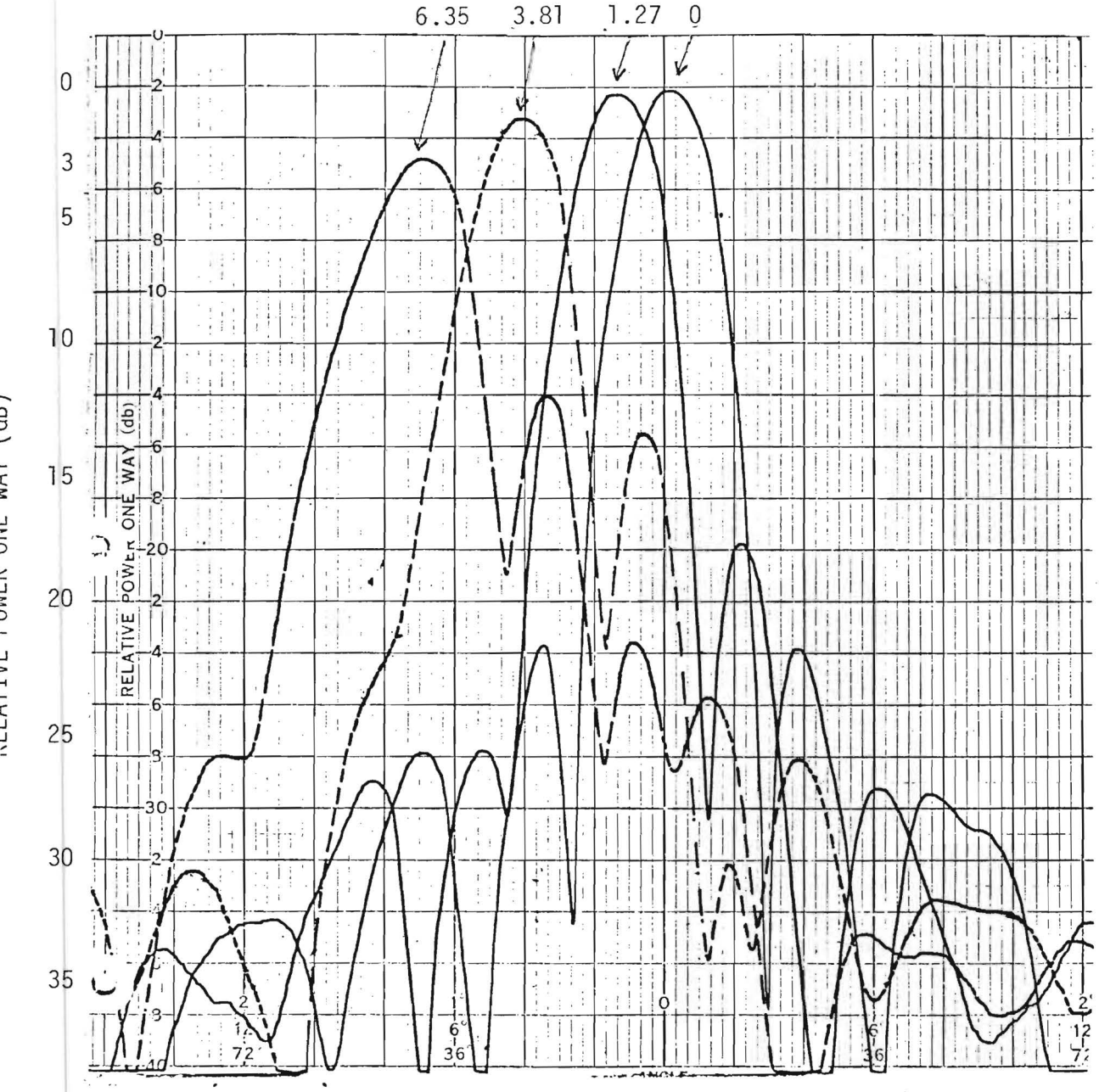

Figure 3-8. Measured E-plane pattern for subreflector translated 0.0, 1.27, 3.81, 6.35 mm. Frequency 94.58 GHz.

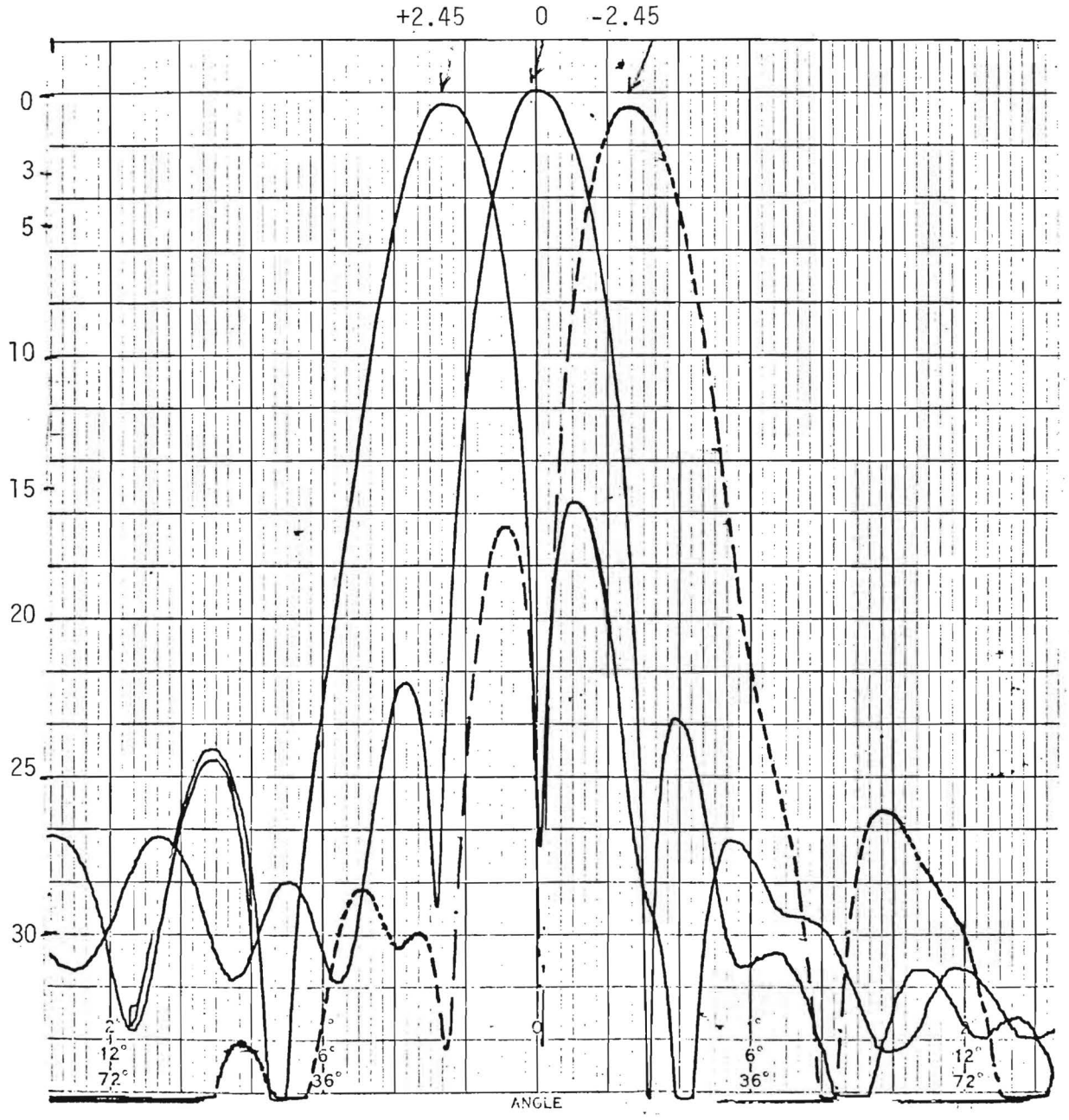

Figure 3-9. Measured E-plane symmetry pattern for subreflector translated +2.45, 0, -2.45 mm. Frequency is 93.51 GHz.

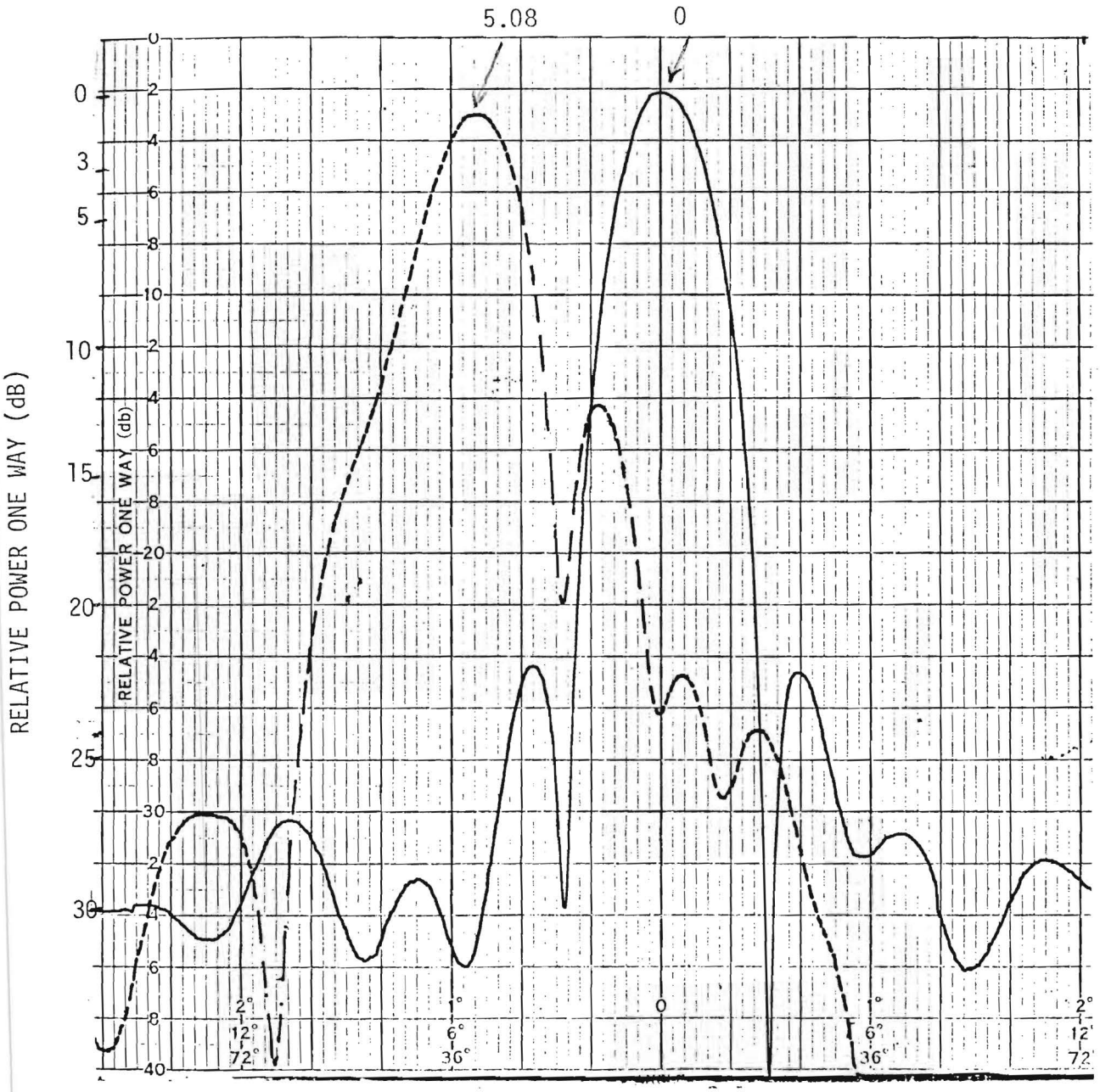

Figure 3-10 Measured E-plane pattern for subreflector translated 0 and 5.08 mm. Frequency 93.51 GHz.

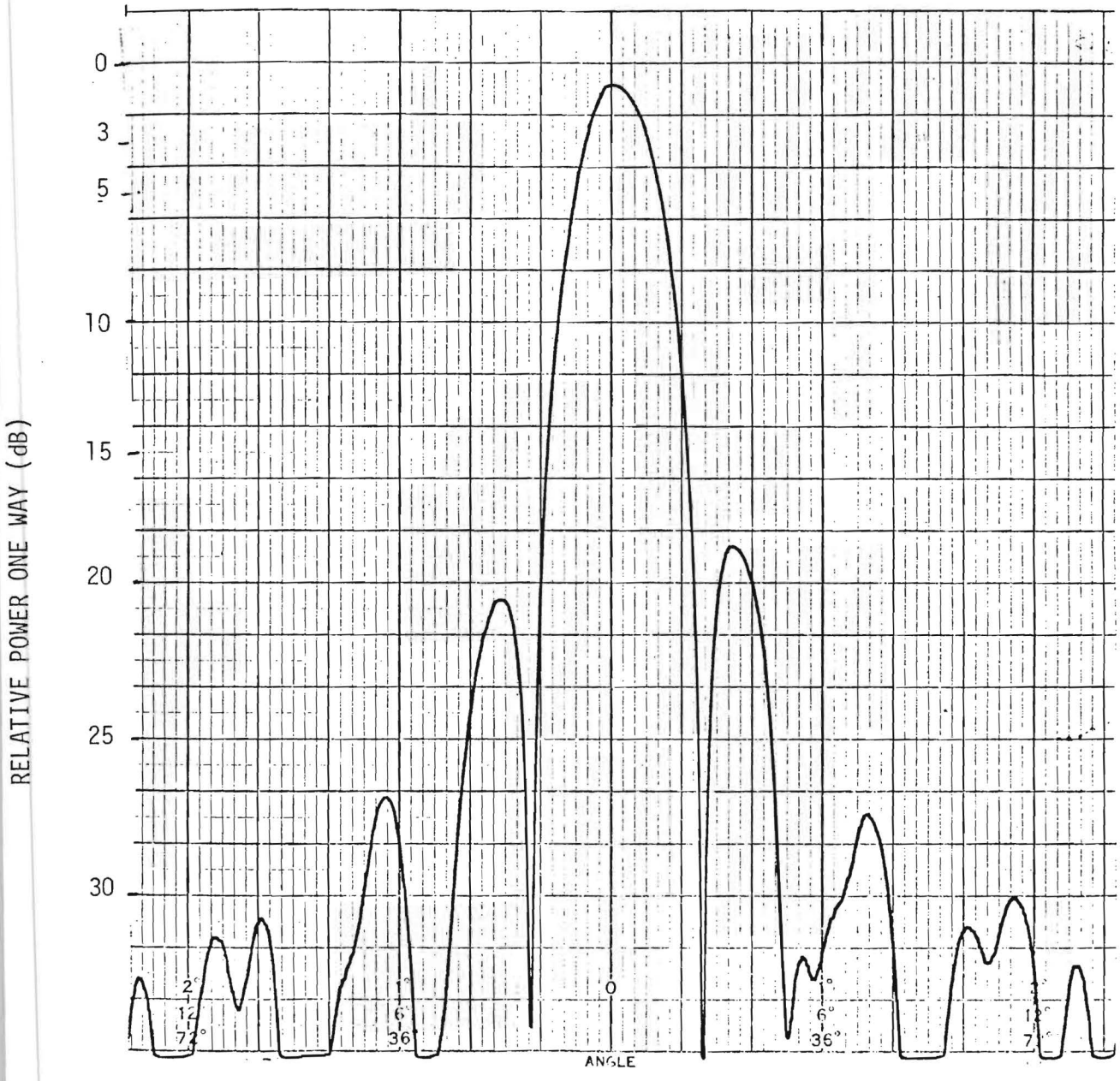

Figure 3-11. Measured H-plane pattern for subreflector translated 5.08 mm. Frequency is 93.51 GHz.

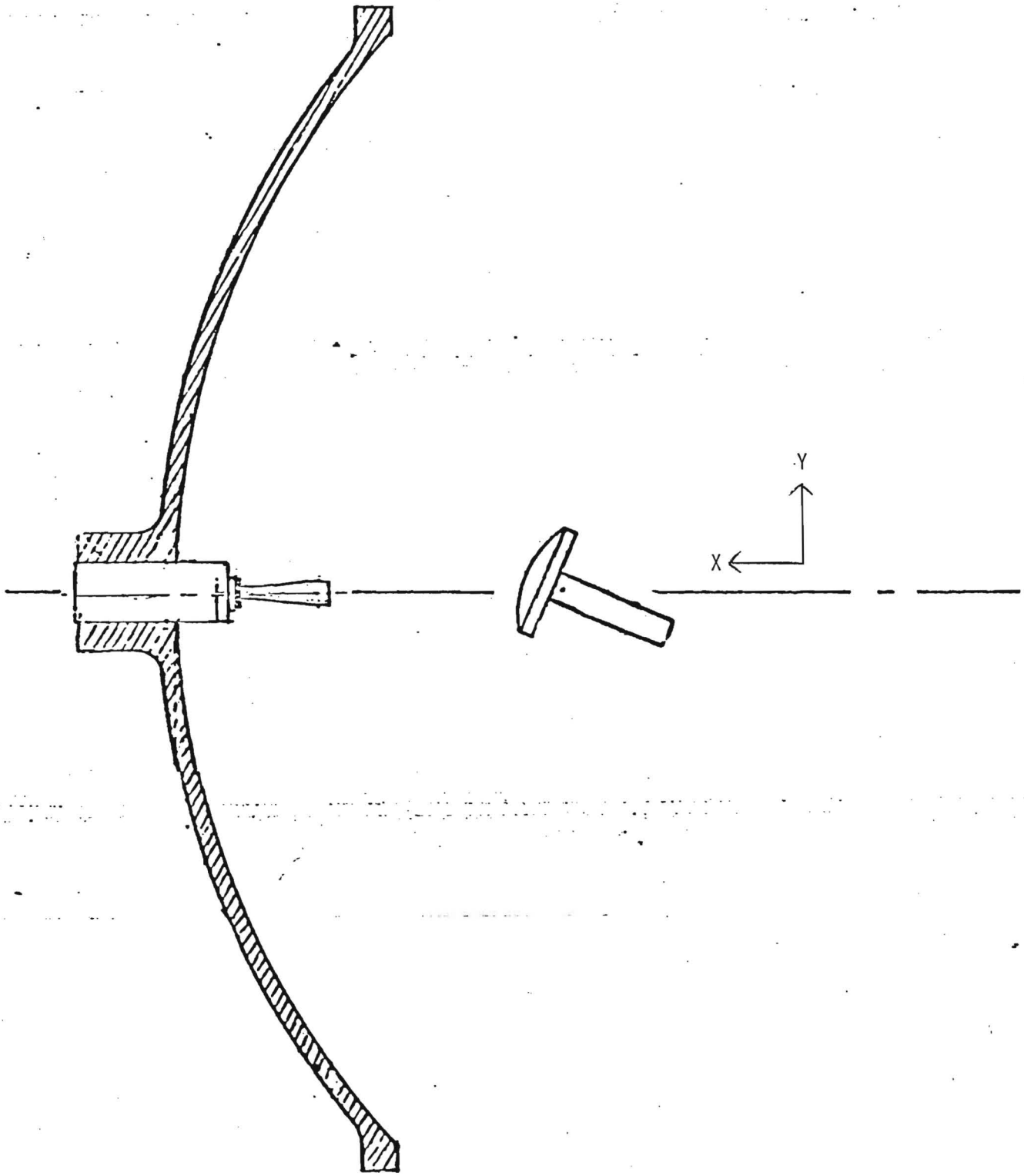

Figure 3-12. E-plane rotation of subreflector about antenna focus. (Top View)

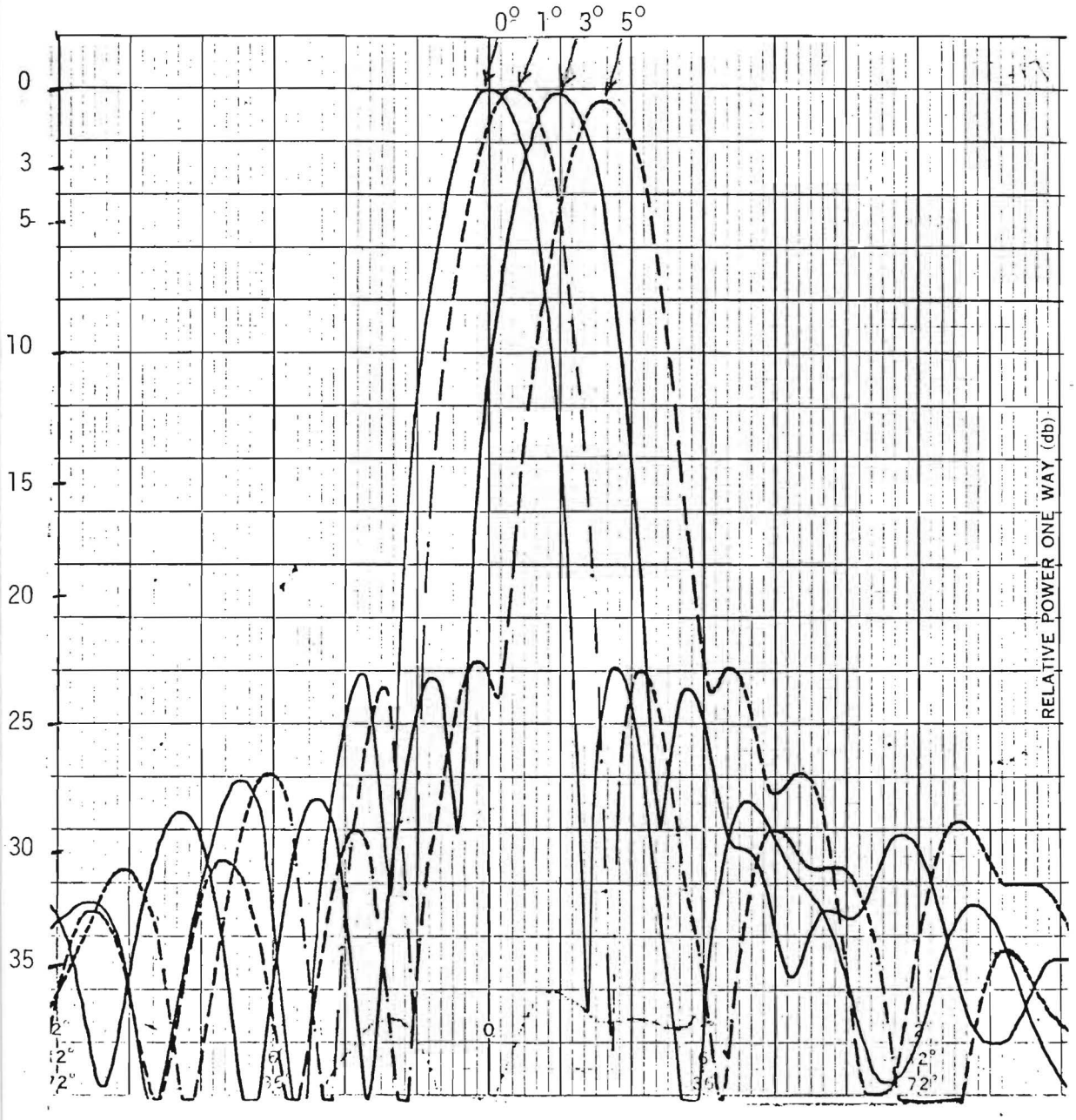

Figure 3-13. Measured E-plane pattern for subreflector rotated 0°, 1°, 3°, 5° about system focus. Frequency is 94.71 GHz.

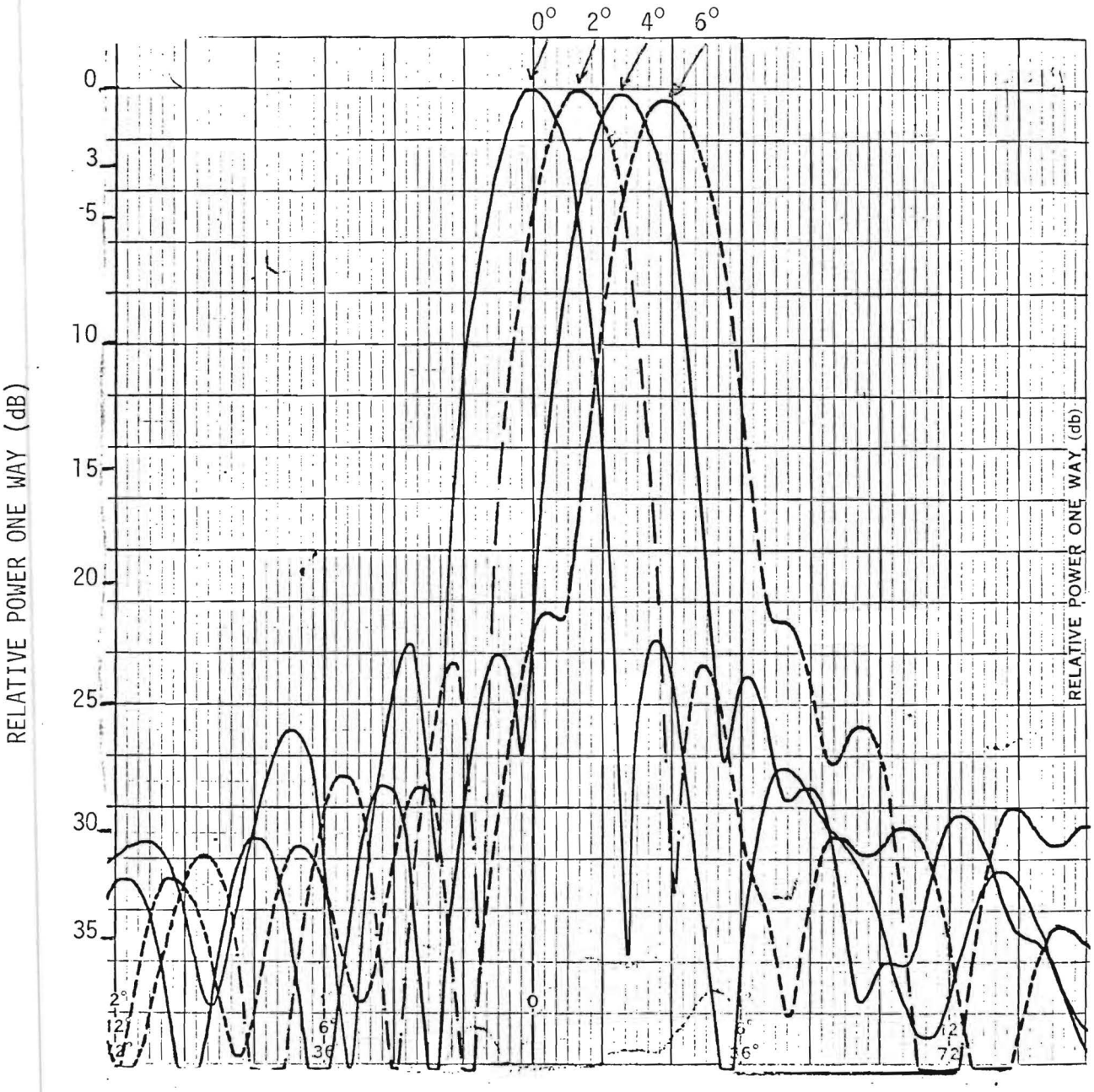

Figure 3-14. Measured E-plane pattern for subreflector rotated 0°, 2°, 4°, 6° about system focus. Frequency is 94.71 GHz.

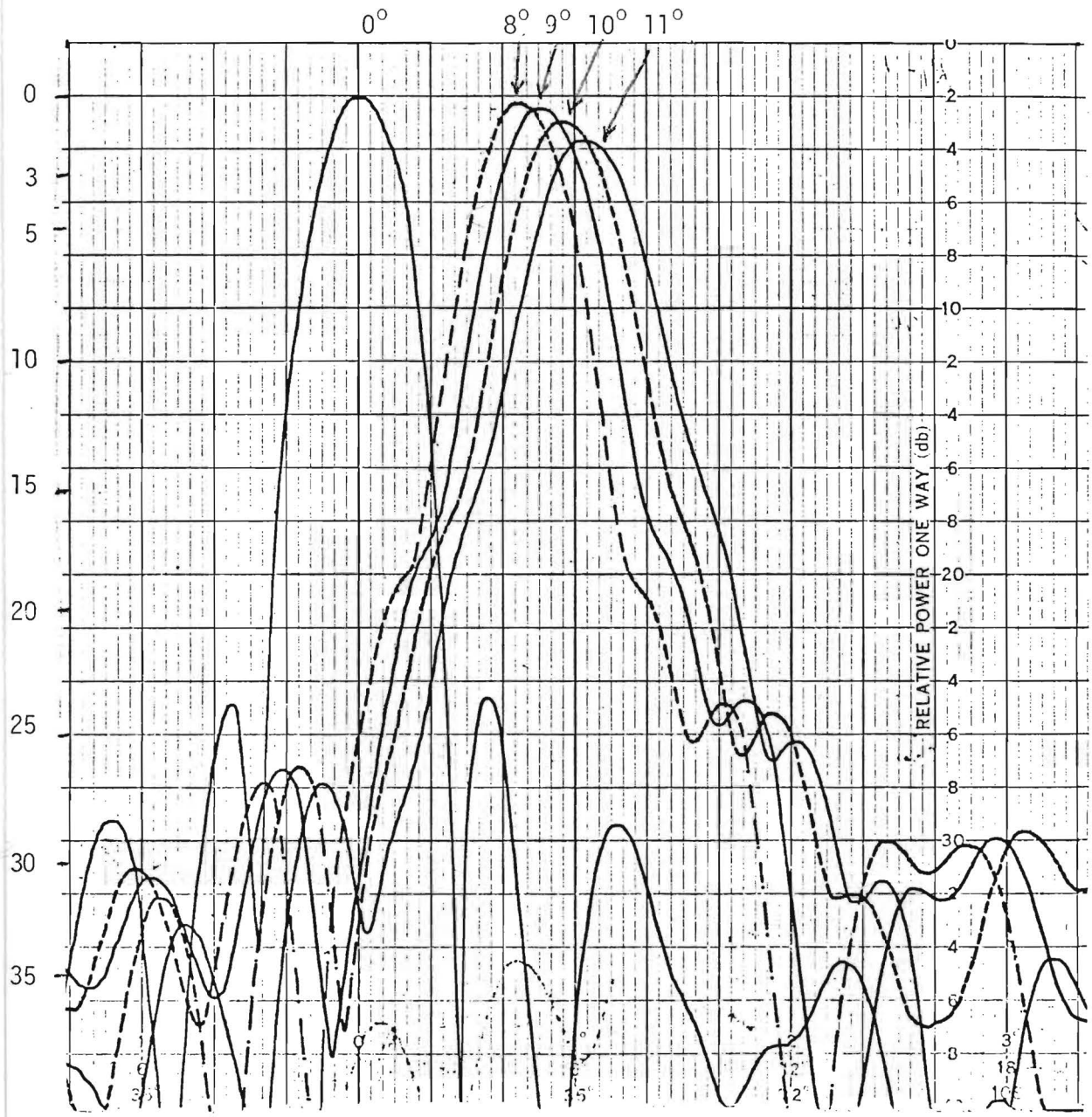

Figure 3-15. Measured E-plane pattern for subreflector rotated 0°, 8°, 9°, 10°, 11° about system focus. Frequency is 94.71 GHz.

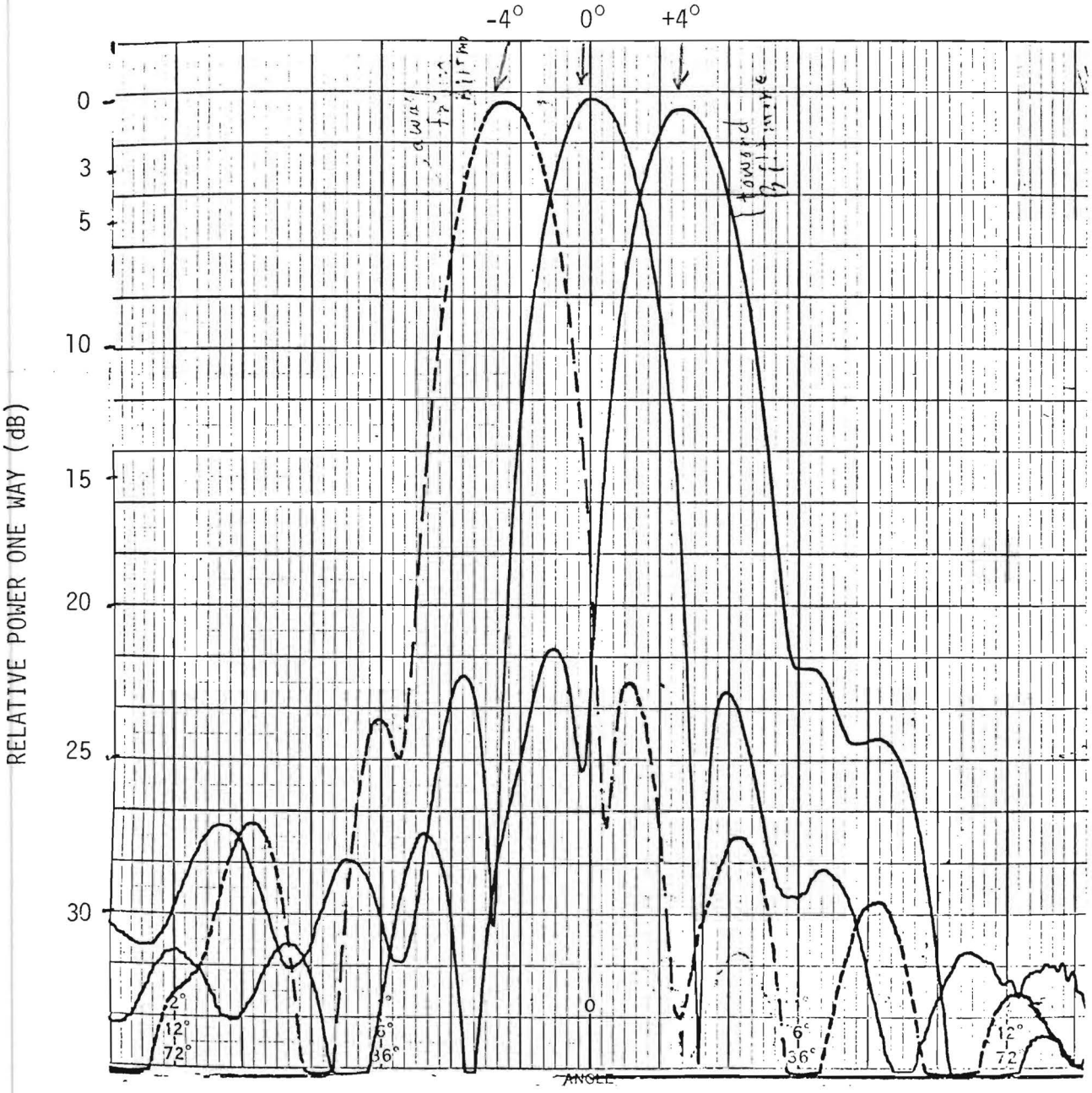

Figure 3-16. Measured E-plane symmetry pattern for subreflector rotated +4°, 0°, -4° about system focus. Frequency is 93.51 GHz.

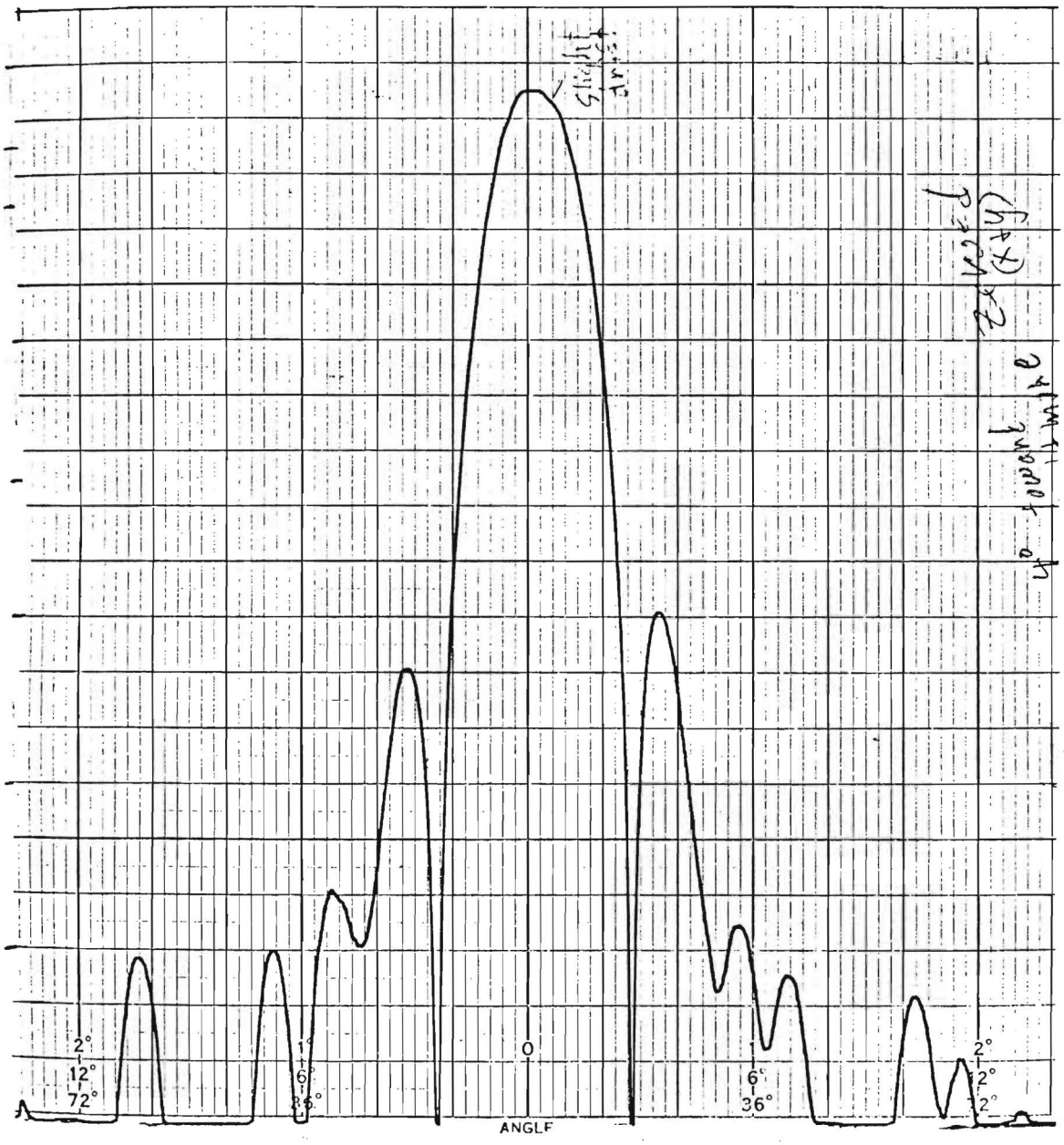

Figure 3-17. Measure H-plane pattern for subreflector rotated 4° about system focus. Frequency is 93.51 GHz.

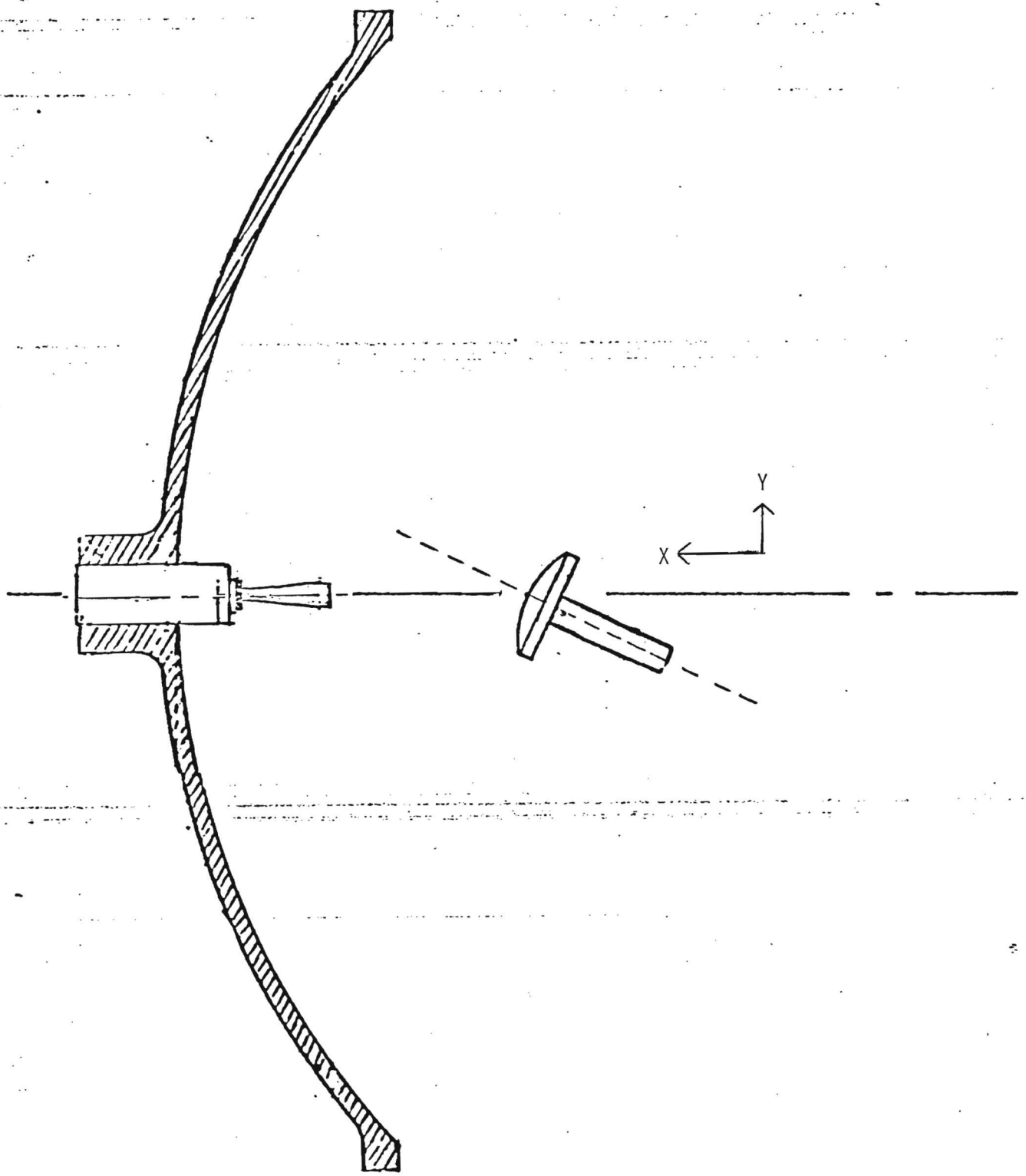

Figure 3-18. Rotation of subreflector about subreflector vertex. (Top View)

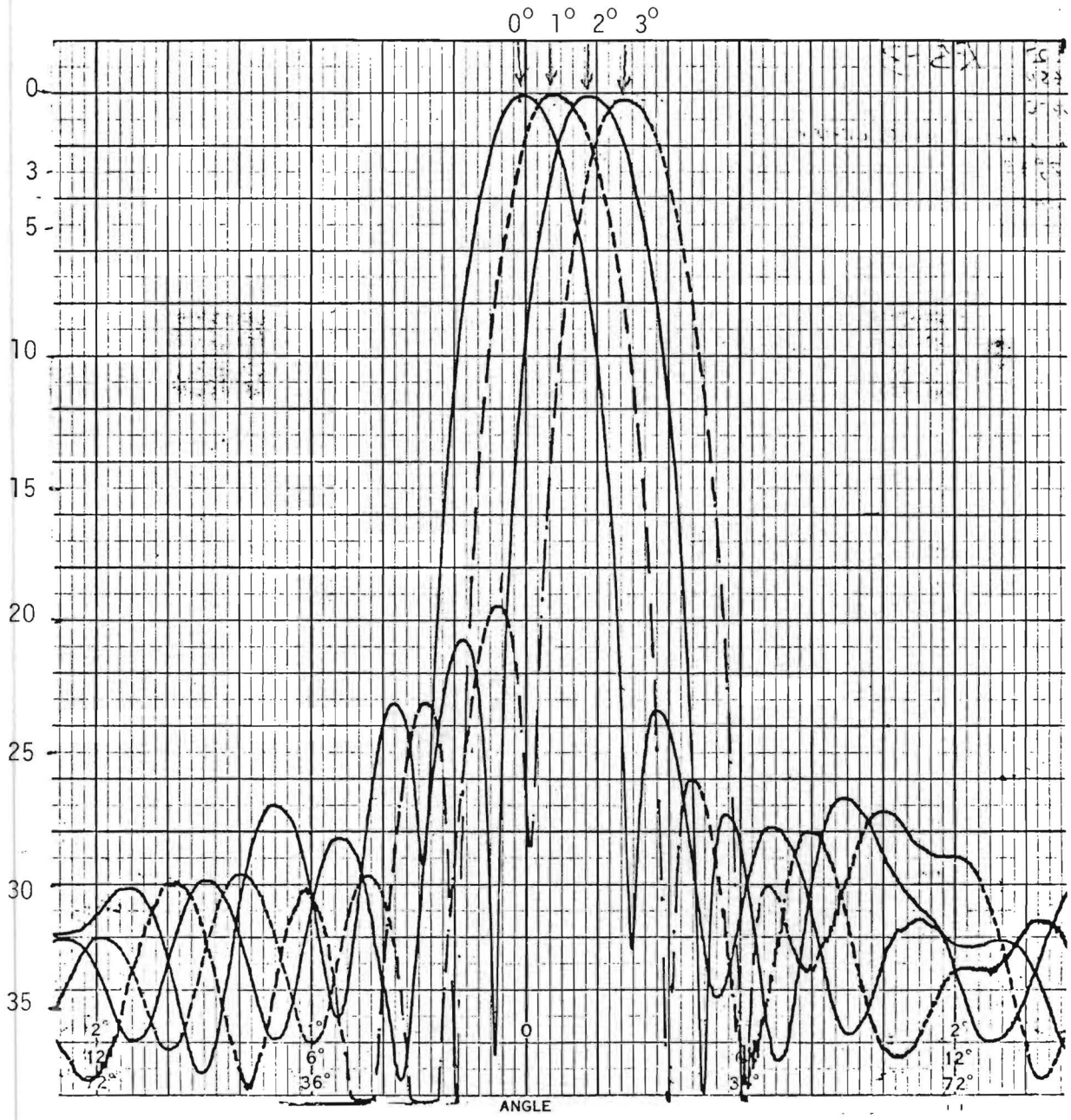

Figure 3-19. Measured E-plane pattern for subreflector rotated 0°, 1°, 2°, 3°, about subreflector vertex. Frequency is 93.27 GHz.

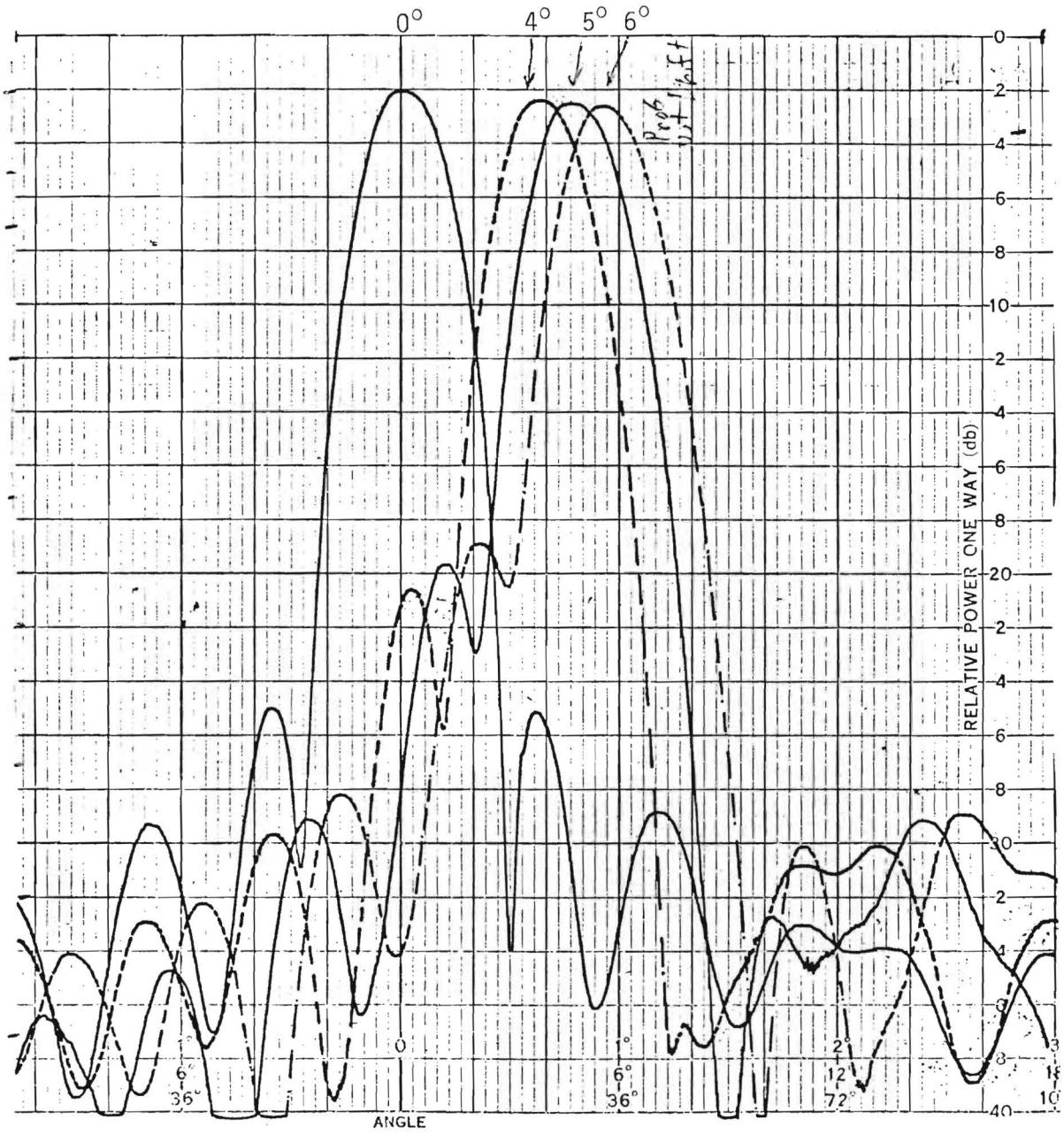

Figure 3-20. Measured E-plane pattern for subreflector rotated 0°,4°,5°,6° about subreflector vertex. Frequency is 93.27 GHz.

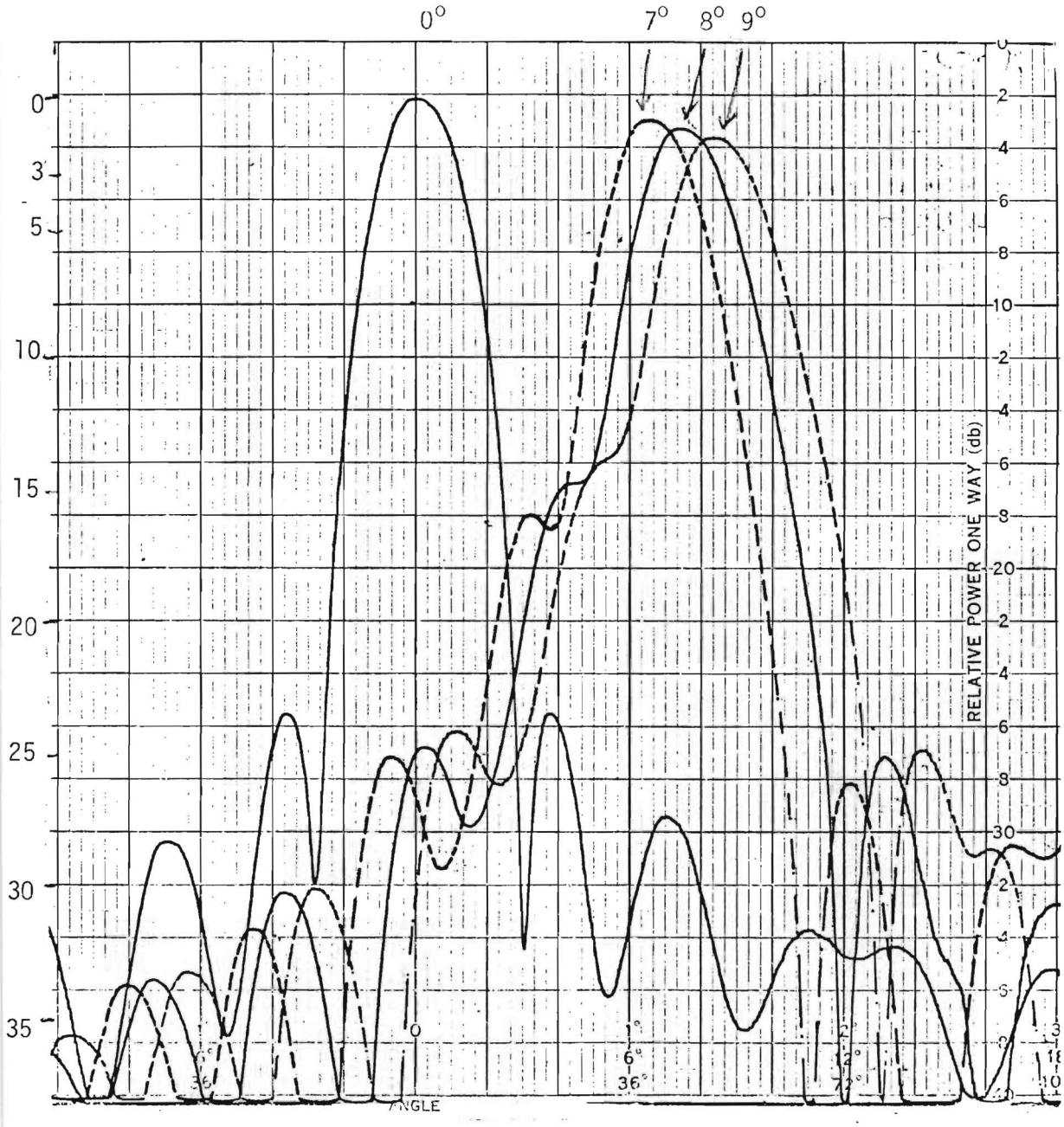

Figure 3-21. Measured E-plane pattern for subreflector rotated 0, 7, 8, 9° about subreflector vertex. Frequency is 93.27 GHz.

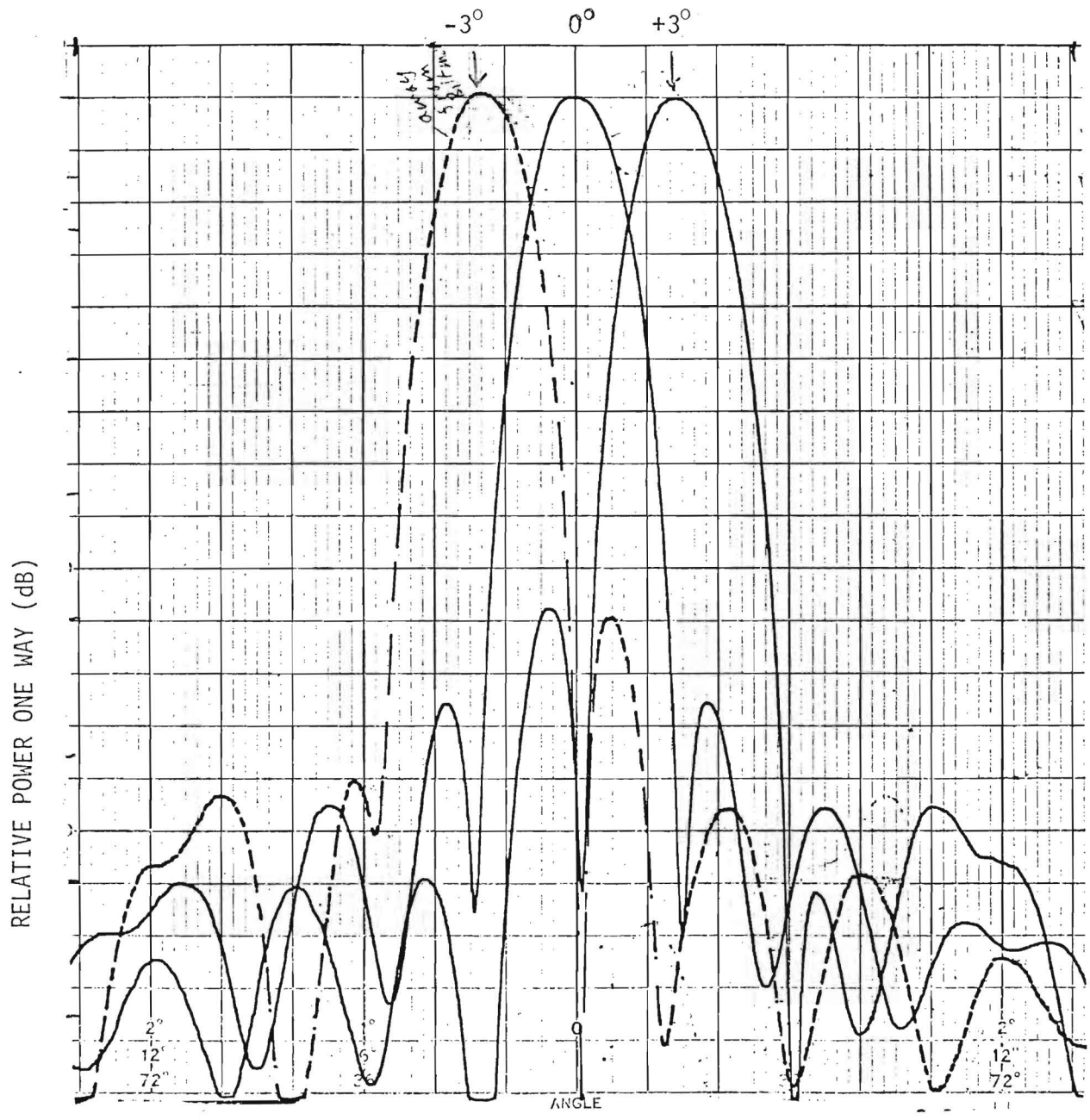

Figure 3-22. Measured E-plane symmetry pattern for subreflector rotated +3°, 0°-3° about subreflector vertex. Frequency is 93.27 GHz.

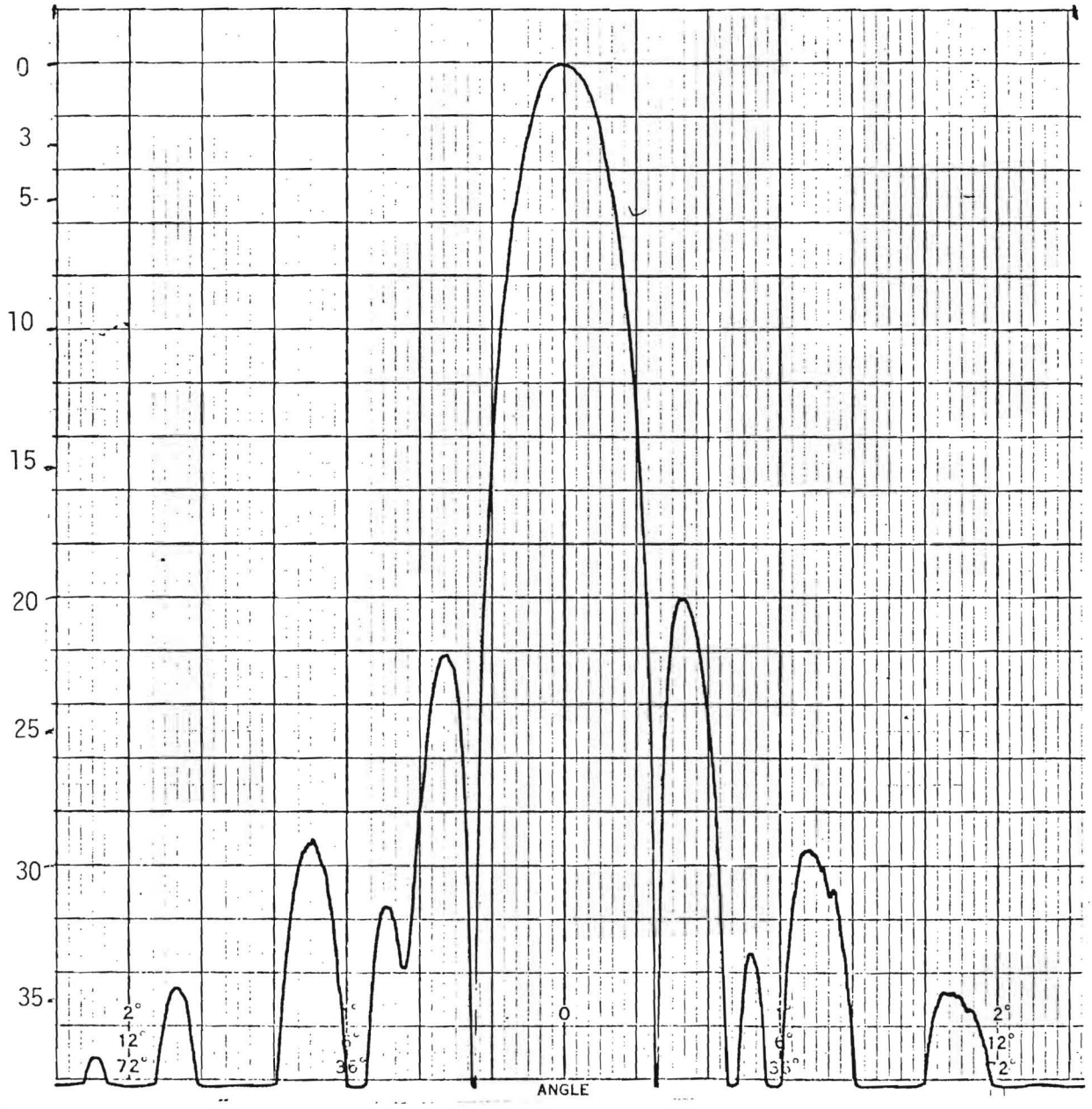

Figure 3-23. Measured H-plane pattern for subreflector rotated 3° about subreflector vertex. Frequency is 93.27 GHz.

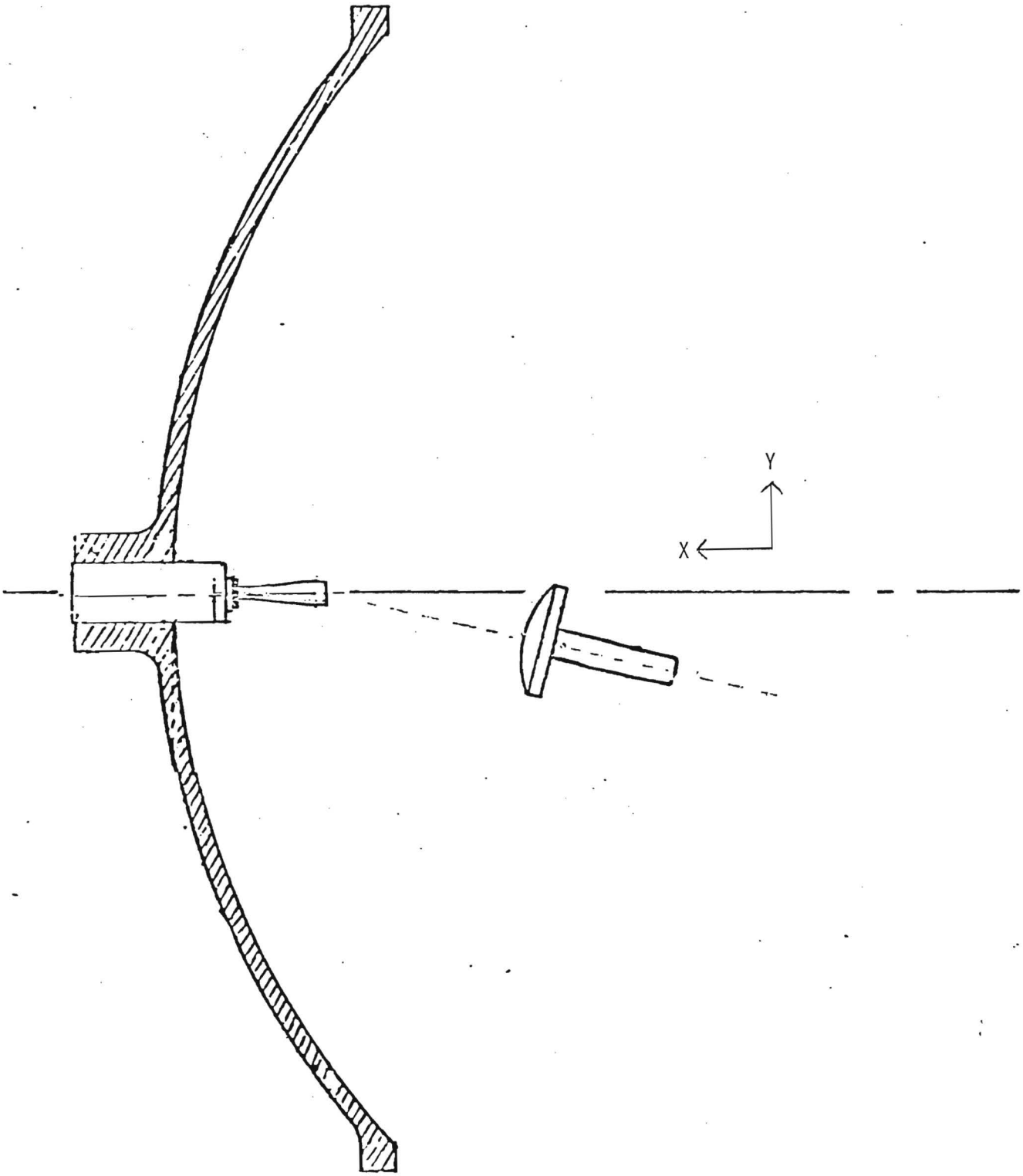

Figure 3-24. Rotation of subreflector about translated subreflector focus. (Top View)

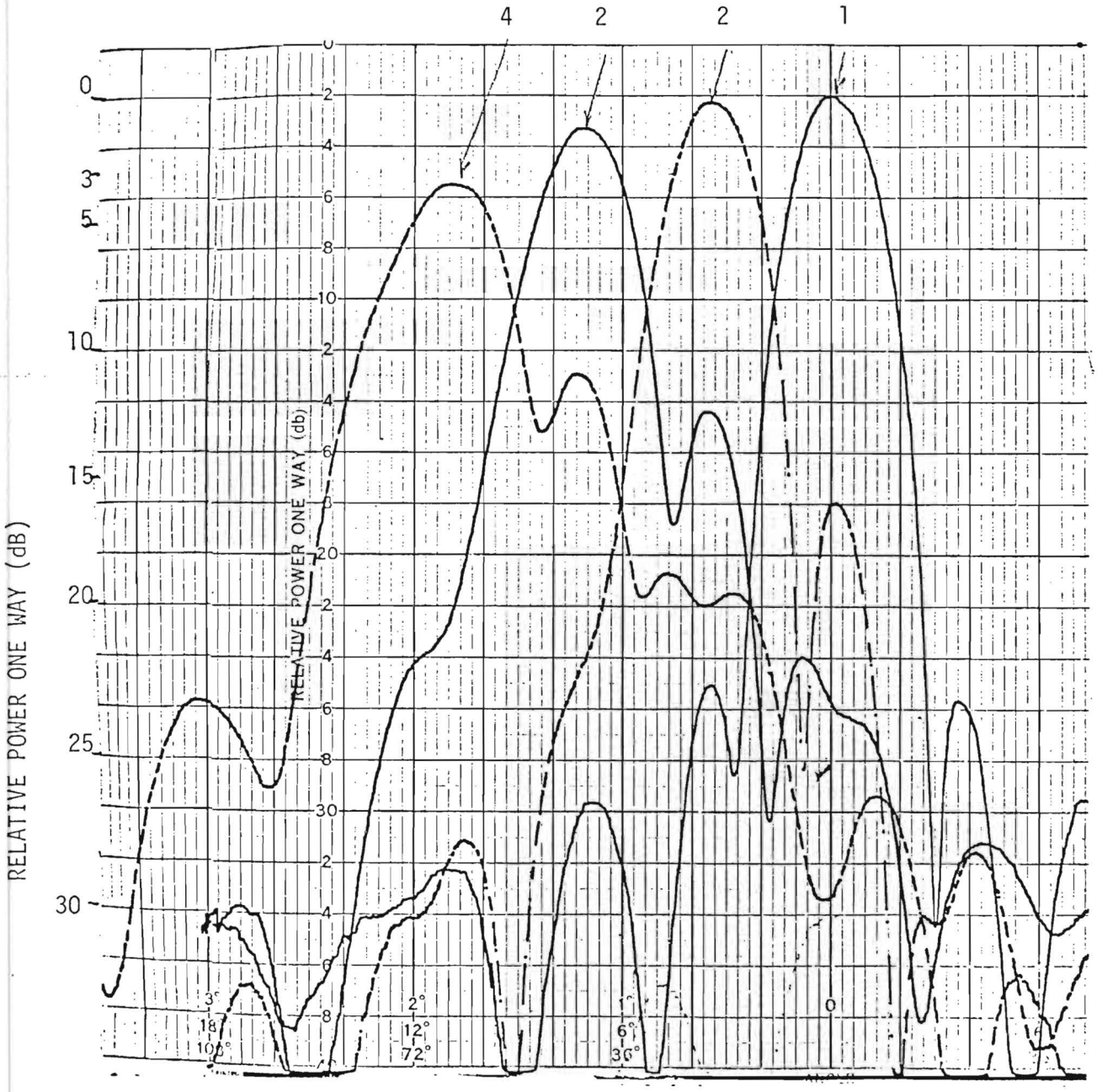

Figure 3-25. Measured E-plane pattern for subreflector translated and rotated toward feed. Frequency is 93.25 GHz.

1.	0	0^{o}
2.	2.54 mm	1.31^{o}
3.	5.08 mm	2.62^{o}
4.	7.62 mm	3.93^{o}

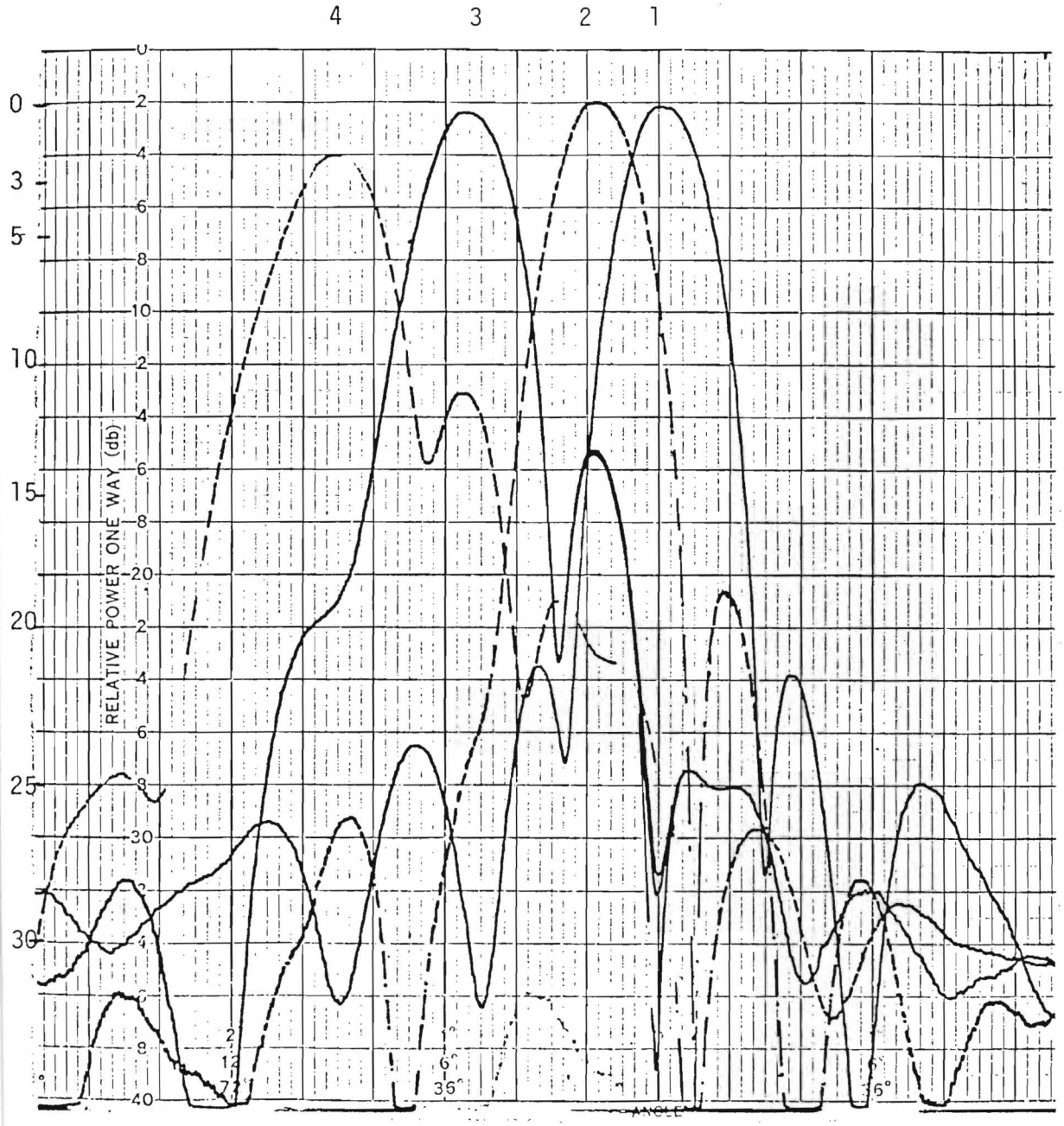

Figure 3-26. Measured E-plane pattern for subreflector translated and rotated toward feed. Frequency is 93.25 GHz.

1.	0	0°
2.	1.27 mm	$.66^{\circ}$
3.	3.81 mm	1.97°
4.	6.35 mm	3.28°

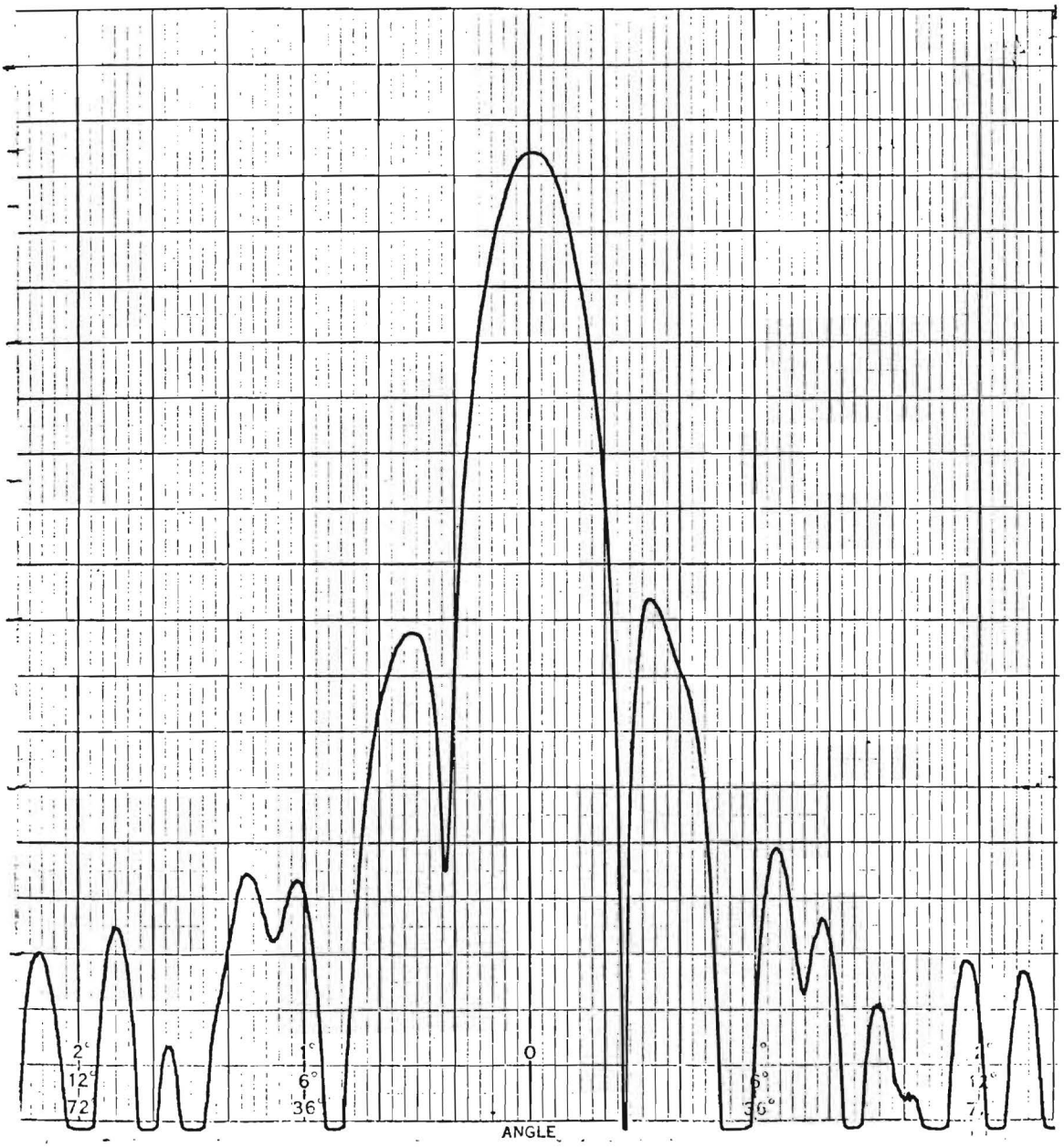

Figure 3-27. Measured H-plane pattern for subreflector translated 7.62 mm and rotated 3.93° toward feed. Frequency is 93.25 GHz.

TABLE 3-1

ROTATION OF SUBREFLECTOR

Angle rotated about focus(deg)	Scan angle(deg)	Scan angle per degree rotation	Side lobe level(dB)	-3dB Beam width(deg)
1	0.11	0.11	22.5	0.36
2	0.21	0.10	22.4	0.35
3	0.31	0.10	22.1	0.36
4	0.42	0.10	21.9	0.36
5	0.53	0.11	21.2	0.36
6	0.62	0.10	coma lobe	0.39
8	0.73	0.09	coma lobe	0.39
9	0.83	0.09	coma lobe	0.40
10	0.94	0.09	coma lobe	0.42
11	1.09	0.09	coma lobe	0.44

Angle rotated about vertex(deg)	Scan angle(deg)	Scan angle per degree rotation	Side lobe level(dB)	-3dB Beam width(deg)
1	0.15	0.15	23.0	0.36
2	0.30	0.15	20.8	0.39
3	0.47	0.16	19.5	0.39
4	0.64	0.16	18.0	0.39
5	0.78	0.16	17.0	0.39
6	0.92	0.15	16.3	0.39
7	1.11	0.16	coma lobe	0.39
8	1.25	0.16	coma lobe	0.42
9	1.39	0.15	coma lobe	0.44

TABLE 3-1 (cont.)

ROTATION AND TRANSLATION OF SUBREFLECTOR

Degrees rotated	mm translated	Scan angle(deg)	Scan angle per mm	Side lobe level(dB)	-3dB Beam width(deg)
0.66	1.27	0.28	0.22	-18.5	0.37
1.31	2.54	0.56	0.22	-16.0	0.39
1.97	3.81	0.89	0.23	-13.0	0.40
2.62	5.08	1.17	0.23	-11.0	0.43
3.28	6.35	1.50	0.24	-09.0	0.47
3.93	7.62	1.80	0.24	-07.5	0.54

TRANSLATION OF SUBREFLECTOR

mm translated	Scan angle(deg)	Scan angle per mm	Side lobe level(dB)	-3dB Beam width(deg)
1.27	0.22	0.17	-17.5	0.35
2.54	0.44	0.17	-14.5	0.36
3.81	0.69	0.18	-12.5	0.39
5.08	0.89	0.17	-10.5	0.40
6.35	1.14	0.18	-09.0	0.43
7.62	1.33	0.17	-08.5	0.50

3.1.2 Feed Reorientation Experiment

E-plane translation and rotation of the antenna feed was accomplished using the modified form of the TRG antenna illustrated in Figure 3-28 (see also Figures 3-29 and 3-30). The subreflector was held in place by its TRG strut mount while the TRG cylindrical feed mount was replaced by a section of WR-10 wave-guide mounted in an L-shaped holder. This holder was in turn mounted to the translation-rotation mechanism used in the first part of the experiment. Feed translation and rotation were limited by the cylindrical feed mounting hole diameter. Translation was limited to approximately 9.25 mm. E-plane patterns corresponding to y axis feed translation are shown in Figure 3-31, and E-plane patterns corresponding to feed rotation about its phase center are shown in Figure 3-32.

A power level change was noted in Figure 3-32 for the 9.25^{o} rotation pattern. A scan angle of only 0.048 degrees/mm was observed for feed translation, and a scan angle of only 0.008 scan degree/rotation degree was observed for feed rotation.

3.2 Experimental Setup and Antenna Range

Figures 3-33 and 3-34 show respectively the transmit and receive stations of the Georgia Tech antenna range used in these experiments. A range length of approximately 1200 ft. easily satisfied far field requirements at 94 GHz for the antenna under test. A 12" aperture transmit antenna produced a 3 dB spot 18 ft. in diameter centered around the antenna under test. This resulted in an approximately flat amplitude taper across the aperture of the antenna under test.

The transmit system is illustrated by Figure 3-35 and is shown pictorially in Figures 3-36 and 3-37. The transmitter tube is an OKI type 90VII klystron with a power output of about 50 mW. The frequency was monitored by a W-band cavity wavemeter. The transmitting antenna is a TRG model W-822-12 Cassegrain. Antenna patterns are calibrated by means of a precision rotary vane attenuator placed in the antenna waveguide.

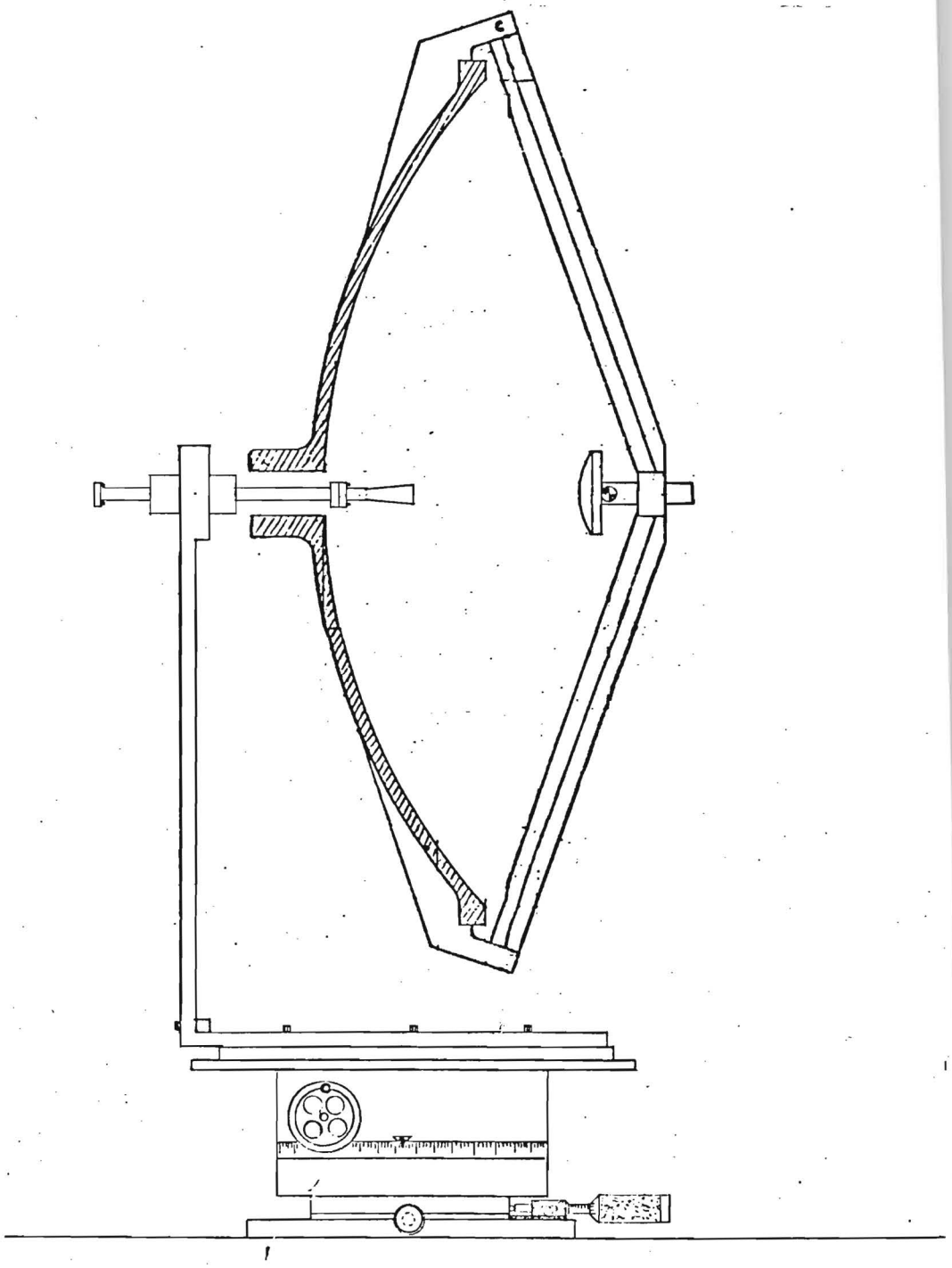

Figure 3-28. Modified Antenna (TRG) system for feed translation and rotation.

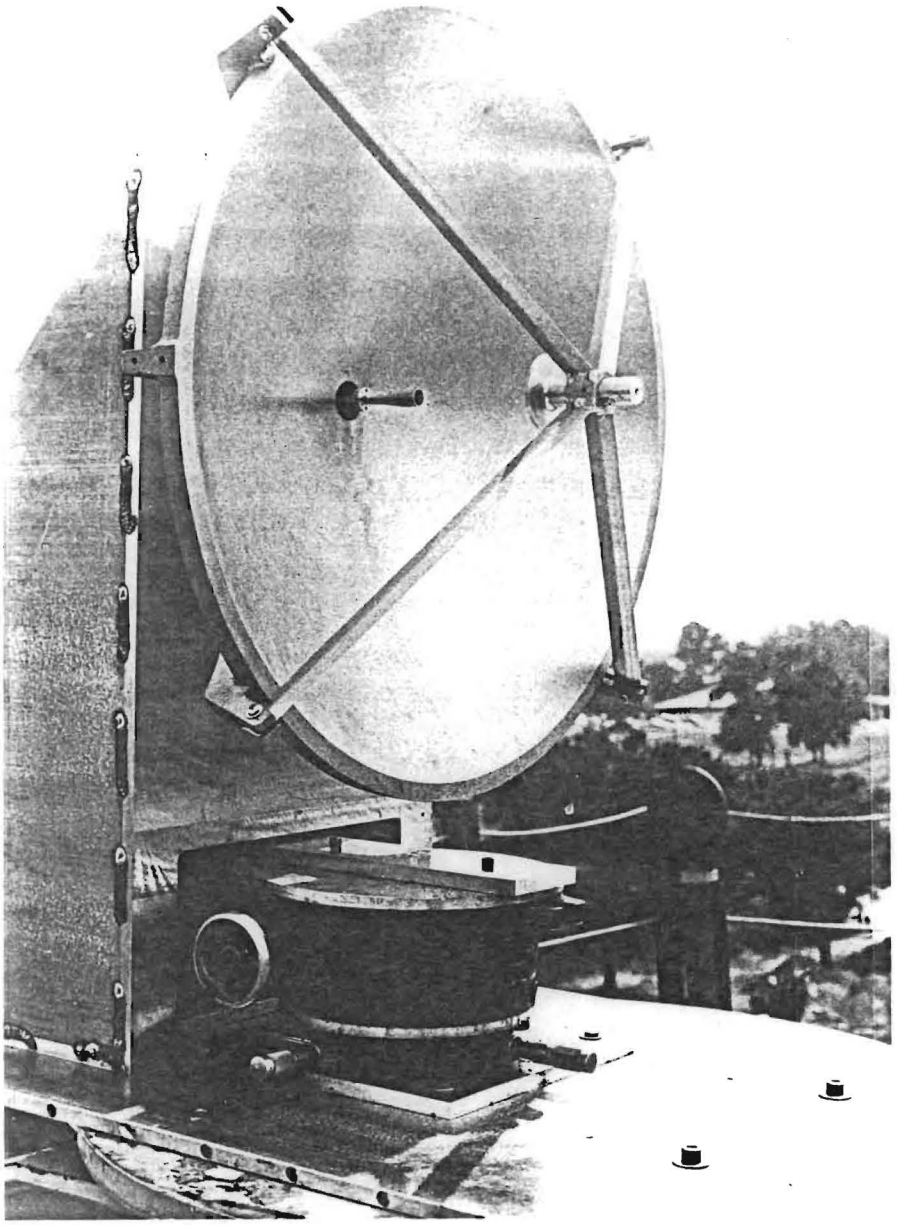

Figure 3-29. Photograph of antenna showing mechanism used for feed rotation and translation. (Front View).

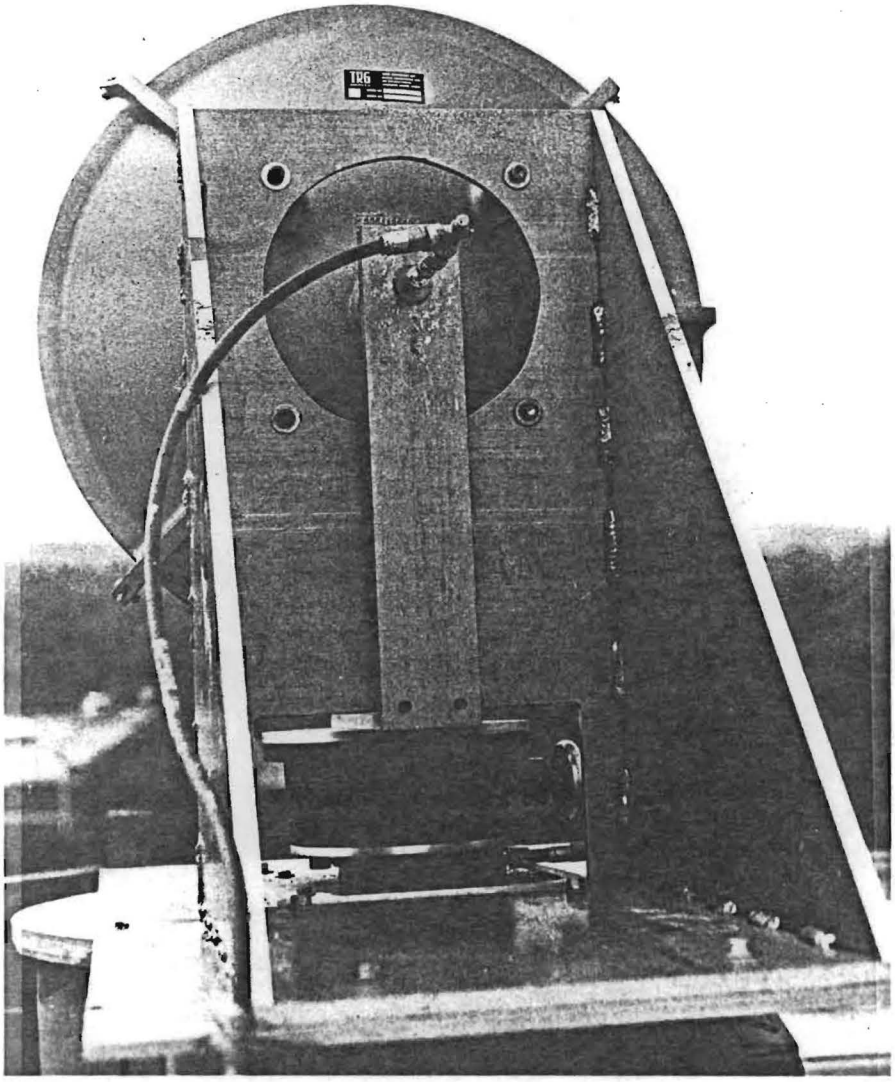

Figure 3-30. Photograph of antenna showing mechanism used for feed rotation and translation. (Rear View).

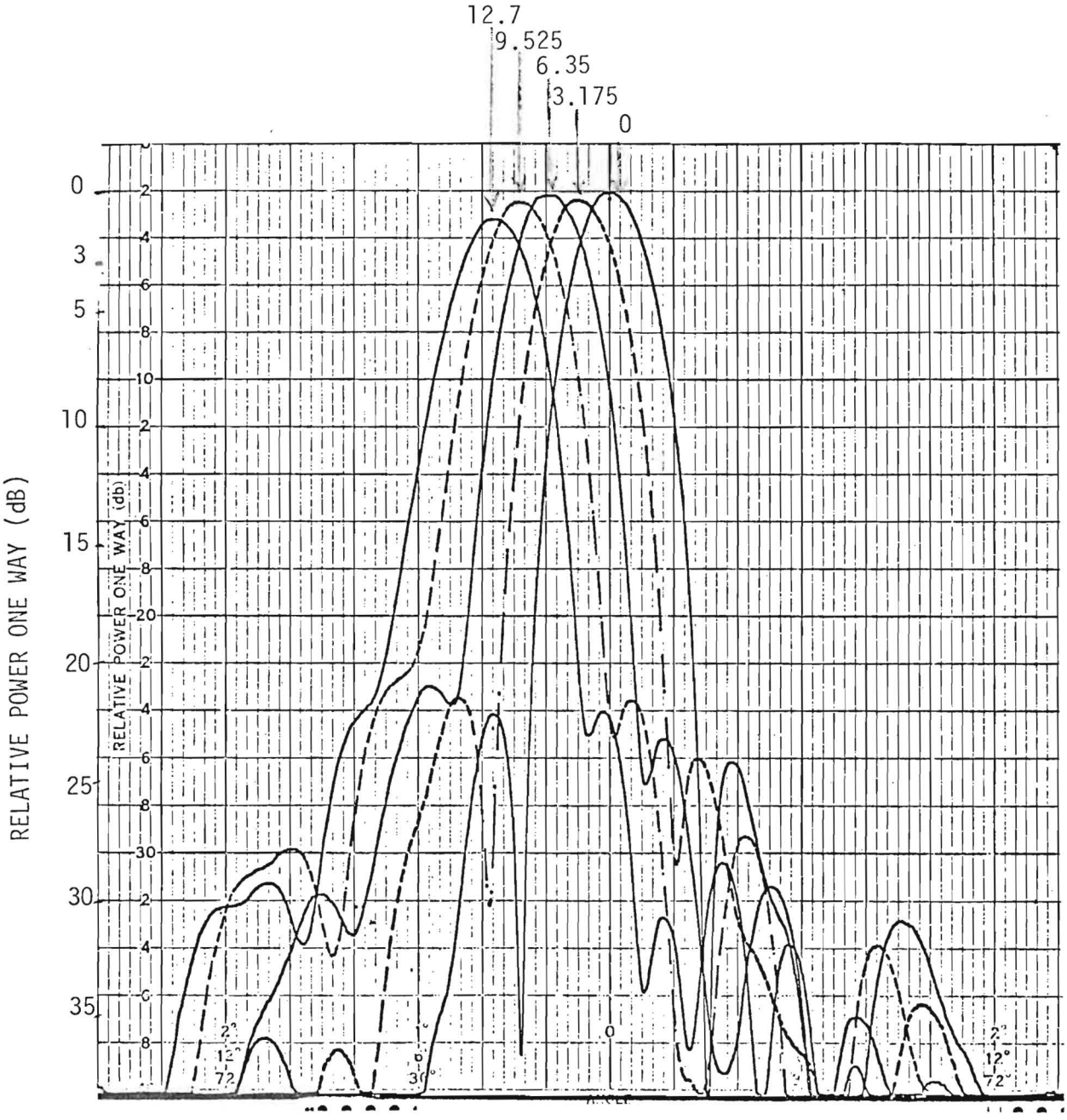

Figure 3-31. Measured E-plane pattern for feed translation of 0, 3.175, 6.35, 9.525, 12.7 mm. Frequency is 93.65 GHz.

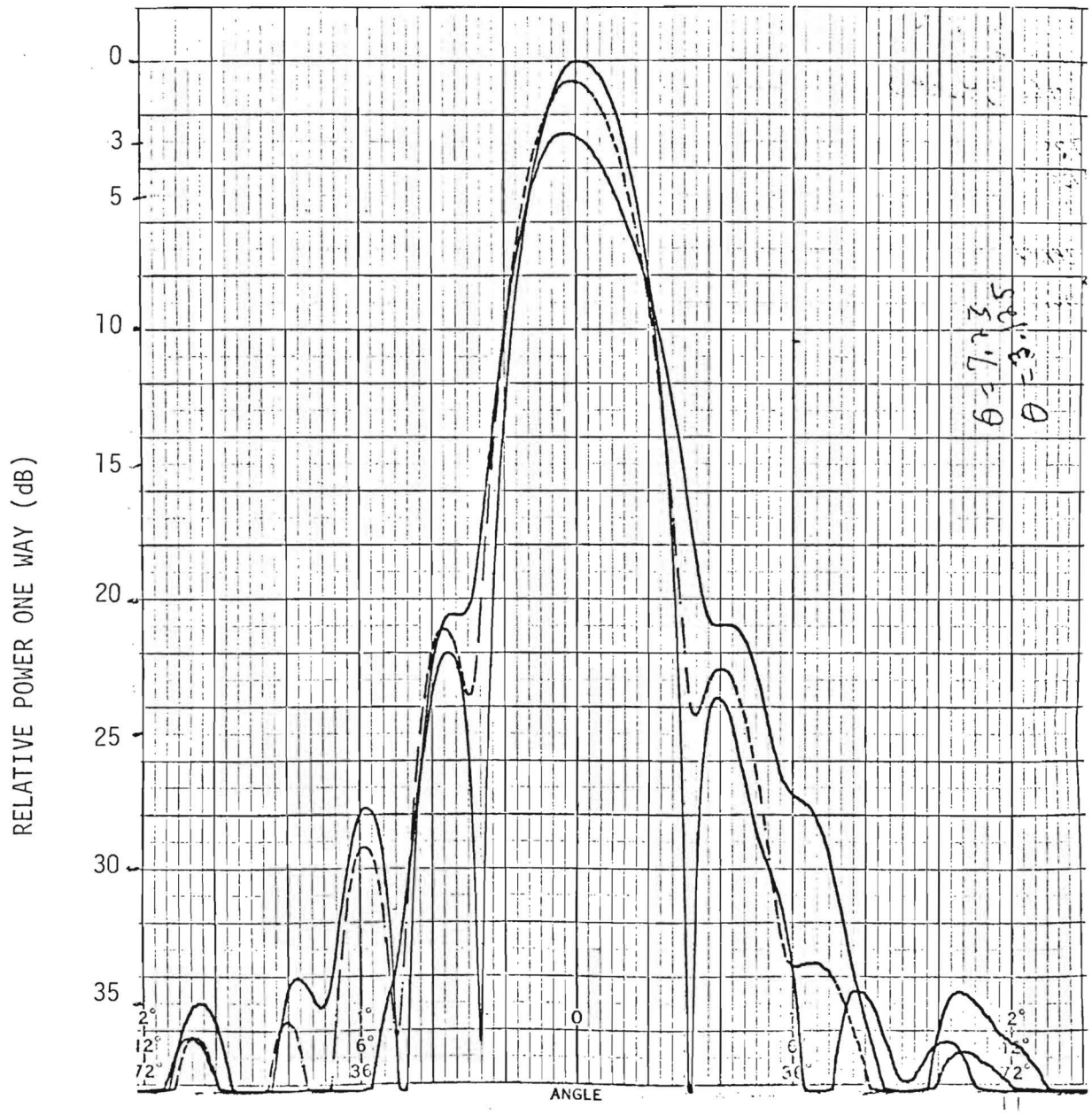

Figure 3-32. Measured E-plane pattern for feed rotated 0°, 4.625°, 9.25° about feed horn phase center. Frequency is 93.65 GHz.

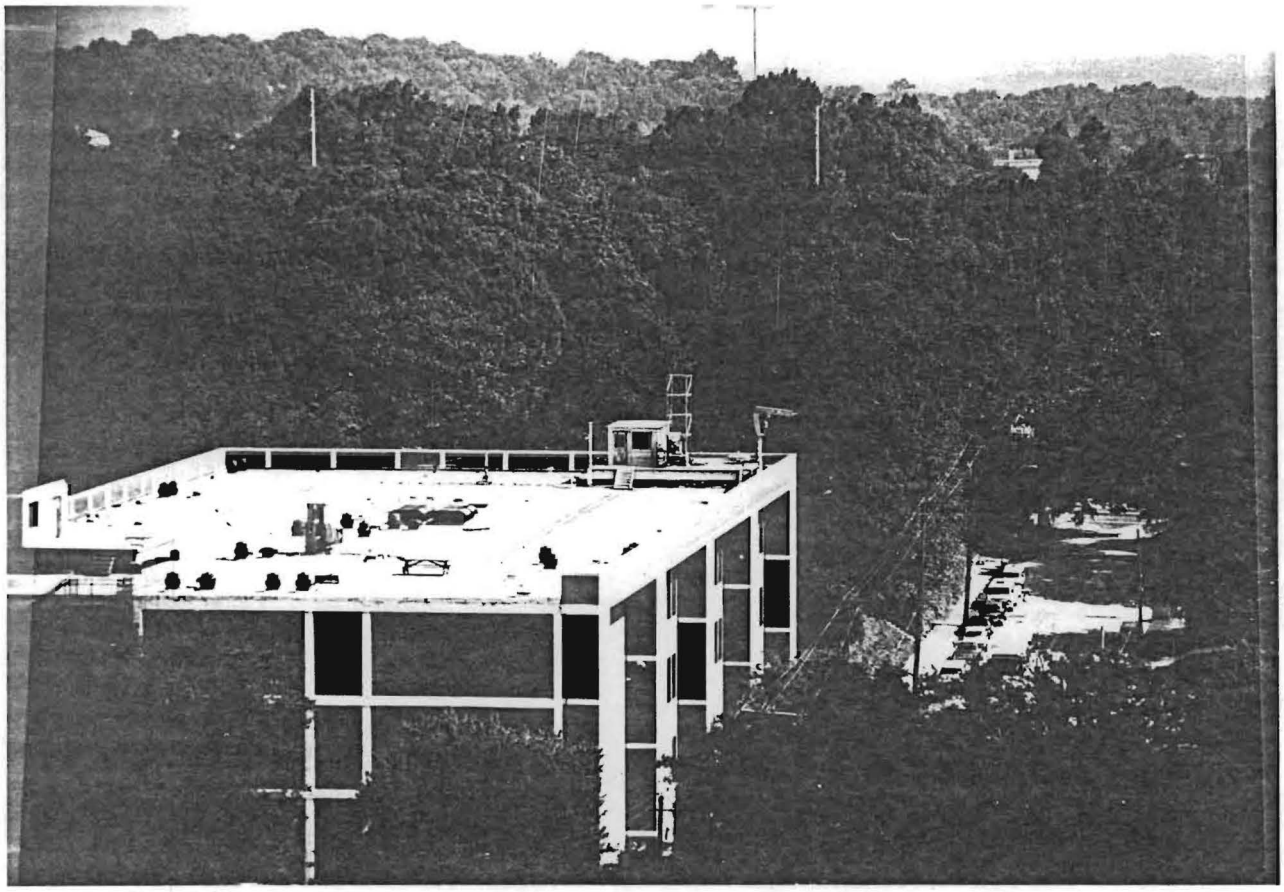

Figure 3-33. Photograph of antenna range transmit station viewed from the receive system.

Figure 3-34. Photograph of antenna range receive station as viewed from the transmit station.

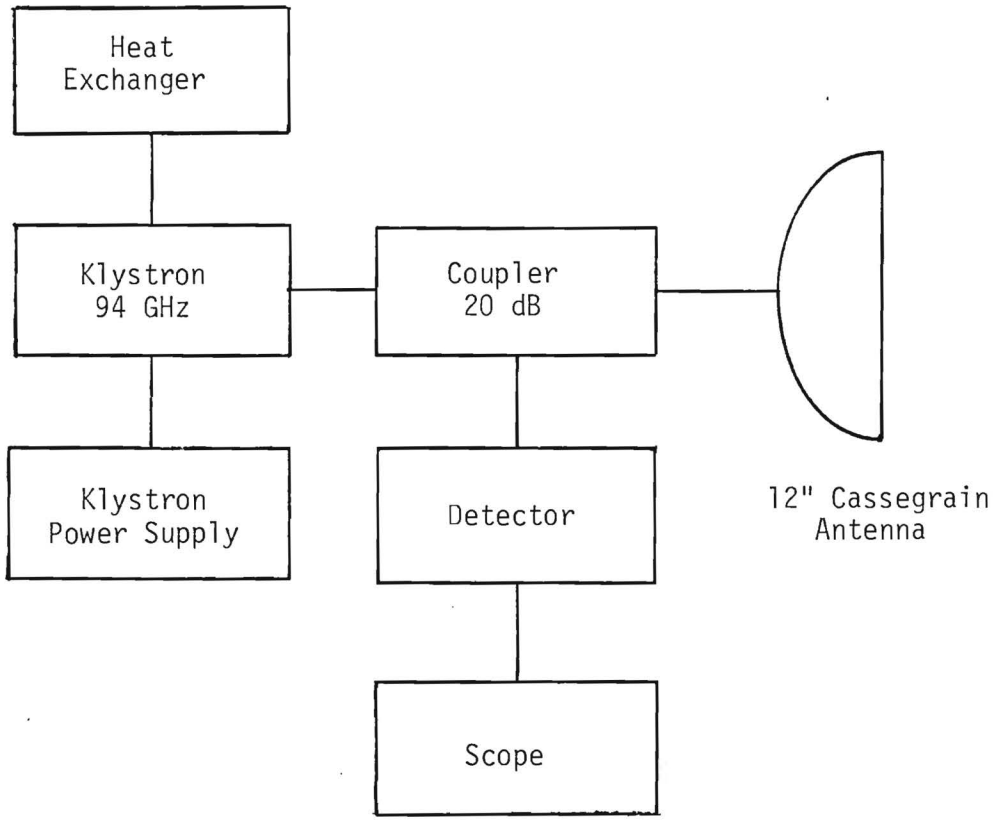

Figure 3-35. Transmit system.

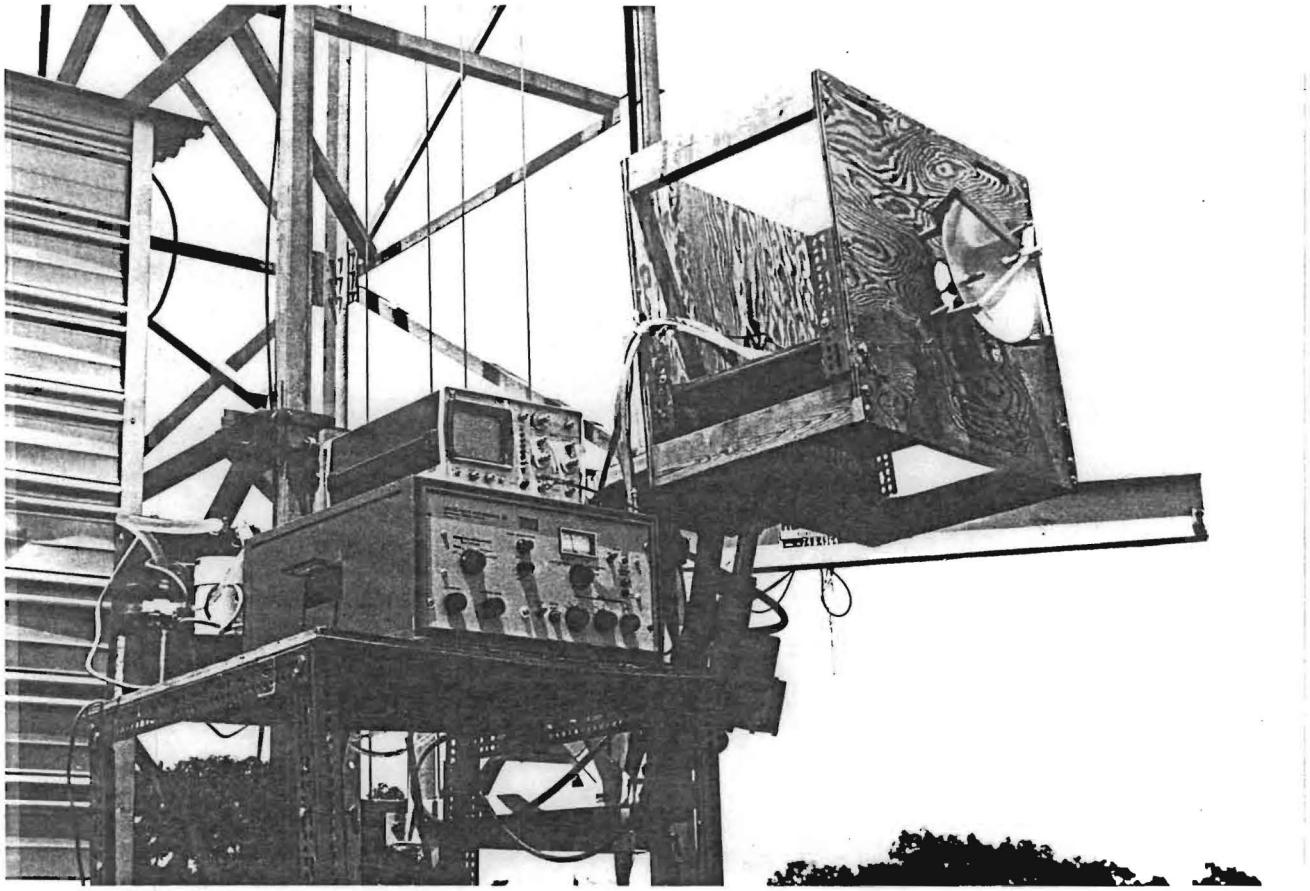

Figure 3-36. Photograph of transmit system.
(Near View)

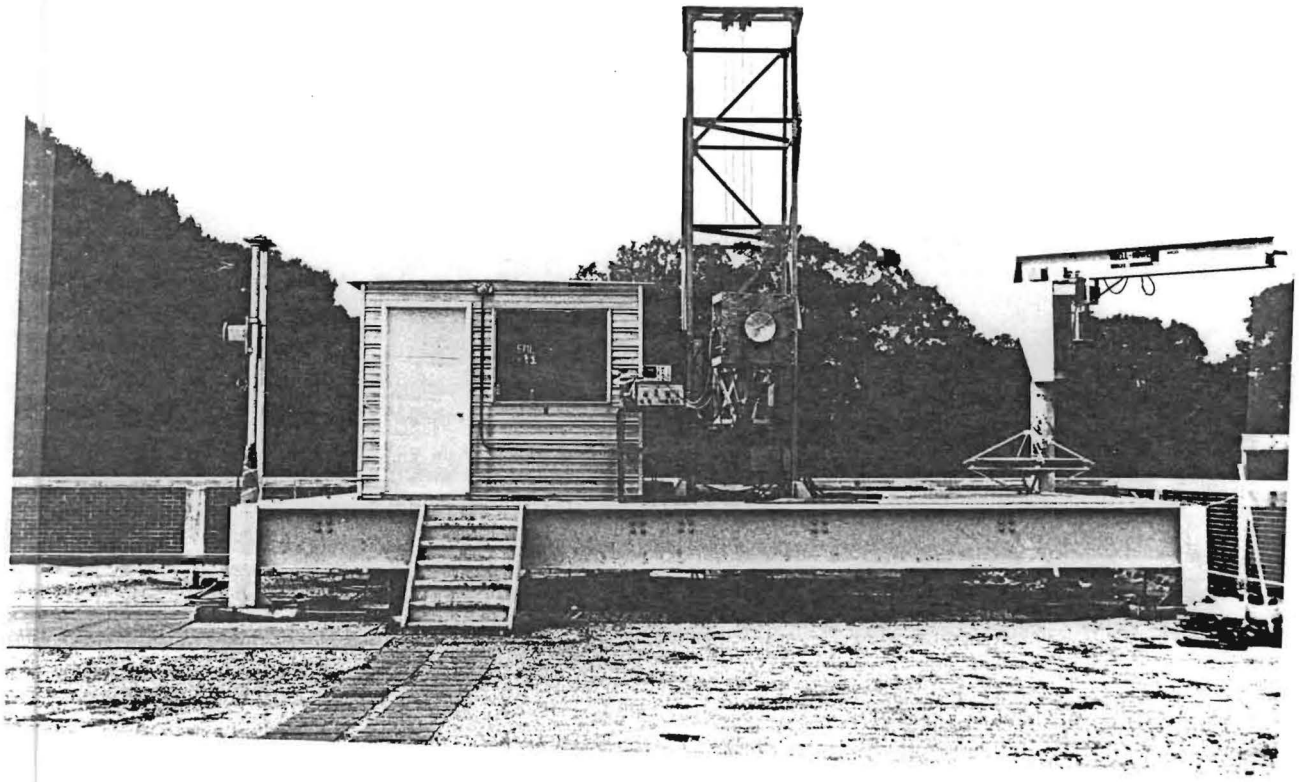

Figure 3-37. Photograph of transmit system.
(Long View)

The receive system is illustrated in Figure 3-38. Here standard Scientific Atlanta equipment was used and is shown in Figures 3-39 and 3-40. The receiver uses a low frequency local oscillator, a harmonic of which is mixed with the incoming 94 GHz signal in a harmonic mixer to generate the intermediate frequency. To give good noise performance and minimize frequency and amplitude drift, the receive local oscillator is locked to a subharmonic of the incoming 94 GHz signal by means of a reference channel.

The antenna under test is mounted on a pedestal which is steerable in azimuth and elevation. In this experiment, the azimuth angle was varied to give the E-plane pattern since the radiation from the transmitter is horizontally polarized. The pattern data are recorded on a chart recorder which is driven in synchronism with the antenna sweep, so that angle readouts are accurate. This feature also allows for recording multiple patterns with a common angle scale.

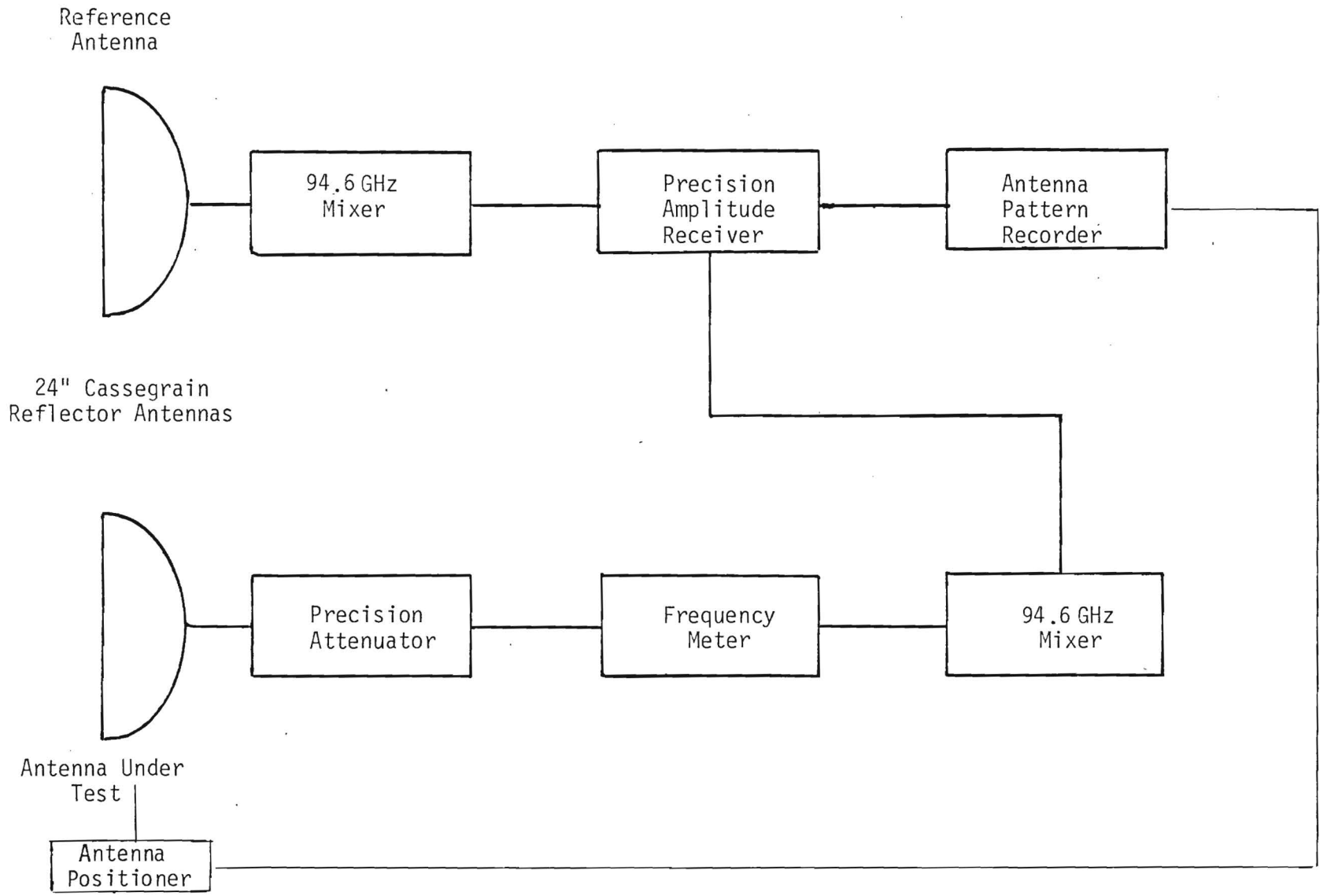

Figure 3-38. Receive system.

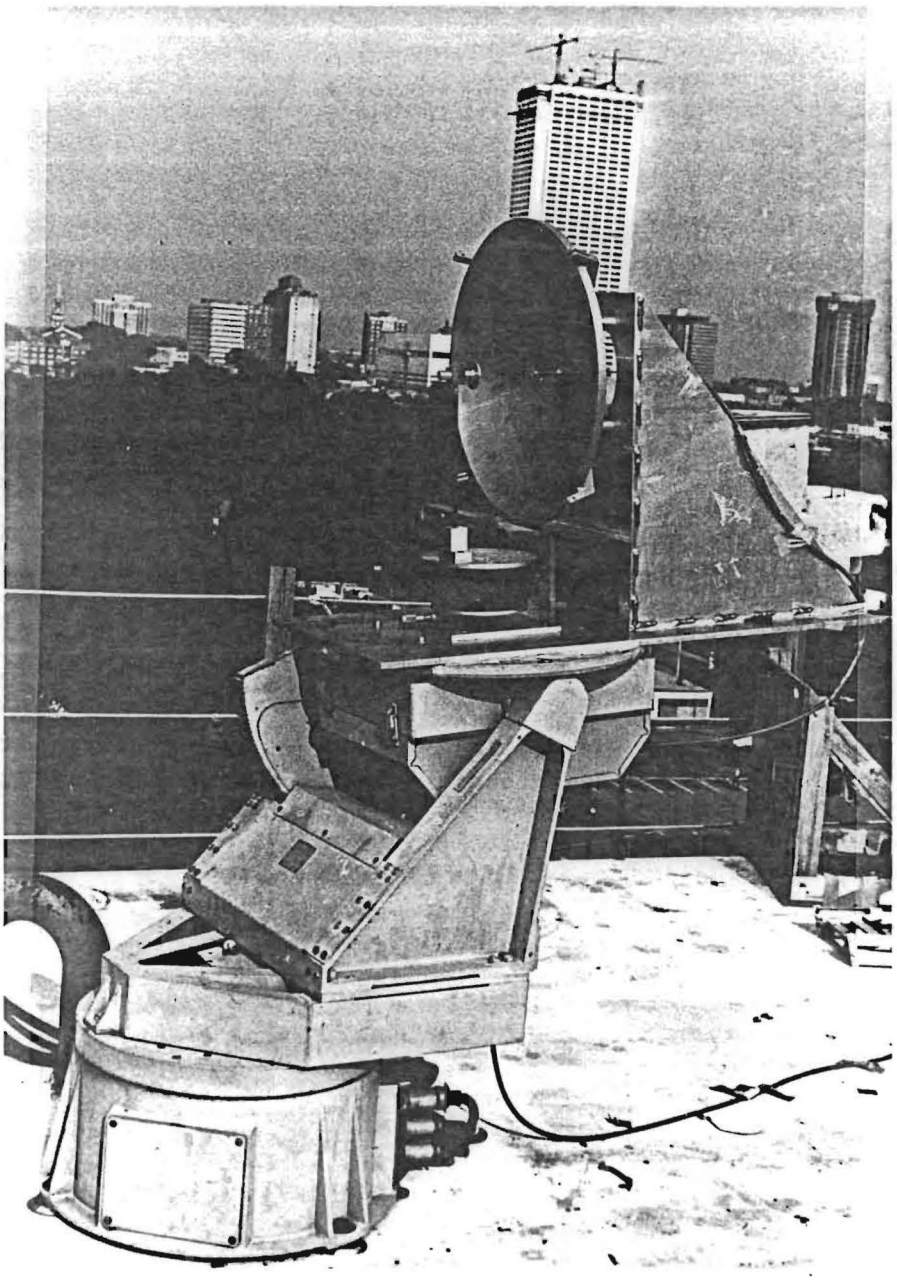

Figure 3-39. Antenna under test mounted on Scientific Atlanta positioner.

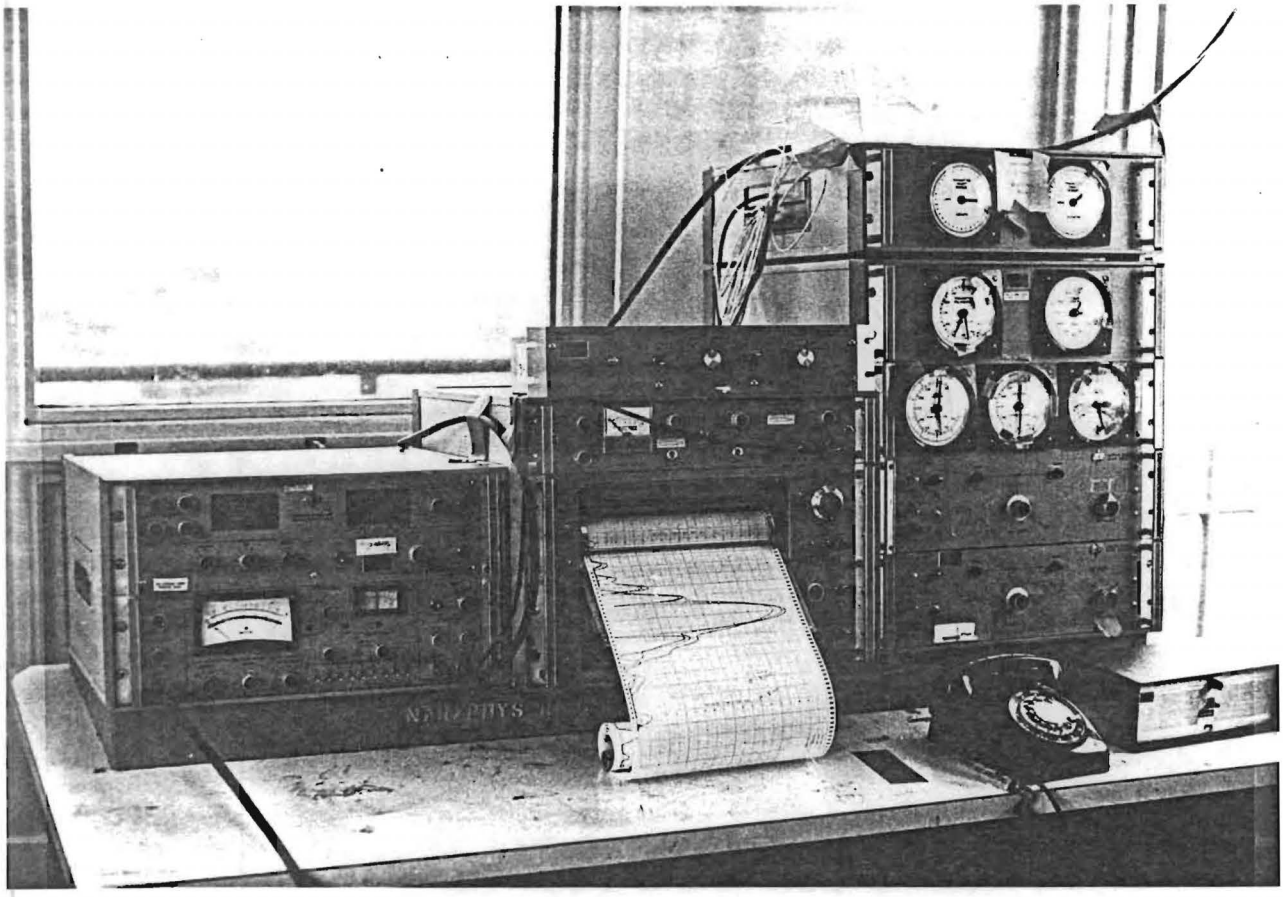

Figure 3-40. Precision amplitude receiver, antenna pattern recorder and antenna position control unit.

4.0 RESULTS

4.1 Comparison of Theory and Experiment

In this section, theory will be compared to experiment in two ways: (1) the simple geometrical theory of beam steering will be compared to the measured main-lobe peak deflections observed, and (2) the measured antenna beam patterns will be compared to the optical diffraction theory.

4.1.1 Geometrical Theory

From Section 2, the equation giving beam steering as a function of hyperbola translation was determined to be

$$\theta_B = \frac{\delta(BDF)\ (M-1)}{Mf}$$

A total of seven patterns for hyperbola translations ranging from zero to 7.5 mm was measured. This value was chosen as the upper limit because of increasingly evident beam distortion at larger translation values. The results of these measurements were shown in Figures 3-7 and 3-8. Two figures are used to show these measurements because of the confusing number of lines on the superposed patterns. Figure 4-1 shows the comparison of the measured peak displacement to the geometrical theory, and indicates that the agreement is quite good.

To show that beam deflections are symmetrical, patterns were made with the subreflector displaced 2.5 mm on either side of the center, and the results of this measurement were shown in Figure 3-9, which does show that the deflections are symmetrical. It is also of interest to examine the antenna pattern in the orthogonal plane to be sure that the desired deflection of the beam in a given plane does not distort the orthogonal pattern beyond that which is useful. Figure 3-11 is a pattern measured in the H-plane with the subreflector translated in the E-plane by 5.08 mm. Note that the sidelobe levels are slightly degraded and also slightly unsymmetrical.

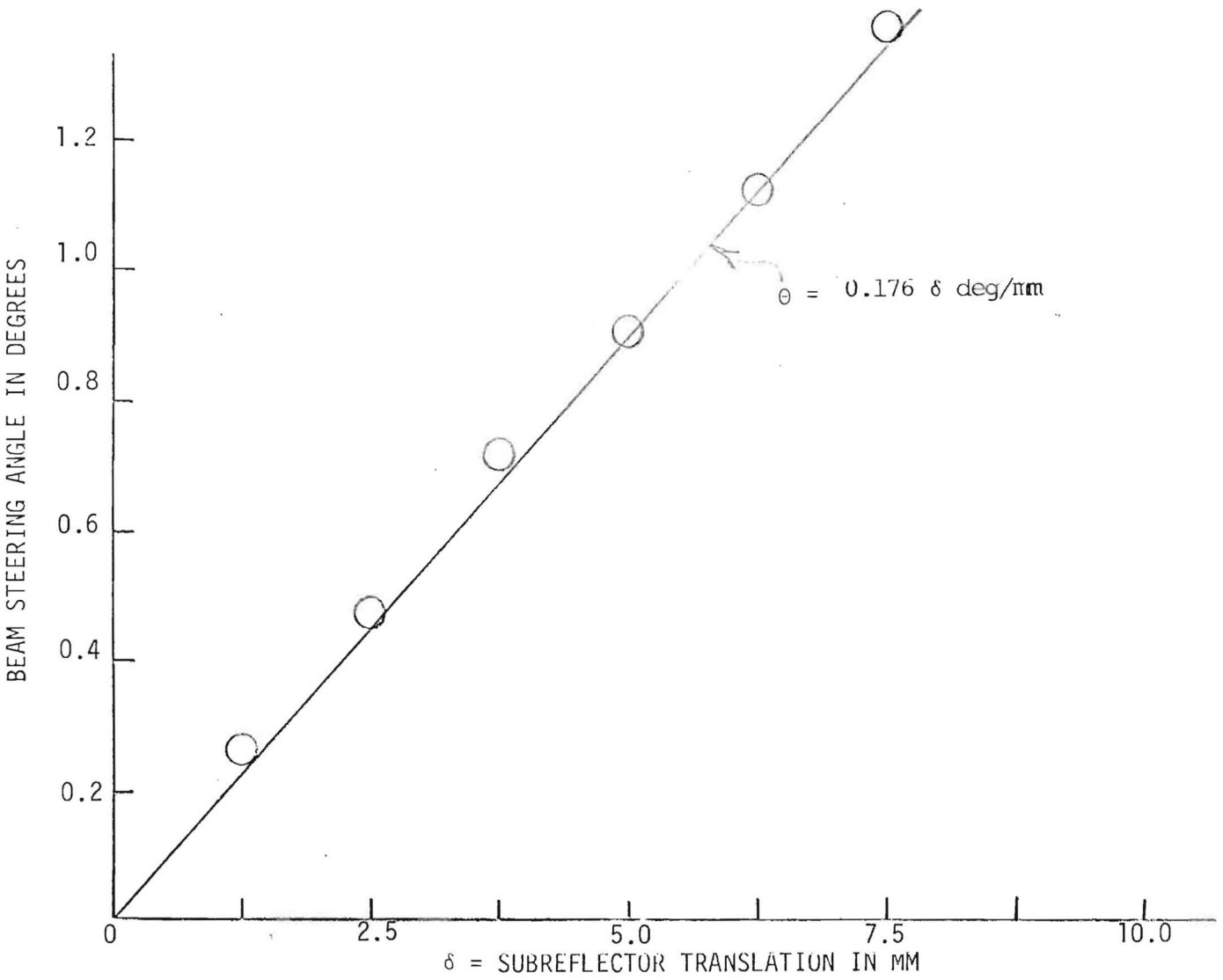

Figure 4-1. Comparison of measured peak beam deviation due to hyperbola translation to theory.

In addition to those made for pure translation of the subreflector, measurements of beam steering were made for a translation of the subreflector followed by a rotation such that its axis is aligned with the center of the feed. This type motion was not treated by the geometrical theory of Isber, but was treated by Ruze using optical diffraction theory. Figures 3-25 and 3-26 show patterns measured in this way. The translation and rotation amounts were noted on the figure. Figure 3-27 shows the H-plane pattern measured for a translation of 7.62 mm and a rotation of 3.95^{o}. As in the pure translation case, the sidelobes are slightly degraded. These results will be compared to theory in Section 4.2.

The equation given in Section 2 for beam displacement as a function of hyperbola rotation is

$$\theta_{sr} = F \tan \alpha \left(\frac{BDF}{f}\right) \left(\frac{M + 1}{m}\right)$$

A total of twelve patterns were measured for this case with the rotation angle varying from 0^{o} to 11^{o} in 12 steps. These results were shown in Figures 3-13, 3-14, and 3-15, and are compared to the simple theory in Figure 4-2. Note that the sidelobe levels are not degraded nearly as badly for this case, but the presence of coma lobes, or small shoulders on the beam profile, is more evident. Figure 3-16 shows that beam deflection is symmetrical for this case, showing symmetrical deflections for rotations of $\pm 4^{o}$. Figure 3-17 is a pattern measured in the orthogonal plane showing that the sidelobe levels are slightly degraded and unsymmetrical as well.

The equation for beam deflection as a function of feed translation was also given in Section 2. This equation is

$$\theta_{fr} = - \frac{\delta_f (BDF)}{Mf}$$

where the variables have already been defined. Substituting the antenna parameters given earlier into this equation gives $\theta_f = -0.041\ \delta_f$ where δ_f is measured in millimeters and θ_f is in degrees. Figure 3-31 shows a

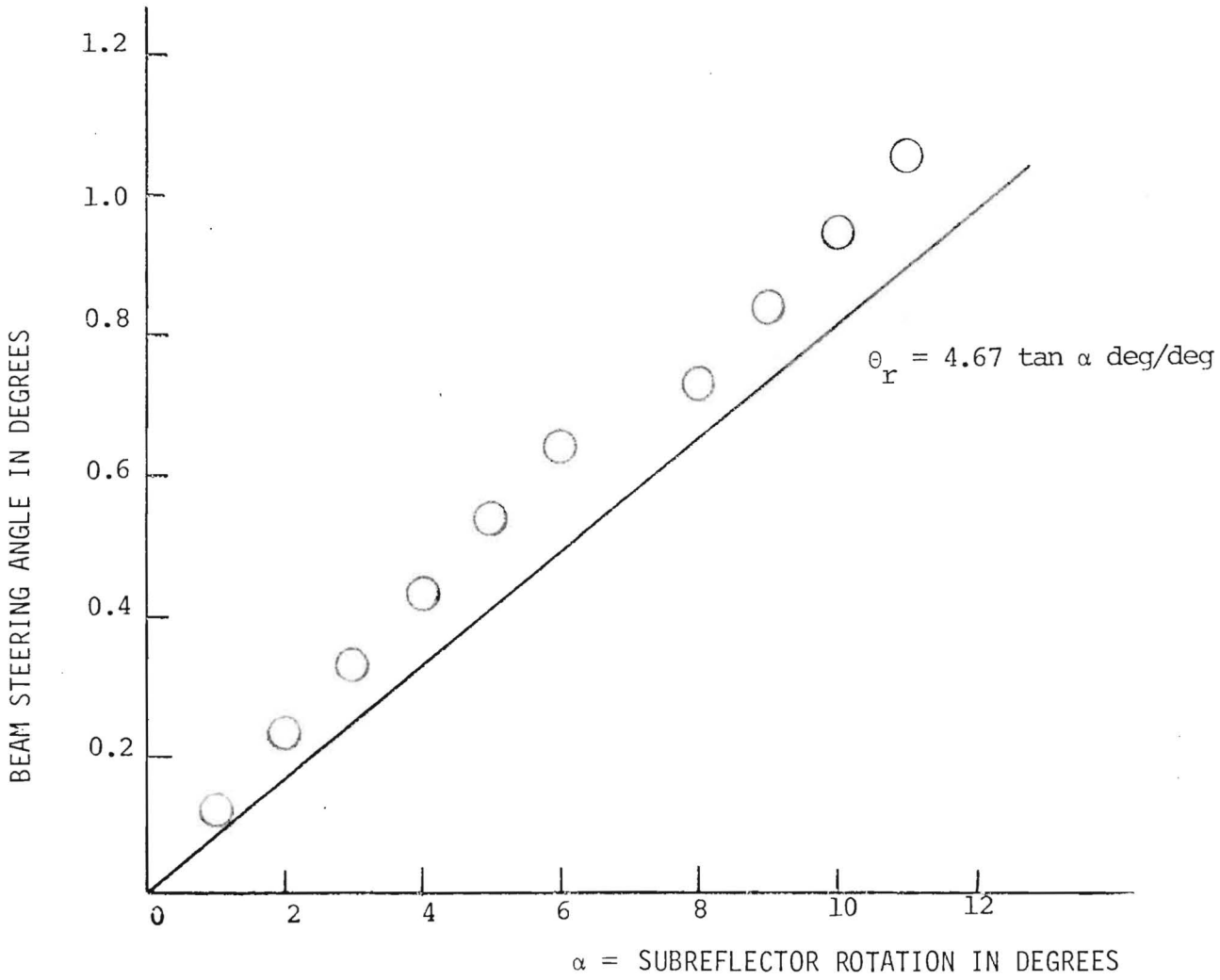

Figure 4-2. Comparison of measured peak beam deviation due to hyperbola rotation to theory.

series of antenna patterns measured for several different feed translations. These deflections were scaled from the figure and plotted against translation and are shown in Figure 4-3. The slope of the calculated variation is less than that of a line drawn through the measured points due to error in determining values of antenna parameters.

From Section 2, beam deflection as a function of feed rotation is given by

$$\theta_{fr} = \frac{\theta_r F(BDF)}{Mf} \quad .$$

Substituting antenna parameters gives $\theta_{fr} = 0.014\theta r$, which is a very low beam scanning efficiency. This low efficiency is also obvious from an examination of figure 3-7, which shows a negligible amount of beam deflection as a function of feed rotation. Since feed rotation is obviously not a viable candidate for a precision tracking antenna, this approach will not be considered further.

There is a fairly severe problem associated with motion of the Cassegrain antenna feed in either mode, caused by the fact that any millimeter wave transmitter/receiver system must be rigidly attached to its antenna feed to minimize losses. This rigid attachment implies that the entire system must be rotated with the feed, which in turn may require a gimbal system almost as large and heavy as that required for the large antenna. It is possible that some method of optical coupling to the feed could be devised to eliminate this problem, but this approach was not considered during this measurement program. In any case, it appears that either method of feed reorientation will not give the kind of scanning efficiency needed for a useful system, and that subreflector motion must be relied upon for building the desired precision tracking antenna.

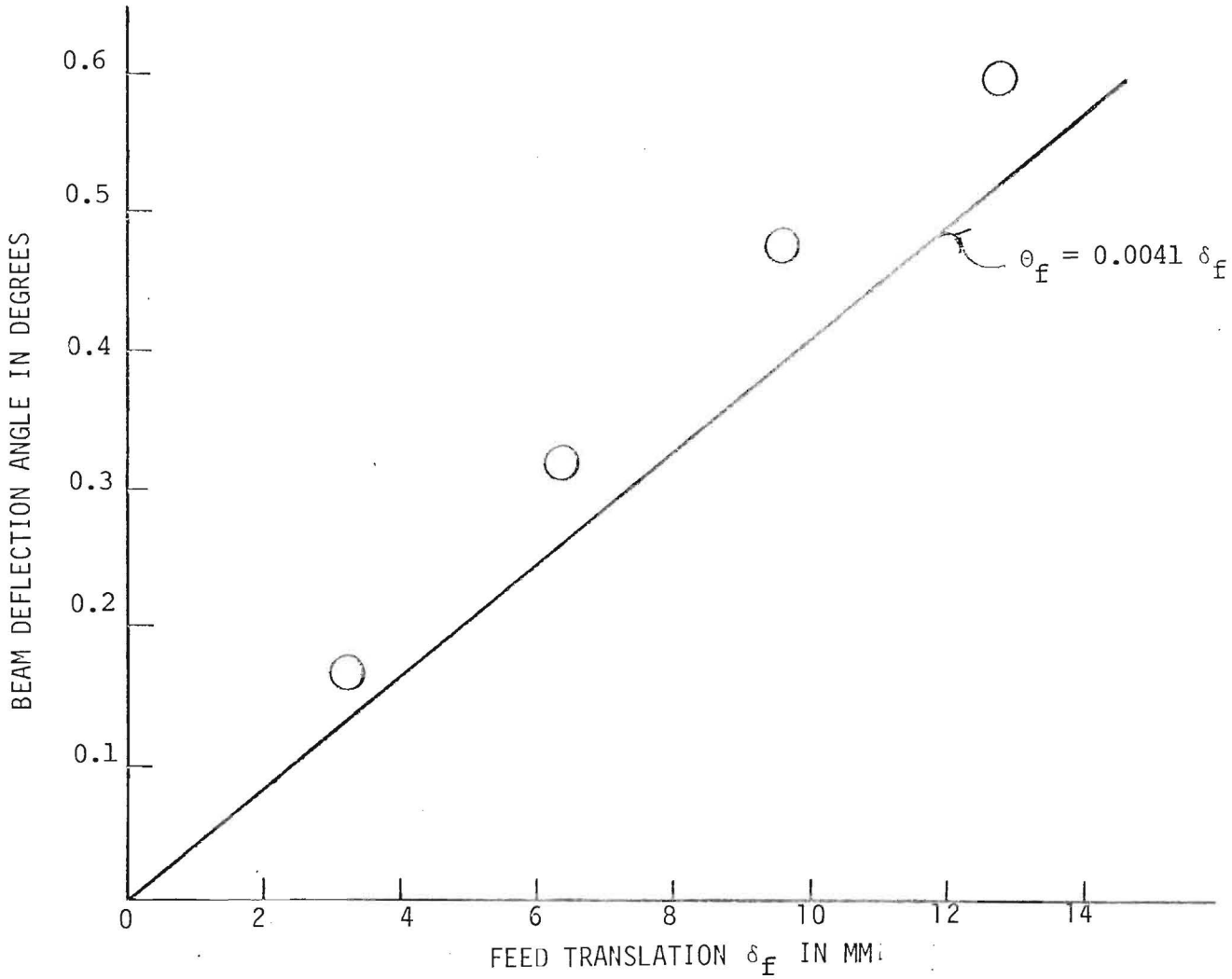

Figure 4-3. Comparison of measured peak beam deviation due to feed translation to theory.

4.1.2 Diffraction Theory

The evaluation of the integral (2-11) was made on the Georgia Tech CDC 6400 computer for the case of a subreflector translation followed by a rotation to point the subreflector toward the feed, as treated in the paper by Ruze [4], These integrals were evaluated for several of the translations and rotations noted on Figures 3-25 and 3-26.

Figures 4-4, 4-5, 4-6, and 4-7 show the calculated antenna patterns for subreflector translation. These figures should be compared to Figures 3-25 and 3-26, which are the corresponding measurement results. Note that this calculation gives good agreement indicating that the state of the theory is good for this case. Figure 4-8 shows the result of comparing the measured deflections of the beam peaks to those calculated by diffraction theory.

Although the combined translational/rational motion of the subreflector yields patterns that agree well with theory, this method of beam deflection is probably not suitable for beam steering because the combined motions are too complicated for practical drivers and position encoders. Such devices are available for pure rotation, and to a lesser degree, for pure translation, but the superposition of these two motions would result in a prohibitively complicated system. Futhermore, the beam distortions evident in the pattern measurements of Figures 3-25 and 3-26 show that thisapproach to beam steering will not be very effective.

The integral (2-15) was also evaluated on the computer for the case of a pure subreflector rotation. The results of these evaluations are shown in Figures 4-9, 4-10, and 4-11 for rotation angles of 3, 6, and 9 degrees respectively. These figures should be compared to Figures 3-13, 3-14, and 3-15 which show the corresponding measured results. Again, the agreement is quite good, although the theoretical curves show deeper nulls than the measured results. This is probably due to a slight defocusing of the hyperbola upon rotation, or possibly to a higher order effect not considered in the theory.

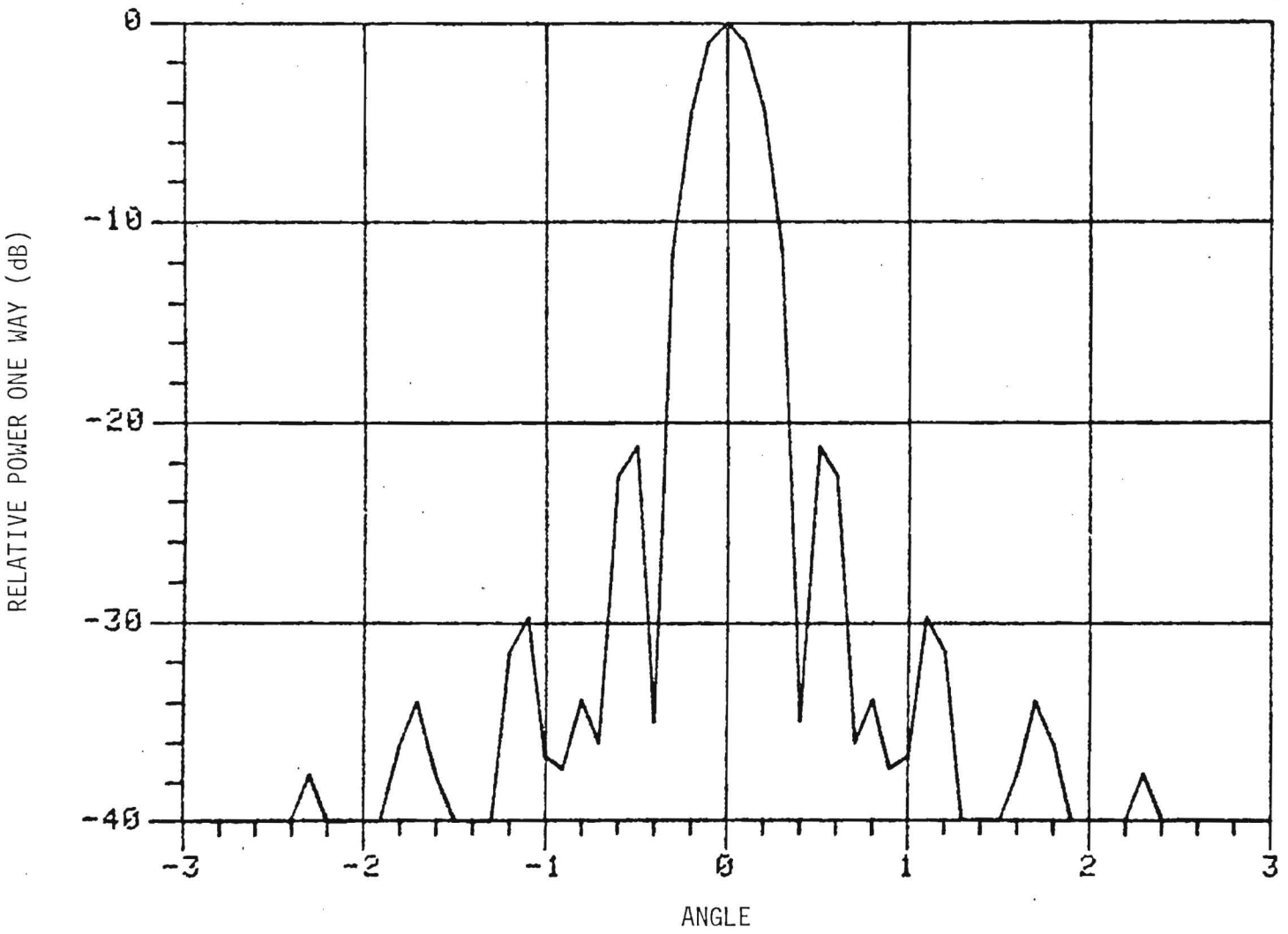

Figure 4-4 Theoretical E-plane pattern for TRG antenna with subreflector in normal position (zeroed).

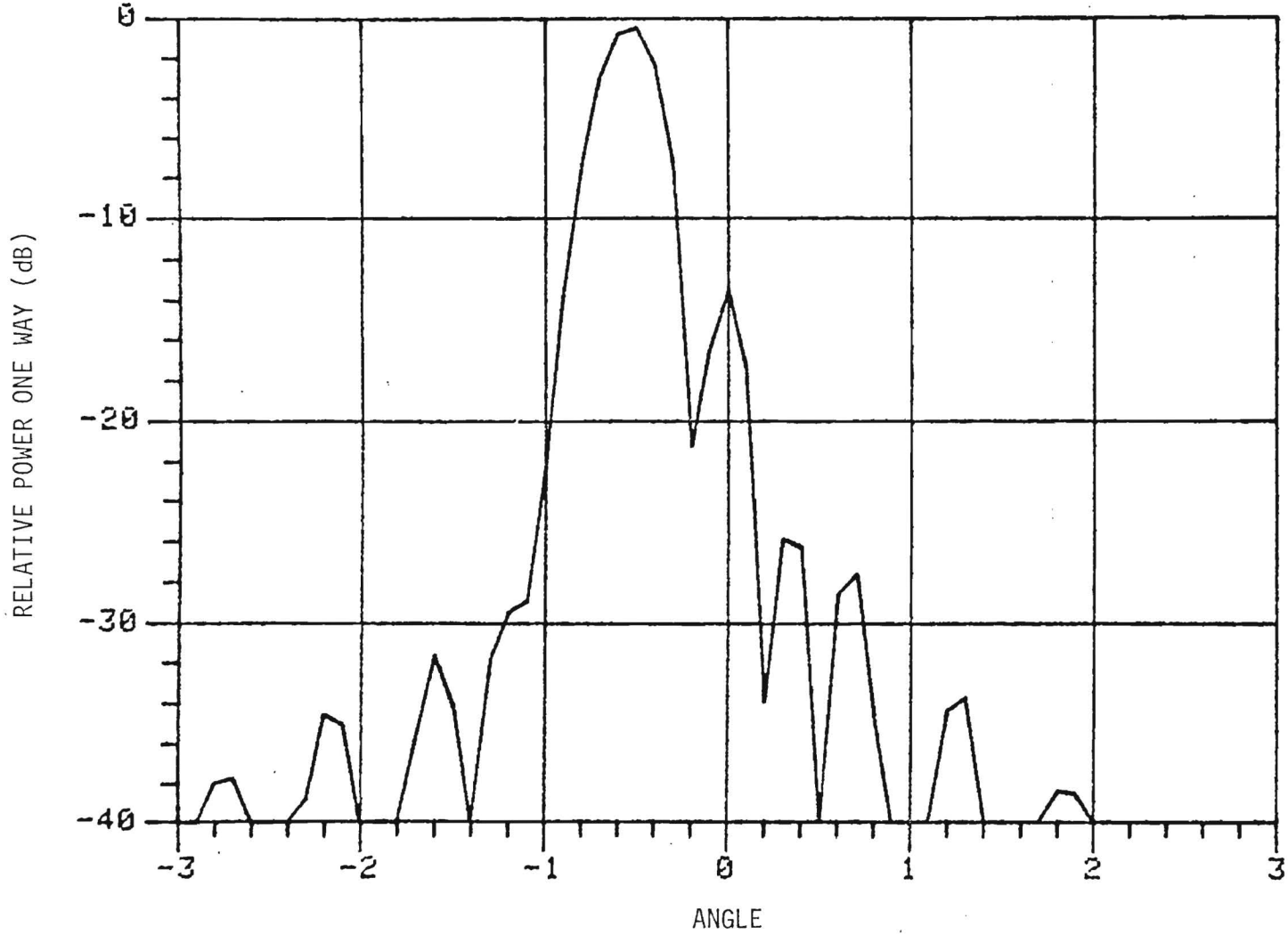

Figure 4-5. Theoretical E-plane pattern for TRG antenna with subreflector translated 2.54 mm and rotated 0.66° toward feed.

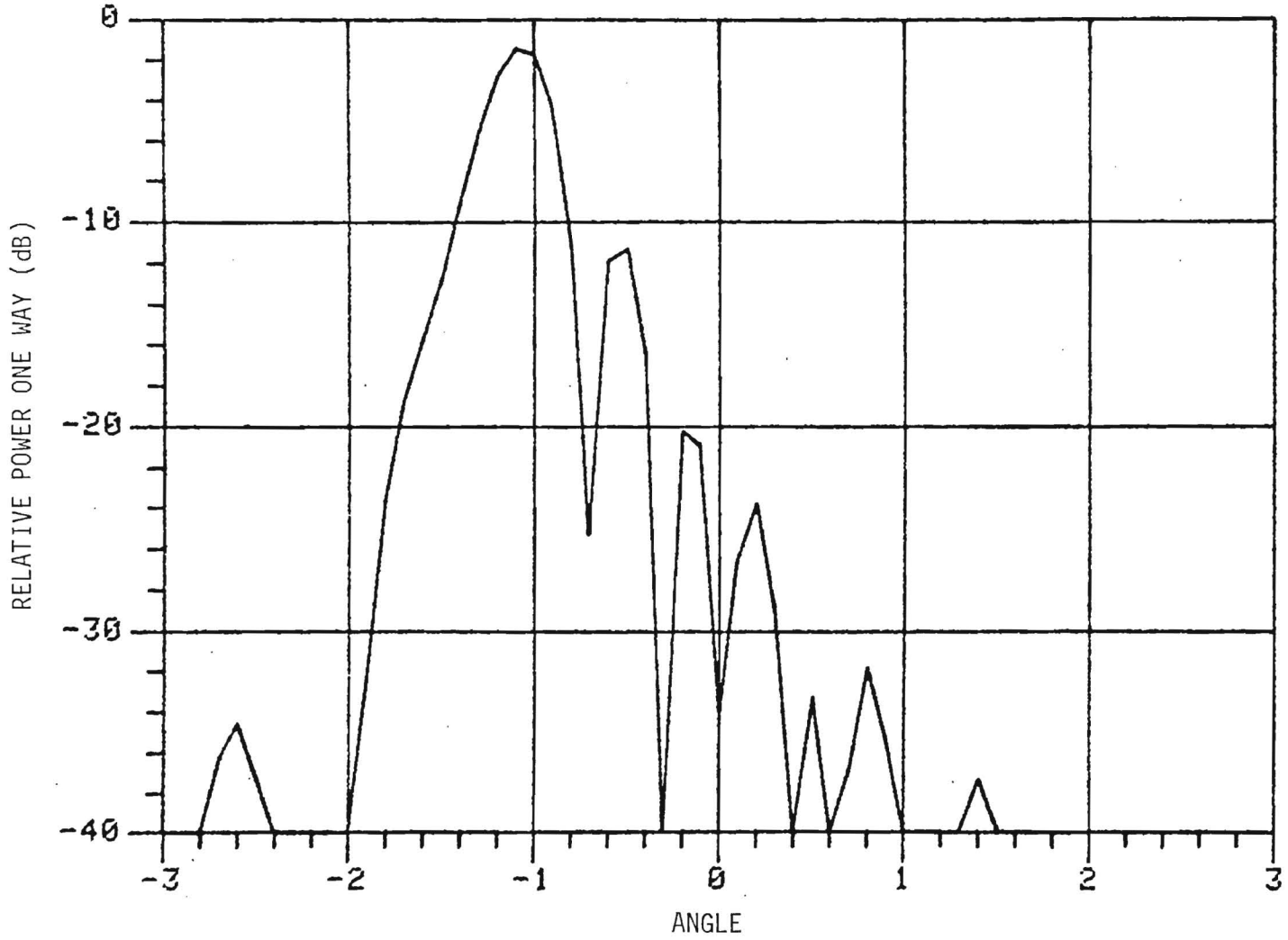

Figure 4-6. Theoretical E-plane pattern for TRG antenna with subreflector translated 5.08 mm and rotated 1.97° toward feed.

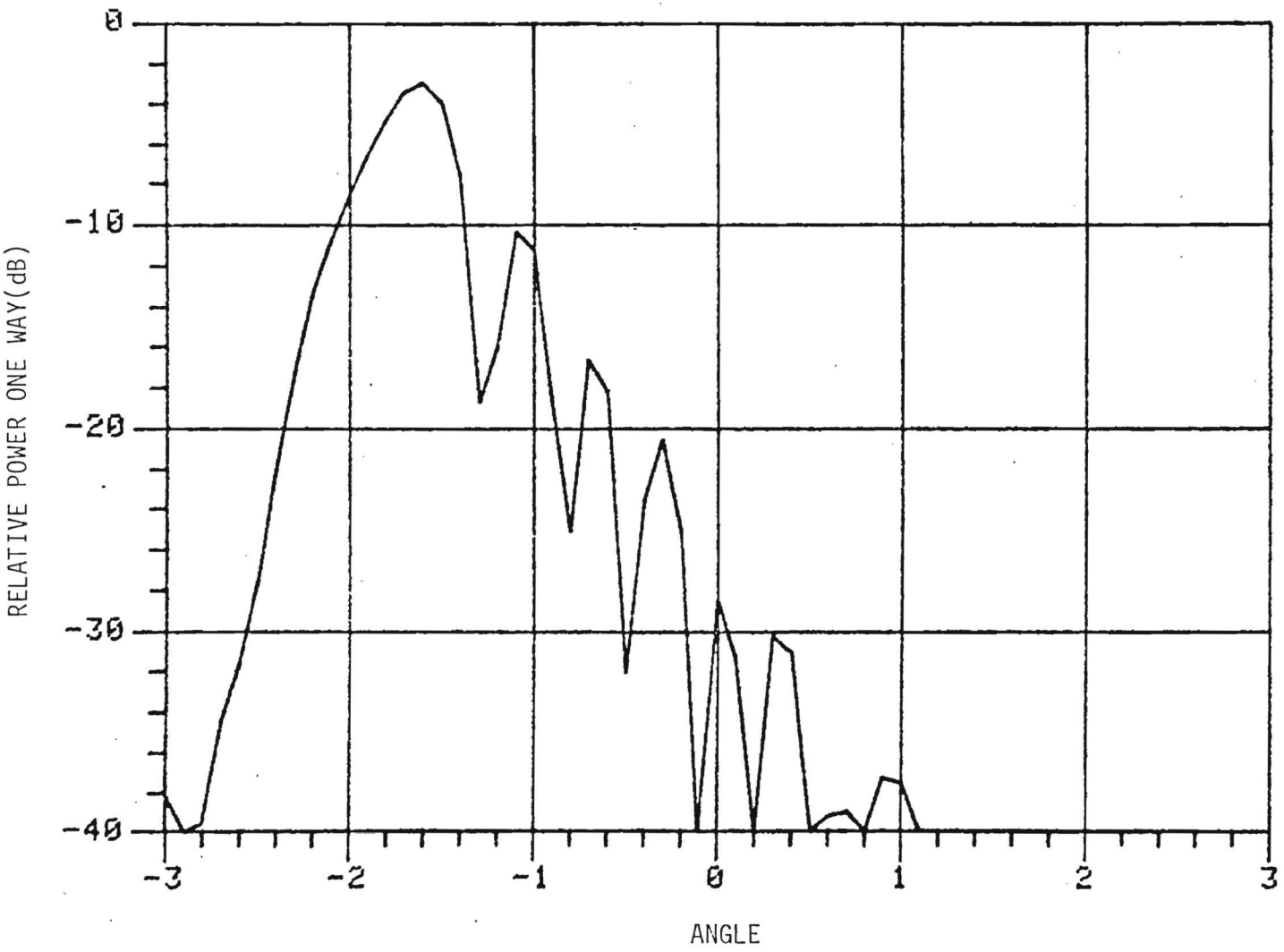

Figure 4-7. Theoretical E-plane pattern for TRG antenna with subreflector translated 7.62 mm and rotated 3.28° toward feed.

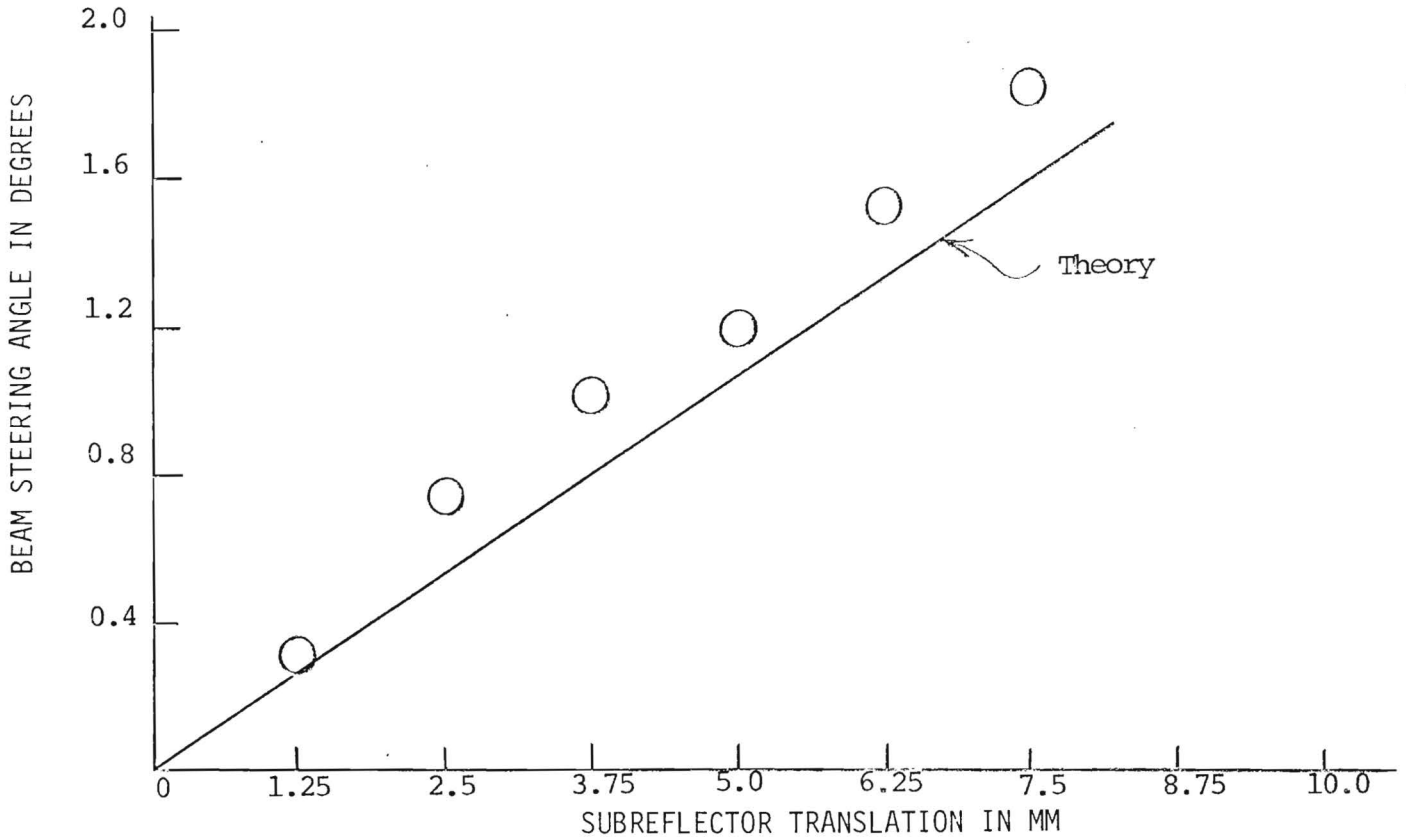

Figure 4-8. Comparison of measured peak beam deviation due to hyperbola translation and rotation to the results of diffraction theory.

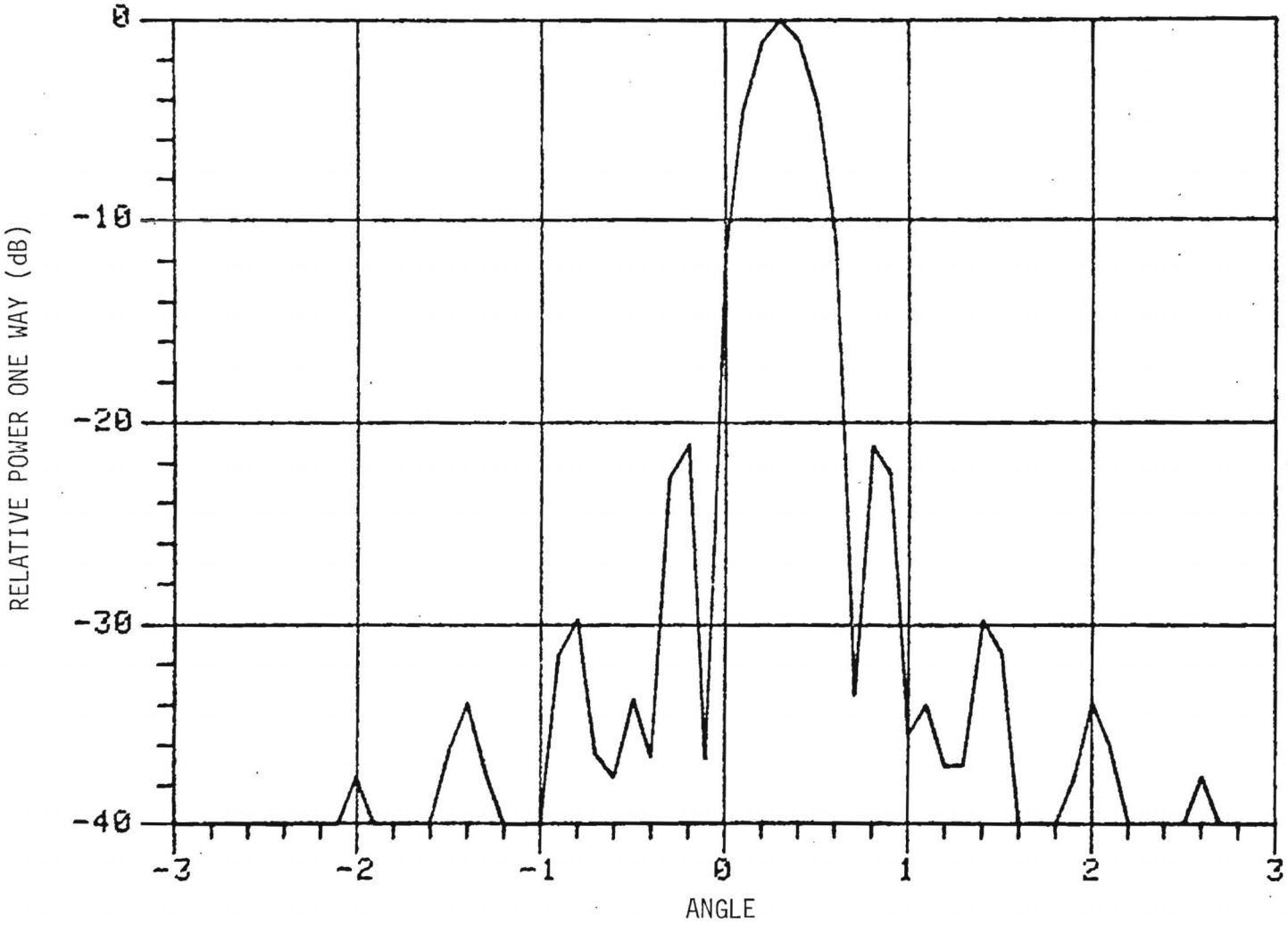

Figure 4-9 Theoretical E-plane pattern for TRG antenna with subreflector rotated 3^{o}.

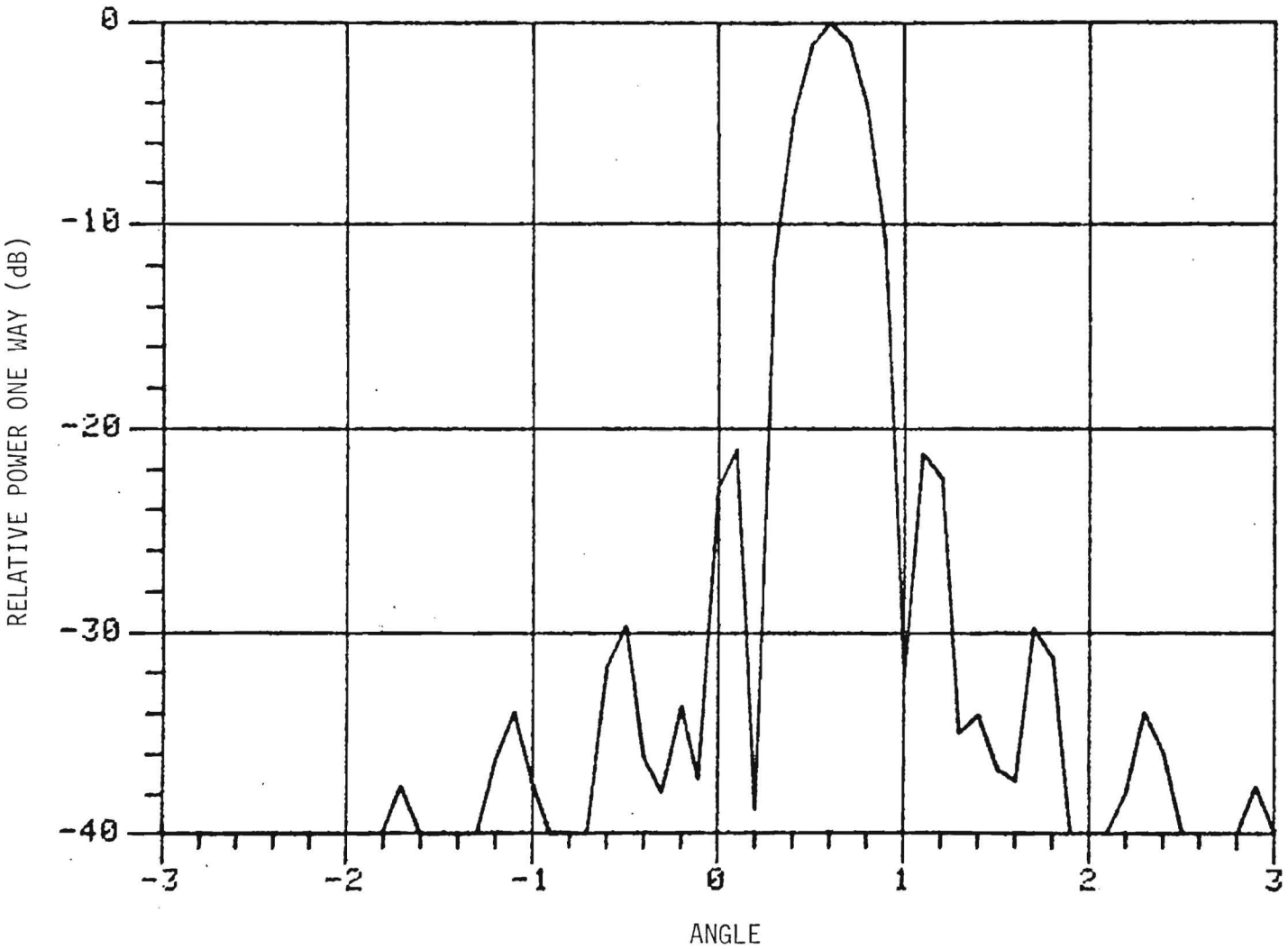

Figure 4-10. Theoretical E-plane pattern for TRG antenna with subreflector rotated 6°.

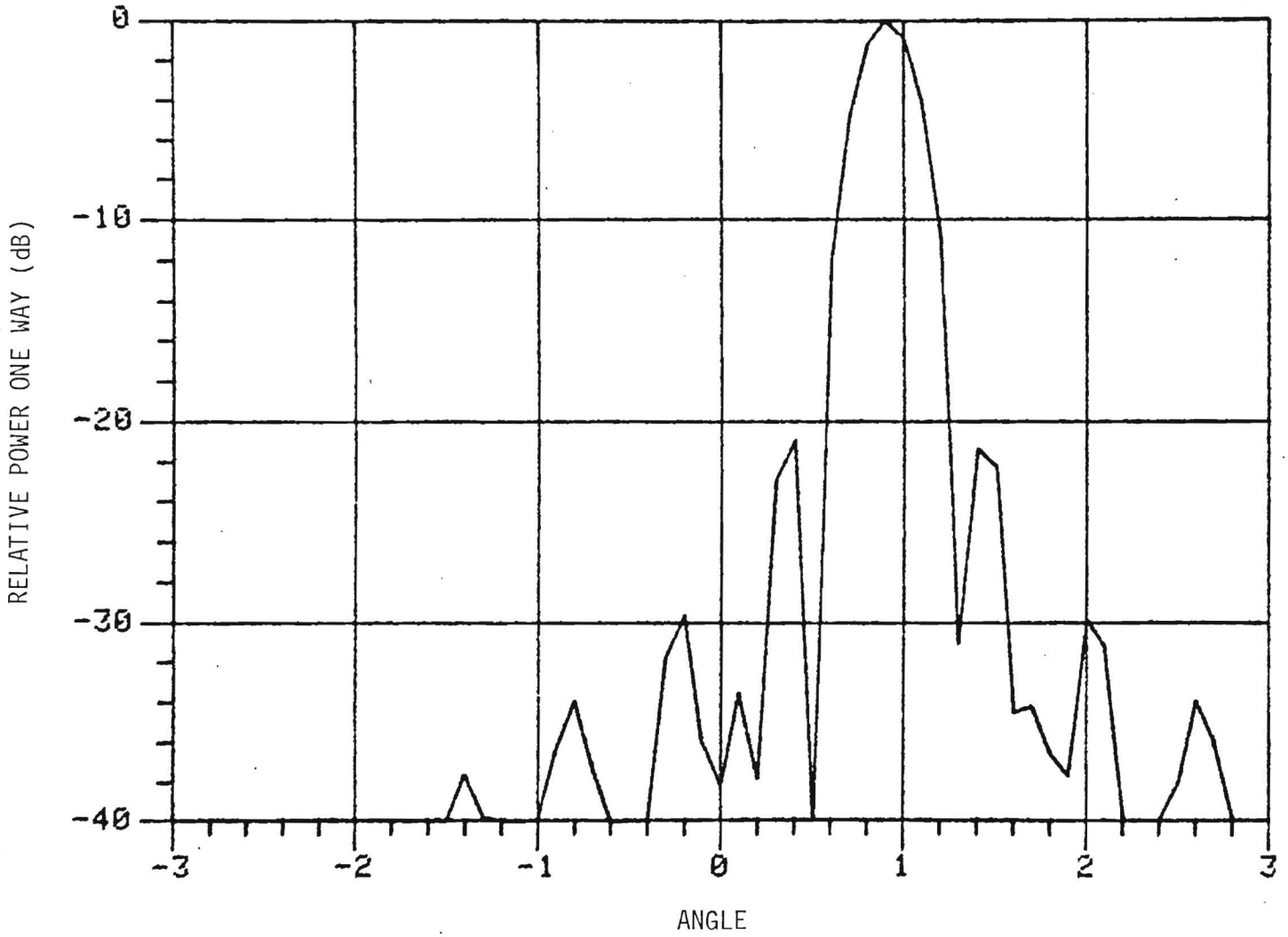

Figure 4-11. Theoretical E-plane pattern of TRG antenna with subreflector rotated 9°.

Since the beam distortion is small for hyperbola rotation, this method is considered to be the best candidate for a fine steering antenna, and will be treated in more detail in Section 5. In that section, an antenna design which would give more effective beam steering than that used for these measurements will be suggested.

4.2 Discussion of Errors

4.2.1 Measurement Errors

In general, the measured antenna patterns discussed in Section 3 agree with theory within about 10%, which is considered to be reasonable agreement for measurements of this type. There are several different sources of error which could cause these disagreements, which will be briefly discussed.

Machining of the antenna feed, subreflector, and main reflector may not be accurate. It has been determined that placement of the subreflector is very critical, and it is assumed that the tolerances of the shape of this element are equally critical, as are the shapes of the feed and main reflector.

Placement and orientation of the antenna elements are also critical to the measurement of an accurate pattern, especially for a short focal length antenna such as the TRG W-822. The nominal patterns shown in this report were determined by repeating pattern measurements until the desired results were obtained, but in some cases there was some residual error in the pattern, evidencing itself as shallow sidelobe nulls or unsymmetrical sidelobe power levels. Failure to obtain the proper nominal pattern could influence the beam steering results obtained. In most cases the nominal patterns obtained were better than the calibration pattern furnished by TRG for the same antenna.

4.2.2 Calculation Errors

The simple geometrical theory of beam steering discussed in Section 2 will predict beam deflection as a function of feed or subreflector motion with good accuracy for small deflections. However, as noted earlier, this simple theory does not give any information about sidelobe levels or beam distortion. For determination of these parameters, it is necessary to solve the diffraction integrals treated near the end of Section 2. The diffraction integrals are not generally solvable in closed form, so that computer solutions must be obtained. The necessity for solving these integrals for a given angle causes the resulting curves to be discontinuous. Many points would have to be taken, and much computer time expended, to obtain smooth curves. The lack of smoothness in the calculation is especially evident in the sidelobes, where the peaks may be discontinuous and the nulls shallow because not enough points were taken for good resolution.

The diffraction integrals also represent approximations to a first order theory. It is possible that a higher order theory might give better results; for example, the measured sidelobe levels due to hyberbola rotation do not agree well with theory, but some of this disagreement may result from a slight defocussing of the reflector as this element is rotated.

In considering the measurements treated during this program, it is slightly surprising to see the quality of the agreement between theory and experiment. This agreement gives credibility to the results of Section 5, which discusses the design of an antenna especially for beam steering.

5.0 CONCLUSIONS AND RECOMMENDATIONS

5.1 Design of an Optimum Antenna for Beam Steering

The TRG model W822-24 antenna is an efficient radiator that appears to be well optimized for its size and F#. However, the results of Section 4 show that the antenna is not very useful for beam steering because of its low F#, a factor which also accounts for the compact axial extent of this antenna. The low F# also causes rapid degradation of beam quality with beam angle, as shown by the measured results of Section 3.

The two requirements for a useful beam steering antenna are: (1) maximum beam steering angle as a function of steered element movement, and (2) minimum distortion of the antenna beam at steering angles of interest. Both of these criteria are approached more readily by using an antenna of large f/D ratio. Practical considerations however, limit this F# to about 1.0; otherwise the axial extent of the antenna would be greater than its diameter. The criterion of minimum beam distortion is also easier to meet for antennas with large F# 's.

Referring to Equations (2-5) and (2-9), it is seen that the effectiveness of beam steering as a function of antenna element movement is linearly dependent on BDF, and very weakly dependent on M, which are the only parameters of interest. Assume that F# = f/d = 1.0 and f = D = 610 mm. As will be seen, the choice of these parameters determines most of the other antenna variables.

In designing this antenna, the straightforward "cook-book" approach detailed in Reference [2] was closely followed. The gain of the antenna is given by

$$G = 2\eta\Pi \frac{D^2}{\lambda^2}$$

where η is antenna efficiency (taken to be 0.5) and λ is wavelength.

For 95 GHz and D = 610 mm, this equation gives G = 51 dB. The half-angle of the parabola is calculated from

$$\tan \frac{\phi_o}{2} = \frac{D}{4f}, \tag{5-2}$$

which gives $\phi_o = 28.1^o$. The equation of the paraboloid surface in polar coordinates is

$$\rho = 610 \sec^2 \frac{\phi}{2} \text{ mm}, \tag{5-3}$$

where ρ is the radial distance from the paraboloid focus and 0 is angular displacement from the paraboloid axis.

For minimum hyperboloid blockage, the diameter of this element is

$$d = \sqrt{2\lambda f} = 62.1\text{mm}, \tag{5-4}$$

and the blockage ratio is B = d/D = 0.102. The hyperpoloid focal length is given by F= f, where the parameter μ is

$$\mu = \frac{2(1 - \ell_c/f)}{\sqrt{1 + 8(1 = \ell_c/f) + 1}} \tag{5-5}$$

and ℓ_c is the distance of the feed phase center from the parabola vertex. If it is assumed that ℓ_c=0, then μ = 0.5. The half-angle of the hyperboloid is given by

$$\tan \alpha = \frac{1}{\frac{2\mu f}{BD} - \frac{1}{\tan \phi_o}} \tag{5-6}$$

which gives $\alpha = 7.17^o$. By using this result for α, the hyperbola magnification, which is a parameter in the deflection equations, may be determined. This magnification is

$$M = \frac{D}{4f} \cos \frac{\alpha}{2} = 3.99, \tag{5-7}$$

and the eccentricity is then

$$\varepsilon = \frac{M + 1}{M - 1} = 1.67, \tag{5-8}$$

These results provide enough information to determine the hyperboloid surface equation, which is

$$r = \frac{\frac{f}{2\varepsilon}(\varepsilon^2 - 1)}{1 + \varepsilon \cos\phi} = \frac{163}{1 + 1.67 \cos\phi} \text{ mm}, \qquad (5\text{-}9)$$

The only parameter left to be determined is the BDF, and Equation (2-3) may be used for its determination. Substituting for D and f in this equation and further assuming that h = 0.5 gives BDF = 0.97.

The above calculations give design parameters for a Cassegrain antenna with f/D = 1 which whould perform well as a beam steering antenna. These results are summarized in Table 4-I. Note that the BDF has increased from 0.82 for the TRG antenna to 0.97 for the antenna discussed in this section. This gives an increase in deflection efficiency of 18%.

These antenna parameters were used in the evaluation of the diffraction integrals (2-15) and (2-17) for this antenna. Figures 5-2, 5-3, and 5-4 show the antenna patterns for hyperbola translations of 0, 2.54, 5.08, and 7.62 mm, respectively; followed by suitable rotations which point the subreflector toward the feed. Note that we have degraded the steering efficiency for this case since the beam steering for a given translation is only about 1/3 of that for the TRG antenna. This result is in agreement with Equation 2-5 since the parabola focal length has been increased by a factor of 3. Note also that the beam quality for a given deflection has improved due to the longer focal length.

Figures 5-5, 5-6, and 5-7 show the antenna patterns for hyperbola rotations of 1, 2, and 3 degrees. The steering efficiency for this antenna has been improved to 50%, compared to about 10% for the TRG antenna. This result is also in agreement with Equation (2-9), because the ratio of hyperbola to parabola focal length has been increased to 0.5. Furthermore, the beam quality is essentially unchanged as a function of steering angle. This high steering efficiency together with good beam quality shows that hyperbola rotation is the best choice for antenna beam steering, and that steering capability can be greatly improved by careful antenna design.

TABLE 4-I

Design Parameters for a Beam Steering Cassegrain Antenna

Diameter	610 mm (24")
Focal Length f	610 mm
Eccentricity of Subreflector	1.67
Magnification of Subreflector	3.99
Diameter of Subreflector	62.1 mm
Gain	51 dB
Equation of Paraboloid Surface	$\rho = 610 \sec^2 \frac{\phi}{2}$ mm
Equation of Hyperboloid Surface	$r = \frac{163}{1 + 1.67 \cos \phi}$
Beam Deviation Factor	0.97

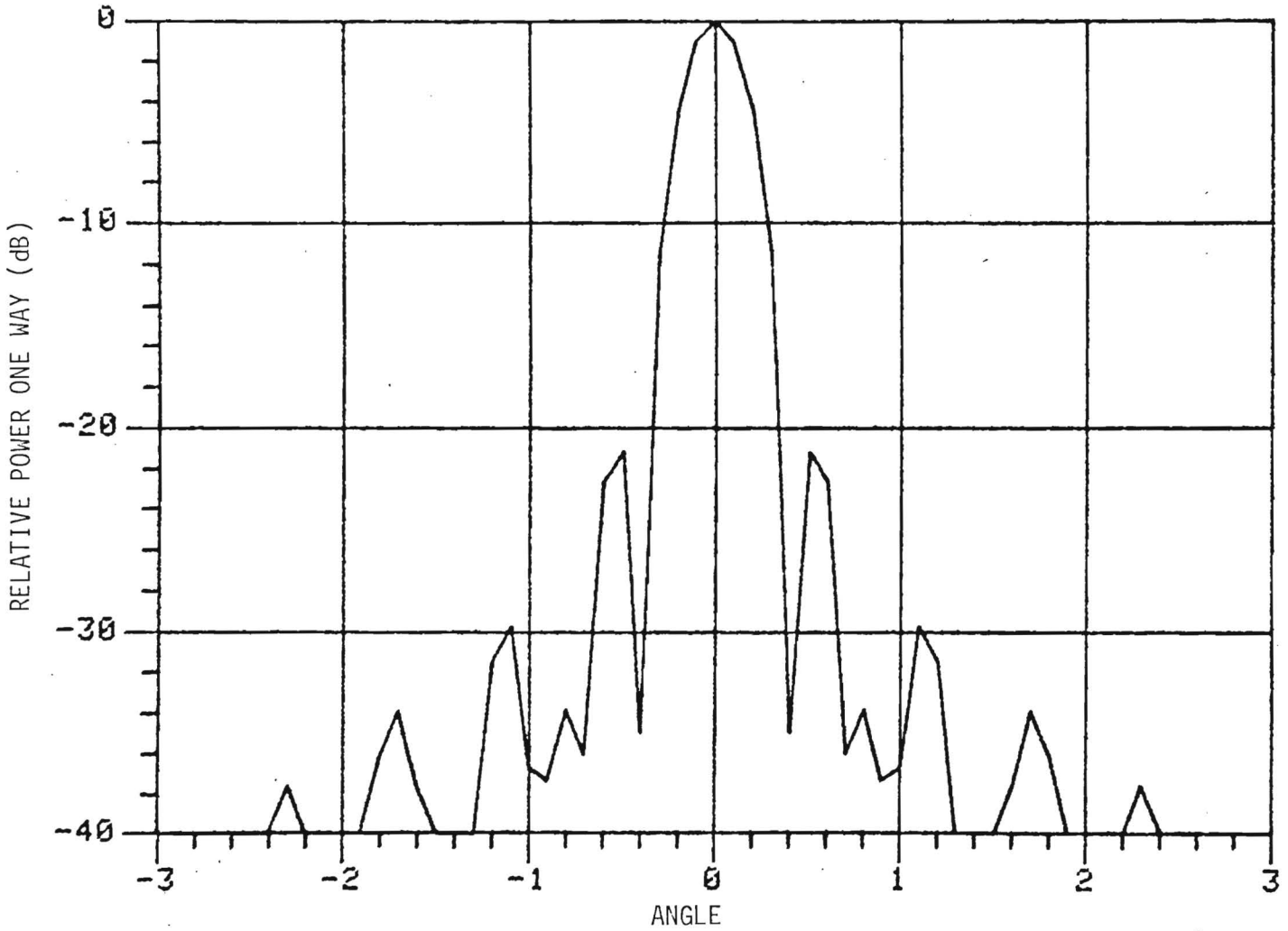

Figure 5-1. Theoretical E-plane pattern for improved antenna with subreflector in normal position (zeroed).

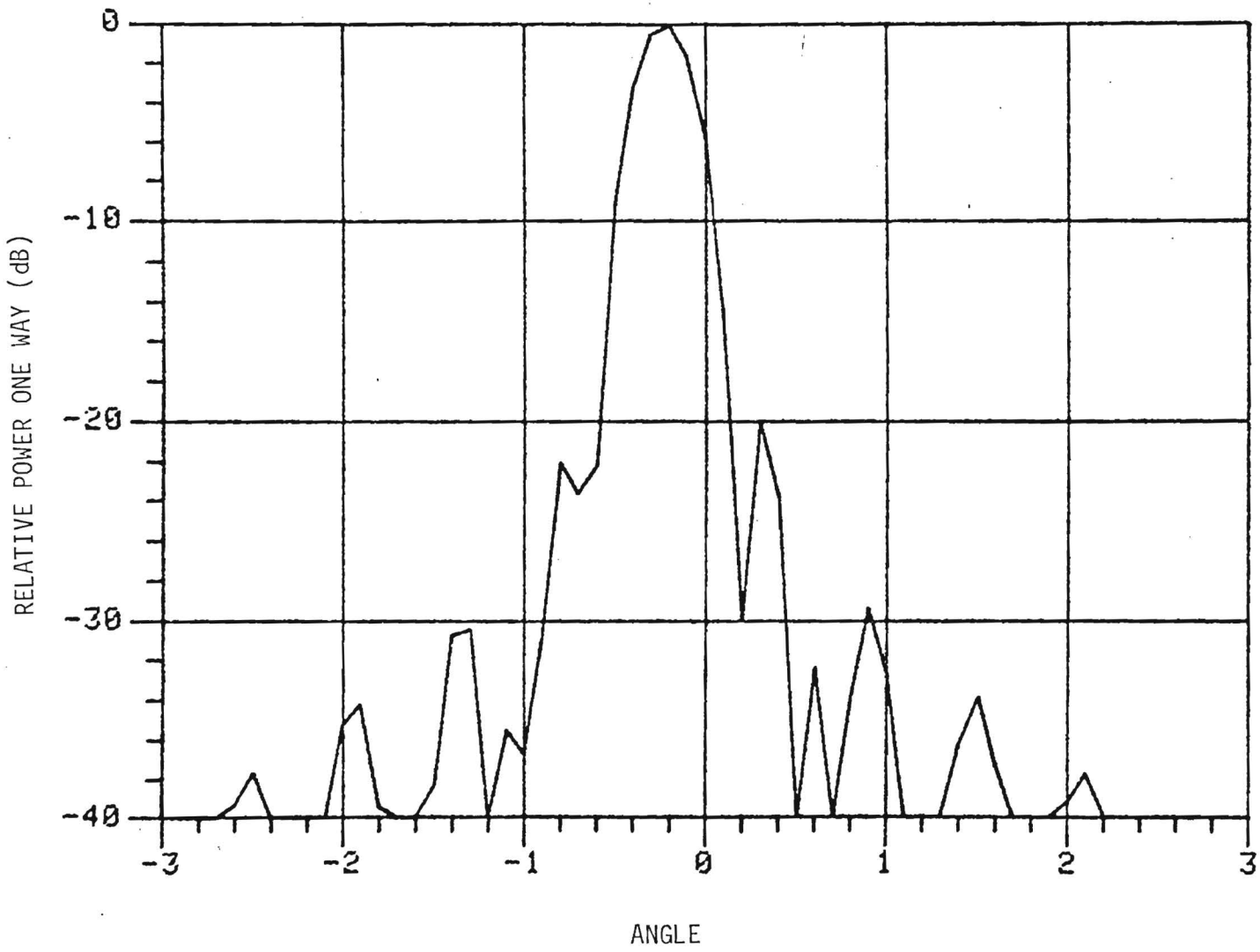

Figure 5-2. Theoretical E-plane pattern for improved antenna with subreflector translated 2.54 mm and rotated 0.24° toward the feed.

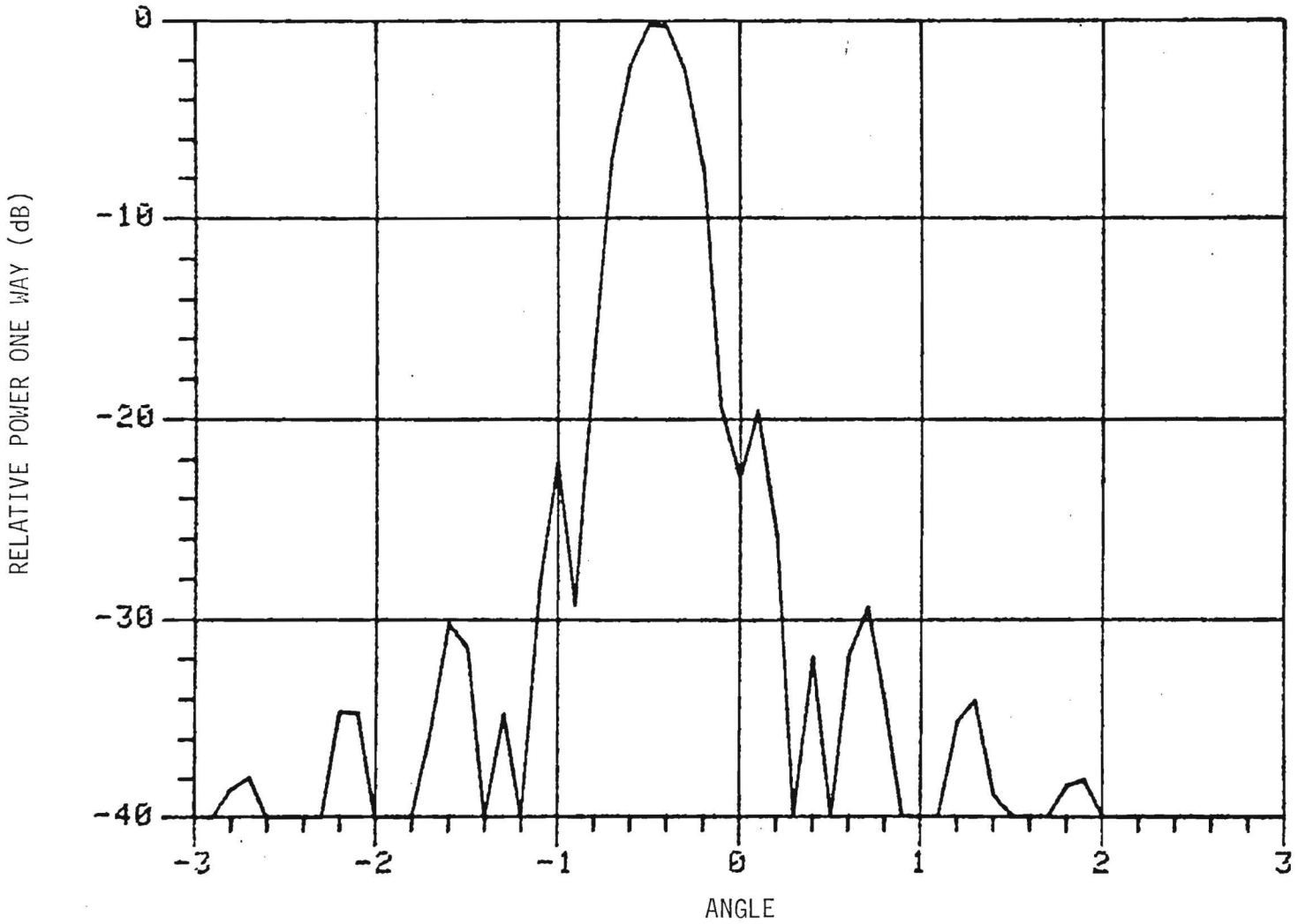

Figure 5-3. Theoretical E-plane pattern for improved antenna with subreflector translated 5.08 mm and rotated 0.48° toward the feed.

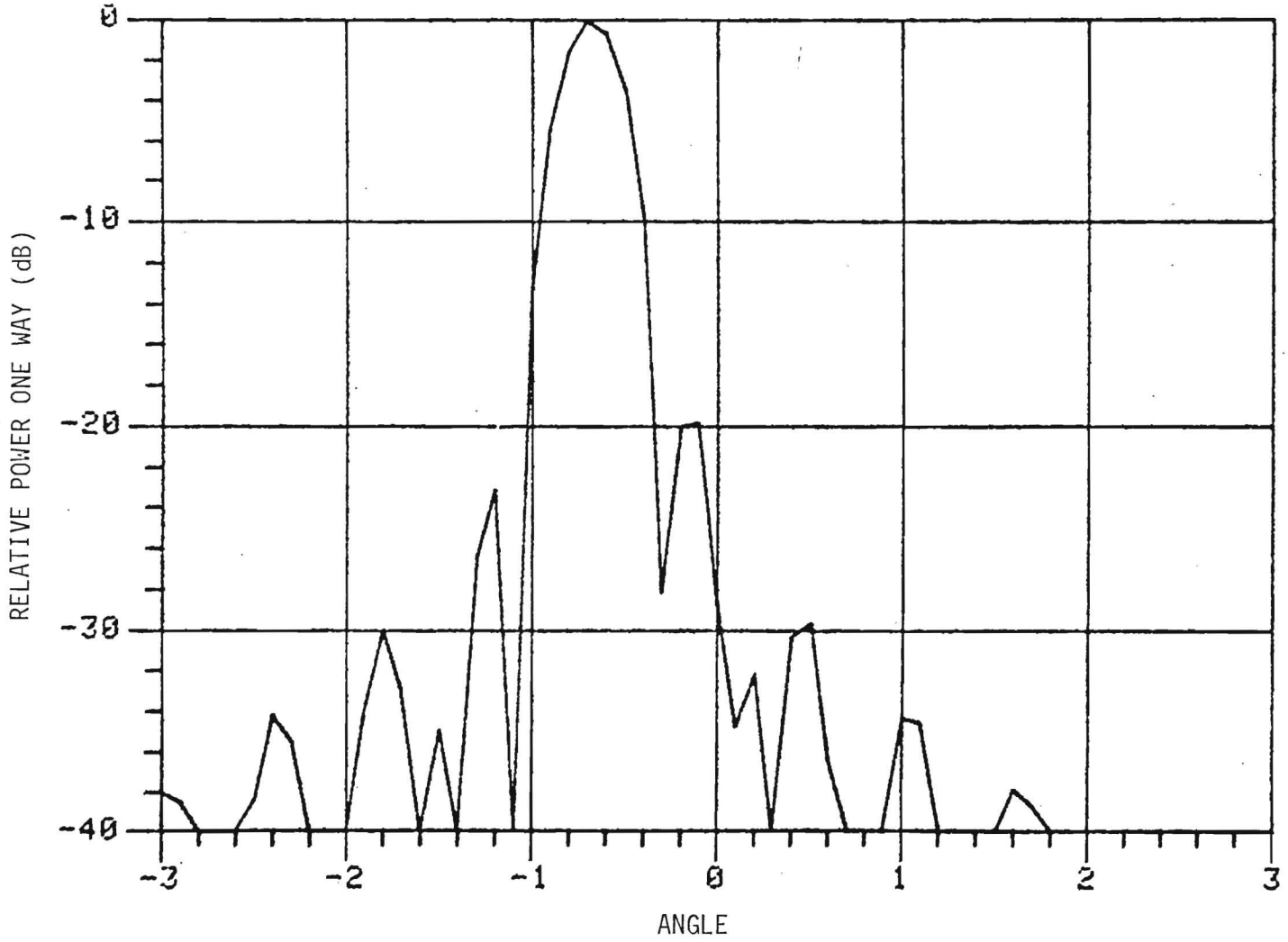

Figure 5-4. Theoretical E-plane pattern for improved antenna with subreflector translated 7.62 mm and rotated 0.72° toward the feed.

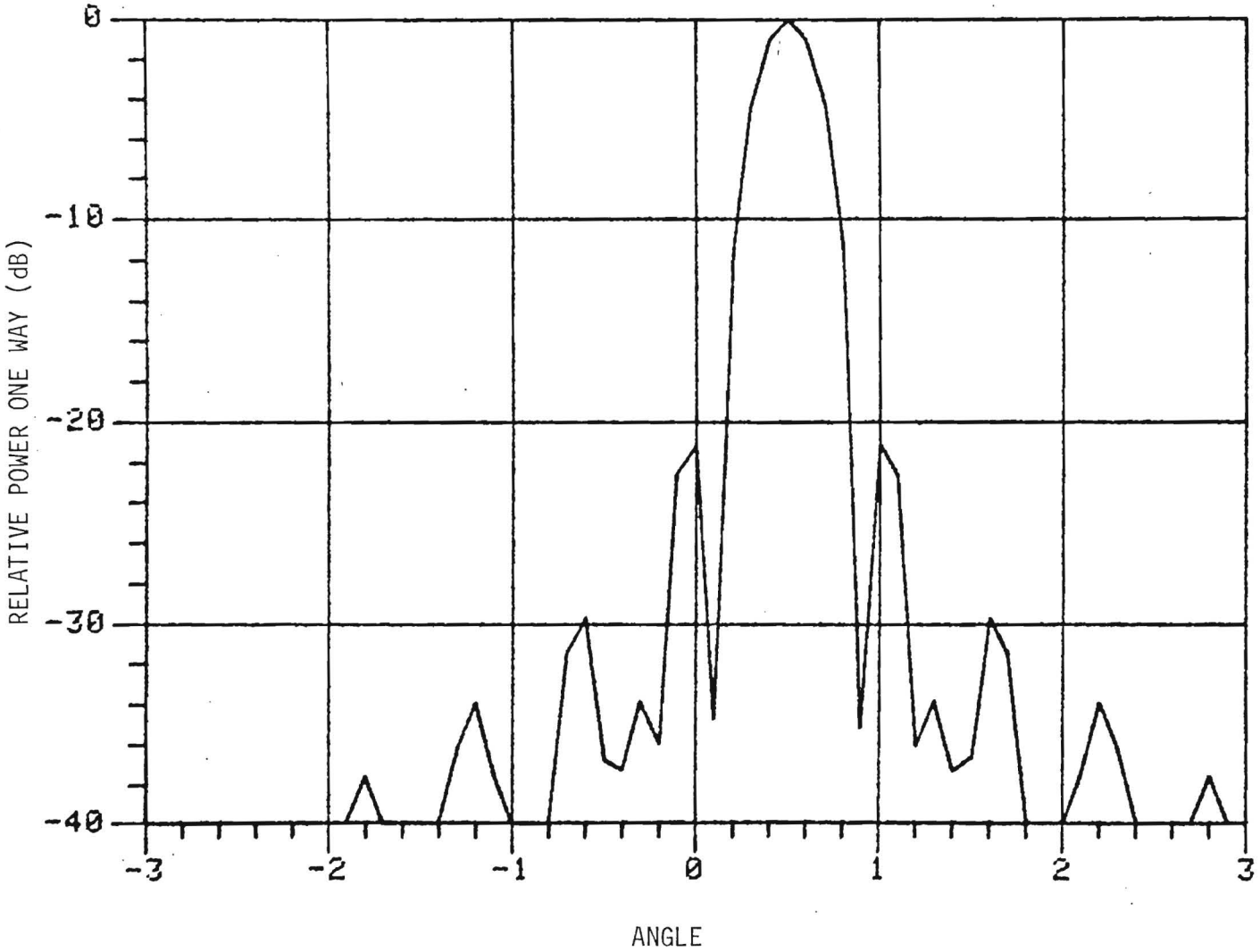

Figure 5-5. Theoretical E-plane pattern for improved antenna with subreflector rotated 1^{o}.

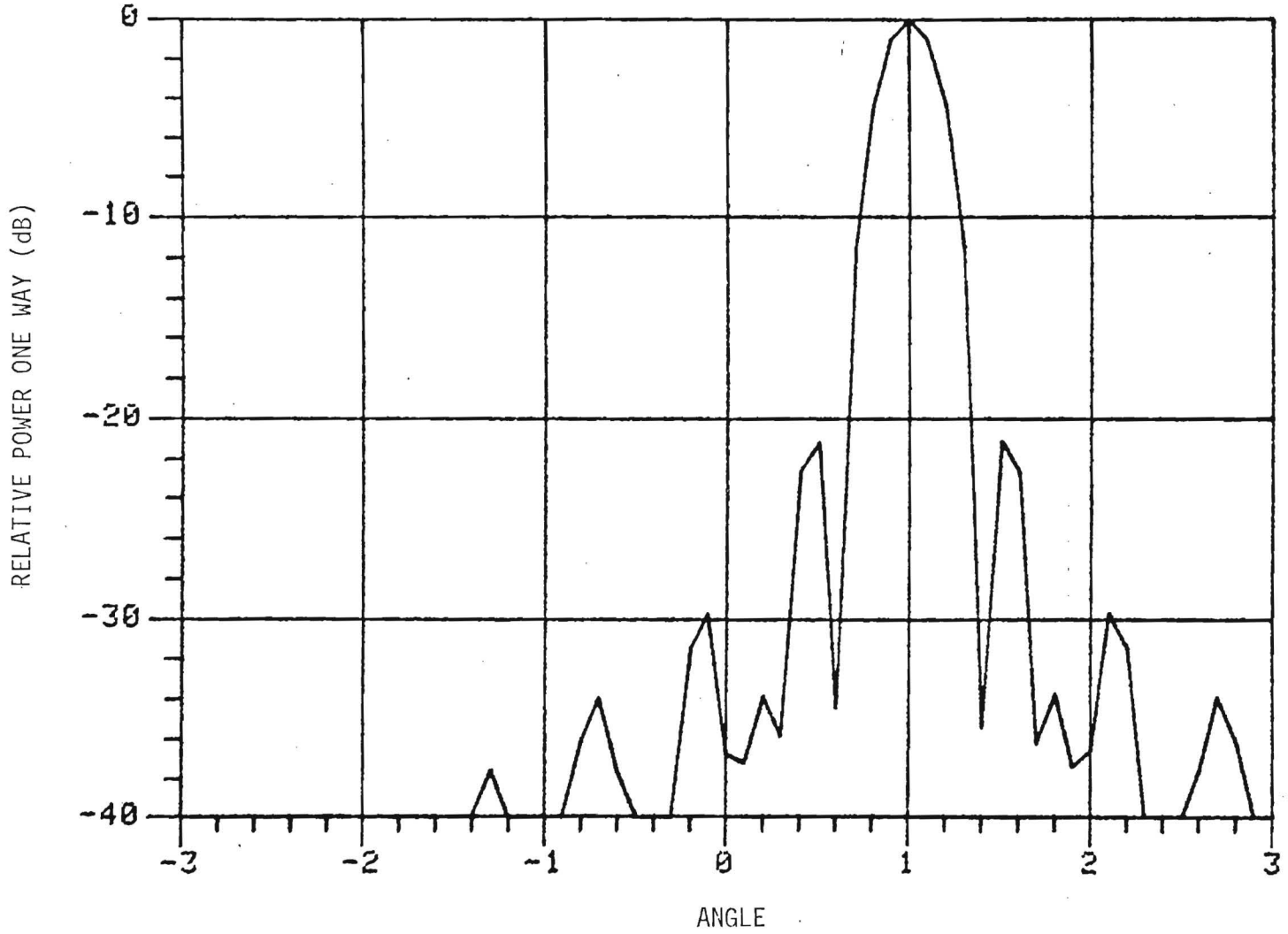

Figure 5-6. Theoretical E-plane pattern for improved antenna with subreflector rotated 2°.

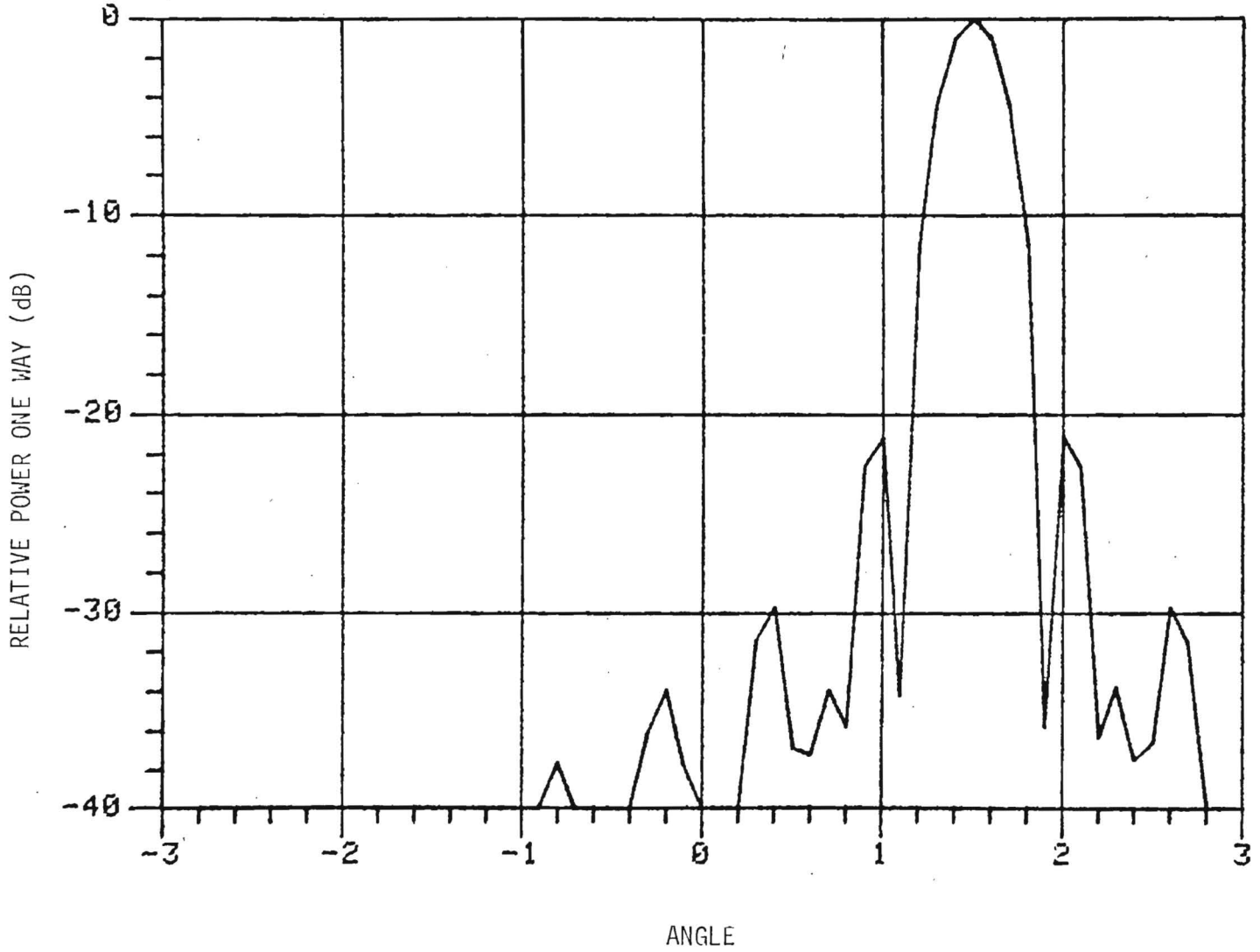

Figure 5-7. Theoretical E-plane pattern for improved antenna with subreflector rotated 3°.

5.2 Conclusions

The experimental and theoretical study outlined in this report has shown that it is possible to predict antenna beam steering by either feed or subreflector motion with reasonable accuracy. Futhermore, solution of the diffraction integrals associated with antenna patterns has given sidelobe levels and beam distortions that also agree reasonably well with experiment. The degrees of agreement for both the simple geometrical theory and the diffraction theory give confidence that an antenna can be designed which will behave as theory predicts. Although the antenna used for the measurements discussed herein is not very suitable for beam steering, it is possible to use relatively simple theory to design such an antenna, and the design can be done with confidence.

An important conclusion reached during this work is that the best method for beam steering is rotation of the subreflector about its focus. This approach gives efficient steering for a well designed antenna with minimum beam distortion while translation and translation/rotation of the subreflector both give prohibitive levels of beam distortion. It was also shown that neither translation nor rotation of the feed is an efficient method of steering the antenna beam.

Although feed motion does give beam scanning with low distortion, it is very inefficient. Besides this efficiency problem, however, there is also the problem caused by feed motion relative to the millimeter wave system, or alternatively, requiring the entire system to move. This required motion could require a larger gimbal system for tracking than the basic Cassegrain antenna, since the system might well weigh more than the antenna.

It is concluded that reorientation of the subreflector provides the best approach to beam steering by a Cassegrain antenna. However, there remains the problem of building a compact and accurate gimbal system which could be installed on the subreflector struts. Any obscuration of

the center of the antenna greater than that already present will cause an increase in symmetrical sidelobe levels which may be prohibitive. This problem is seen to be especially severe when one considers that the resolution of angular position encoders required for accurate tracking will be on the order of 0.1 mrad, and that such encoders are generally about 150 mm in diameter and 25 mm thick. If such a system were to be built, it would be necessary to expend a major effort to obtain parts which, when mounted on the subreflector, would not cause excessive beam distortion. This problem is perhaps the most severe of any confronting the designer of an antenna whose beam is steered by subreflector motion.

5.3 Recommendations

It is recommended that the antenna treated in Section 5.1 be built. In building such an antenna, the initial effort should be expended in verifying the design and refining the beam profile calculations until all of the fairly slight differences noted between theory and experiment in this report are resolved. The antenna should then be constructed without a gimbaled subreflector and measurements similar to those discussed in this report should be performed on it to verify the design. In a parallel task, an intensive effort should be expended to locate torque motors, encoders, and other gimbal components which have high resolution and small size. If such components cannot be located, steering of a Cassegrain antenna beam by subreflector motion is not a viable concept.

The most effective method for machining the parabolic and hyperbolic surfaces required for a Cassegrain antenna is to use a programmable milling machine to fabricate a cutting tool of the proper shape for the desired curve. The equation of the surface is entered into the machine computer, which drives the tool head to give the desired figure. This method has been extensively used to fabricate lenses for millimeter wave systems, including a 60 cm rexolite lens machined at Georgia Tech.

As an alternative, it might be possible to avoid machining the large parabolic reflector by purchasing an astronomical telescope reflector made of glass and coating it with an aluminum reflecting surface. Such a mirror would be too heavy for a practical millimeter wave system, but would suffice to prove the beam steering principle. The hyperbolic reflector could then be easily machined by the method discussed above.

In summary, it is concluded that an antenna suitable for precision tracking by steering of the subreflector can be built with good steering efficiency and negligible beam distortion. The most severe problem facing the implementation of such a device is the possible increase in central obscuration caused by the gimbal being mounted on the subreflector. It is recommended that this antenna be designed and built.

REFERENCES

1. R. W. McMillan and G. E. Riley, "Precision Tracking Radar Antenna," Technical Report RE-CR-80-4, U. S. Army MICOM, Redstone Arsenal, AL October 1979.

2. A. M. Isber, "Obtaining Beam-Pointing Accuracy with Cassegrain Antennas", Microwaves, August 1967, pp. 40-44.

3. P. A. Jensen, "Designing Cassegrain Antennas", Microwaves, December 1962, pp. 12-19.

4. J. Ruze, "Lateral-Feed Displacement in a Paraboloid", IEEE Trans. Antennas and Propagation Vol. AP-13, No. 5, pp. 660-665, September 1965.

5. Y. T. Lo, "On the Beam Deviation Factor of a Parabolic Reflector," IRE Trans. Antennas and Propagation, Vol. AP-8, No. 3, pp. 347-349, May 1960.

6. Alpha/TRG Millimeter Microwave Products and Capabilities, Catalog, Alpha Industries, Inc. 1978.

7. W. R. Ronis, Alpha Industries, Private Communication, April 1980.

8. E. Jahnke and F. Ende, Tables of Functions with Formulas and Curves, 4th Ed., Dover Publications, New York, 1945, Chapter VIII.